Active-Contracting Fabrics for Wearable Compression Applications

A THESIS
SUBMITTED TO THE FACULTY OF THE GRADUATE SCHOOL
OF THE UNIVERSITY OF MINNESOTA
BY

Rachael Margaret Granberry

IN PARTIAL FULFILLMENT OF THE REQUIREMENTS
FOR THE DEGREE OF
MASTER OF SCIENCE

Dr. Bradley T. Holschuh
Dr. Julianna Abel
Dr. Lucy E. Dunne

September, 2018

Acknowledgments

In addition to the immense support from my advising committee at the University of Minnesota, including Dr. Brad Holschuh, Dr. Julianna Abel, and Dr. Lucy E. Dunne, I would like to thank NASA's Space Technology Research Grants (STRG) program for funding this work through a NASA Space Technology Research Fellowhsip (NSTRF, Grant # 80NSSC17K0158). Without their support, this research would not be possible. Additionally, I would like to acknowledge the crucial role Amy Ross, my NSTRF mentor, has played in the development and continuation of this work. I'm looking forward to following up this Master's thesis with a Ph.D. dissertation under her mentorship.

Other supporting individuals include Dr. Linsey Griffin, Dr. Karen LaBat, and Dr. Karen Ryan from the Human Dimensioning Lab, who provided helpful guidance with anthropometric analysis. Additionally, Kevin Eschen, Ph.D. ME candidate from the Design of Active Materials and Structures Lab, has provided invaluable contributions to this manuscript. His work to mechanically model knitted SMA structures has provided a significant foundation for applications work - for compression garments and many others. While Kevin's work is cited throughout this thesis, I would like to particularly acknowledge the role he played in developing self-fitting fabrics. Additional students to thank include Julia Duvall, and Megan Clark from the Wearable Technology Lab, and Robin Carufel from the Human Dimensioning Lab. Thank you.

Finally, I would like to acknowledge non-academic support from my husband and our cats, to whom this thesis is dedicated. Additionally, a big thank you to my parents, Sheri and Michael Granberry, and my parents-in-law, Kathleen and Urs Keller, for their endless encouragement and support. Last (but certainly not least) thank you to my friends, Rachel Gregory, Katherine King, and Vanessa Sanchez, for always being there for me.

Dedication

This thesis is dedicated to my husband, Michael Keller, and our cats, Gala Dali, Kiki Smith, and Egon Schiele, who loved and supported me every day of this Master's program. Thank you for being my family.

Abstract

Compression garments are worn articles of clothing commonly used in medicine, astronautics, sports, and ready-to-wear fashion to provide a wide range of on-body pressures for purposes such as pressure therapy, enhanced mobility/performance, anatomical anchoring, or simple aesthetics. Current compression garment technologies are limited to pneumatic garment and undersized garments, each with their own challenges. Inflatable garments are dynamic, meaning pressures can be varied in quantity, duration, and location; however, these garments inhibit mobility and have a large mass, two factors which limit their use to stationary situations. Undersized garments are designed with stretch fabrics and/or cinching mechanisms, such as straps or lacing, to increase fabric tension around the body. Undersized compression garments are preferred when pressure is desired during daily and/or mobile activities because they are low-profile, do not inhibit mobility, and do not require a power source; however, the trade-off is lack of dynamic functionality.

Active-contracting fabrics are an emerging area of research that could advance the capabilities of compression garment design by contracting on command. Shape memory alloys (SMA), for example, are active materials with shape memory properties and can be engineered to remember prescribed forms through an annealing process. Traditional weft knit architectures can be engineered to produce contraction if individual yarns incorporate SMA wire, causing large, dynamic displacements and contractive forces across the fabric surface that can be turned on/off or achieve various compression levels.

This research addresses the compression garment technology gap by evaluating active-contracting fabrics, specifically contractile SMA knitted actuator fabrics, for on-body compression applications. Because the effectiveness of compression garments is dependent on the relationship between the garment and the body (i.e. fit), 50% of this work seeks to define the dimensions, range, and variability of the human body, while the remaining 50% seeks to quantify the performance of active-contracting fabrics. Specifically, this work (1) defines lower body static anthropometric variability through the development of a sizing system, (2) defines lower body dynamic anthropometric variability between different working positions to determine average dimensional fluctuation, (3) develops self-fitting, self-stiffening garments using active-contracting fabrics to address individual and population fit challenges, and (4) characterizes the actuation force of active-contracting fabrics for on-body

compression applications.

The outcomes of this manuscript are the following. (1) Lower body dimensional variability is vast. To accommodate 95% of the consumer population with a fitted, non-compliant lower leg garment would require hundreds of size categories, an approach that is not appropriate for the ready-to-wear market in the absence of mass-customization. (2) Lower body dimensional variability due to posture is minimal at the ankle and calf (max, 8%); however, changing dimensions at the knee and thigh (max 13% and 17%, respectively) may require special design consideration. (3) Active-contracting fabrics can be used in the design of self-fitting, self-stiffening garments that can accomplish actuation contraction up to 40%, a range that is suitable to reduce hundreds of sizes to a handful of sizes for a fitted, non-compliant, lower leg garment. (4) When displacement is fixed, or blocked, active-contracting fabrics can reach fabric tensions between 43 and 359 N/m. When wrapped around the body, these tensions translate to pressures ranging from 15-65 mmHg, depending on body radii. Additionally, these results revealed that increased SMA wire diameter and increased strain produce higher actuation forces.

The results of this research endeavor conclude that active-contracting fabrics could be used in two distinct ways to accomplish the design of active-contracting compression garments. Self-fitting, self-stiffening fabrics could be actuated first to pull the garment close to the body and apply necessary strain to high-force compression fabrics. Once strained to their optimal actuation length, the high-force compression fabrics could apply the desired pressures. The results is a controllable, low-profile compression garment design that will be developed in future work.

Contents

List of Tables

List of Figures

Chapter 1

Introduction

Compression garments (CG) are articles of clothing designed to reduce body volume, an action which increases body pressure. Recognizable uses for on-body compression include medical CGs that increase body pressure for the purpose of manipulating fluids. Additionally, some medical CGs increase peripheral body awareness through circumferential pressure. Ubiquitous, but less obvious uses of compression include body shapewear (e.g. bras, bodysuits) and everyday clothing/accessories that require anchoring to the body through waistbands, wristbands, headbands, shoe tops, should straps, and many more.

CGs are designed to reduce body volume through strategic garment dimensional reduction. Therefore, functionality is dependent on garment fit, or the relationship between garment dimensions and body dimensions. Two presently used CG technologies include pneumatic and undersized CGs. In the former, inflatable bladders distend to increase garment mass, an action which causes the garment to balloon towards the body. In the latter, the length of fabric wrapped around the body is less than the circumference of the body, placing the garment in a strained state and the body in a compressed state. Undersized CGs can be designed with stretch fabrics with dimensions less than body dimensions so that the garment strains when donned. Alternatively, they can be designed with minimum-stretch or non-compliant fabrics with dimensions greater than body dimensions, which are reduced post-don through adjustable closures, such as lacing or straps. Although undersized CGs designed with stretch fabrics are the least complex (i.e. no manual manipulation of closures, no inflation source), they are also the most sensitive to garment fit because dimensions cannot be adjusted post-manufacture.

This work evaluates the garment-body interface, specifically garment fit, to improve

upon current CG technologies. The following sections present the trade-off between pneumatic and undersized CGs before proposing an alternative solution - active-contracting fabrics for CG design. The objectives for this research endeavor are outlined, followed by a summary of chapter content that pursues these objectives. The chapter ends with a synopsis of major thesis findings.

1.1 Problem Statement

This research addresses functionality and wearability challenges of present CG technologies, specifically the challenge of achieving desired pressures through fit manipulation in a form-factor that encourages patient compliance and/or consumer acceptance. Pneumatic garments are frequent used in medical setting for their controllable and high-pressure capabilities; however, pneumatic CGs could pose medical and situational risk to patients due to the fact that they inhibit wearer mobility [10, 11, 12], cause edema in cut-away areas (e.g. knees, feet, groin) [10], increase metabolic cost and user exertion [12], do not allow for controllability away from air supply [12], deflate with movement [12], and exert uneven pressure due to the mechanics of inflatable structures [11]. Consequently, pneumatic CGs are best restricted to bed-rest or otherwise stationary conditions. Undersized CGs are an alternative technology that are prefered for their superior mobility [12]. While they are capable of exerting pressure on the body without substantially impeding movement [13], undersized CGs inflict unpredictable regions of too-high and too-low pressures on the user in response to the variable nature of the body [14, 6, 15]. Additionally, undersized CGs are notoriously difficult to don/doff, especially at high pressures (i.e. increased garment dimensional reduction) and for elder patient populations with limited dexterity and upper body strength, [16]. Finally, undersized CGs are not dynamic, meaning pressure magnitude and duration cannot be changed [17], a limitation that prevents them from providing effective compression treatment for disorders such as lymphedema and deep vein thrombosis that require controllable pressures.

In addition to the previously outlined functional flaws, neither pneumatic nor undersized CGs were designed to anticipate or respond to changes in the body (i.e. shape, volume) [6]. The result is large swings in pressure magnitude with a change in joint angles, fluid volume, orientation in relation to gravity, and/or body composition (i.e. fat, muscle, bone ratio) [14]. Because a change in body dimension alters the fit, or body-to-garment relationship, pressure will always respond accordingly unless the garment is designed to respond dynamically.

This research addresses the body-garment interface challenges by proposing a new type of CG technology that could adapt to the body's shape change without ballooning away from the body or impeding movement, two key wearability challenges. The following section introduces active-contracting fabrics, actuating fabrics that are capable of contracting on command, and proposes their use for the design of dynamic, low-profile CGs for a variety of medical, aerospace, and consumer uses.

1.2 Motivation for Low-Profile, Active-Contracting Fabrics

Active fabrics are an emerging area of research that could advance the capabilities of CG design by contracting on command [18, 19]. Shape memory alloys (SMA), for example, are active materials with shape memory properties that can be engineered to remember a prescribed form through a heat-treatment process and then recover that form when heated above a material-specific temperature [20]. SMAs can recover high strains ($\approx 8\%$) [8] and produce amplified actuation strokes when configured in certain geometries [18, 19]. Knit architectures, primary used to construct stretch fabrics, are one type of geometry that enhances actuation stroke across large surface areas. Knit fabric structures are particularly suited to the design of active-contracting fabrics because their looped architecture enables surface-wide, mechanical compliance that can be leveraged with active materials.

Figure 1.1 depicts a traditional knit structure composed of alternating courses of knit and purl stitches, defined by either an overlapping or underlapping loop crest. If an SMA wire, trained to remember a straight configuration, replaces the yarn, upon actuation the loops attempt to straighten, causing surface-wide, uniaxial contracting. Prior research has observed up to $\approx 40\%$ length reduction [4] of SMA knits. Furthermore, mechanical contraction can be design by modifying traditional knitting variables, such as weight of yarn (or wire diameter), loop length, and loop enclosed area (or knit density) [4]. While prior research has limited exploration to weft knit structures, as depicted here (e.g. garter stitch, jersey stitch, rib stitch) [18], warp knit structures also offer exciting actuation potential.

If an active knit CG is constructed using knitted SMA, the garment could be donned during an off, or a loose, relaxed state, contract on command, exert various pressure profiles, and adapt to the bodys dimensional change. Additionally, active-contracting fabrics could be designed to exert specific pressures on the body through design choices that would determine actuation stroke, such as type of knit structure, SMA wire diameter, density of knitted structure, and pre-fit of the garment (i.e. fit before actuation). Like passive

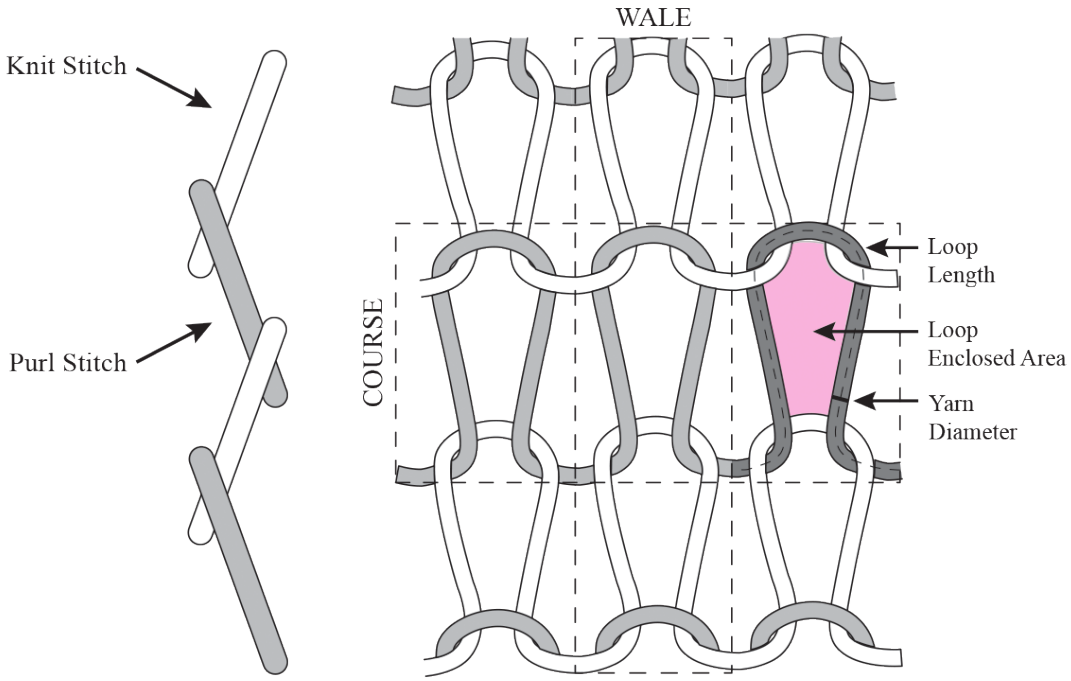

Figure 1.1: **Knit Fabric Structure (Garter Knit):** Alternating courses of knit and purl stitches make up a traditional garter knit fabric. A knit course is a row of knit stitches. Likewise, a knit wale is a column of knit stitches. Important design features of knit fabrics include the yarn diameter, the loop length, and the loop enclosed area.

knit medical garments designed with gradient pressures that decrease from the ankle to the thigh, an active-contracting fabric CG could have a functionally gradient design, incorporating regions of various pressure profiles and active shape change across the lower body. Consequently, active-contracting fabrics offer the novel possibility to develop advanced CGs that are simultaneously controllable, mobile, and untethered.

1.3 Research Objectives

The objective of this research is to investigate the garment-body interface through parallel anthropometric and active-contracting fabric research. By characterizing body dimensions and variability in tandem with the actuation characterization of active-contracting fabrics, this manuscript aims to provide a foundation to further active-contracting fabric development, tailored to the dimensional and performance requirements of the body. To work towards these big-picture objectives, the following sub-goals are pursued.

- Characterize the number of unique sizes that would be required to design a conformal, non-compliant low-leg garment for the North American consumer population and define the dimensional range within each size.
- Characterize the percentage of circumferential dimensional change at key, low-leg locations (i.e. ankle, calf, knee, thigh) for North American women.
- Characterize actuation force of active-contracting fabrics and approximate on-body pressure potential to determine appropriate uses for the technology.
- Determine the suitability of active-contracting fabrics to self-fit and self-stiffen around the body and reduce population sizing challenges by pairing prior actuation contraction characterization data with anthropometric analysis.

1.4 Thesis Overview and Structure

The success of CGs is dependent on fit, or the relationship between the garment and the body; therefore, this thesis content is split between: (1) anthropometric, sizing, and fit analysis for the lower body and (2) active-contracting fabric characterization for the use in CG applications. By defining the behavior and identifying the challenges of both the lower body and active-contracting fabrics in parallel, this work lays groundwork for future development. The following section breaks down the contents of each chapter.

- **Chapter 2** presents the challenges of anthropometric variability, sizing, and fit for the lower body, assuming a static posture. The simplified analysis (which does not include dynamic, working postures) is the first known attempt to develop a sizing table for a conformal, non-compliant low-leg garment.
- **Chapter 3** adds complexity to the challenges presented in Chapter 2 by presenting a dynamic anthropometric analysis of the leg. Specifically, the study evaluates the change in leg dimensions between a standing posture and a sitting posture (working posture).
- **Chapter 4** begins the characterization of active-contracting fabrics by evaluating their pressure potential in CG applications. Specific areas of analysis include actuation force, or the force differential between actuated and unactuated state, at different blocked lengths (strain). The chapter ends by defining the range of theoretical pressures active-contracting fabrics could exert on the body when used to design a CG.

- **Chapter 5** presents collaborative work completed with Kevin Eschen, University of Minnesota Mechanical Engineering Ph.D. student and uses prior applied force-displacement analysis paired with new anthropometric analysis to design and fabricate a self-fitting, self-stiffening leg garment. The chapter ends with supplemental analysis that simplifies the sizing table at the end of Chapter 2 by incorporating the performance of the new, self-fitting, self stiffening fabric technology.

- **Chapter 6** concludes the work by synthesizing analysis from all four body chapters into a systems-level discussion. The chapter ends by identifying shortcomings, challenges, and future work for CG design using active-contracting fabrics.

1.5 Brief Summary of Thesis Findings

The findings of this thesis work are fourfold. (1) Maintaining low-leg garment fit across a population without fabric compliance, added dimensional ease, or bidirectional adjustability produces unreasonable production expectations and retail complications in the absence of mass-customization (i.e. hundreds of unique garment sizes) [2]. (2) Leg dimensions were found to change circumferential dimension between standing and sitting postures (i.e. max 8% ankle, 6% calf, 13% knee, 17% thigh), suggesting CG fit must be dynamic, as well as precise [21]. (3) The maximum actuation force of active contracting fabrics produces actuated fabric tensions ranging from 43 to 359 N/m, a range that could exert on-body pressures between 30 and 65 mmHg around body radii between 0.04 and 0.17 m. (4) The minimum dimensional increase for a low-leg garment to be pulled over the foot for don/doff is within 40% of body dimensions, suggesting actuation contraction of active-contracting fabrics (max 40% [4]) is suitable for the design of self-fitting garments [22]. The thesis findings are synthesized in Chapter 6 to discuss implications for future CG systems design.

Chapter 2

Static Anthropometric Analysis for the Fit & Sizing of the Lower Body

This static anthropometric analysis of the lower body for the fit and sizing of advanced functional garments began as a collaborative conference manuscript with Julia Duvall, M.S. graduate of the University of Minnesota's Apparel Studies program. The original manuscript was presented at the 2017 International Symposium on Wearable Computers in Maui, Hawaii. J. Duvall made contributions by means of background writing and figures, which will be referenced, but not included in this text. Additionally, I would like to acknowledge the contributions of Megan Clark, a B.S. graduate of the Apparel Studies Program who spent substantial time collecting data for this analysis, and the Human Dimensioning Lab (HDL), who provided access to CAESAR, the anthropometric database used in this analysis. At the time of the study, the HDL only had access to CAESAR; consequently, a supplemental analysis is included at the end of the chapter that evaluates SizeUSA, an additional anthropometric database with a larger quantity of readily accessible data. The chapter ends with male/female size charts for a non-compliant, conformal lower-leg garment.

2.1 Introduction

Functional garments are worn articles of clothing that are designed to meet a specific, and often complex set of user needs accomplished by merging apparel design and science [23].

Examples of functional garments include clothing that affords the user enhanced environmental protection, medical or therapeutic benefits, sports performance, or vanity satisfaction (e.g. body shapewear). Many garments provide multi-functionality (e.g. spacesuits), and special needs services (e.g. wheelchair gloves) [24]. Advanced functional garments are functional garments that achieve their function through integrated sensing and/or actuating components (e.g. electrocardiography (ECG) shirt (sensing garment), robotic exosuit (actuating garment) [25, 26].

The success of advanced functional garments is often dependent on proper placement of sensing and/or actuating components on the body as determined through garment sizing/fitting methodologies in the absence of customization [25, 27]. While clothing fit is defined as the relationship between the garment and the body, sizing is the method of adjusting all garment dimensions to maintain the desired fit across a designated population [23]. Poor fit and subsequent poor placement of actuators/sensors on the body can result in under-performance (e.g. sensing garments might pick up a weak signal; actuating garments might deliver a weak force to the body) and counter-performance (e.g. misplacement of sensing components could cause noise that obstructs the sensed signal or sends the wrong signal; misplacement of actuating components could deliver force to the wrong area of the body and hinder movement) [25, 27].

Due to the sensitivity and criticality of sensor-body and actuator-body interfacing, common ready-to-wear (RTW) apparel sizing methodologies do not meet the fit requirements of advanced functional garments for a consumer market. This research seeks to develop novel sizing and design strategies for advanced functional garments to maintain proper fit/placement across a large population. For the purpose of this research, we evaluated anthropometric variability and developed advanced functional garment sizing methodologies around a novel, active compression garment (CG) design for the lower leg.

2.2 Background

2.2.1 Active-Contracting Compression Garments (CG)

Here we evaluate geometric variability of the lower leg and seek to develop a sizing and fitting methodology for a novel, shape memory alloy (SMA) activated compression garment (SMA-CG), as detailed in [5]. This advanced functional garment for the calf (depicted in Figure 2.1) delivers therapeutic pressures to the body by integrating contracting SMA springs,

as outlined by Holschuh et al [19]. The pressure generated by the garment is dependent on precise fit, specifically the ratio between the garments circumference and the limbs circumference. Consequently, to maintain fit across a population, garment circumference must vary in response to (1) individual dimensional changes (e.g. ankle circumference vs calf circumference) and (2) variability in population anthropometrics. Consequently, to design an SMA-CG or any other CG designed for a North American consumer population, we need to know the lower leg dimensional variability of our population, determine the critical dimensions for SMA-CG design, and develop methods for adjusting critical dimensions across our population to maintain fit.

Figure 2.1: **Shape memory alloy activated compression garment (SMA-CG):** For more information on garment design, refer to [5].

2.2.2 Anthropometric Resources

To evaluate geometric variability of the lower leg for a large population representative of the consumer market in North America, we first explored available anthropometric resources. Some anthropometric databases contain measurements that are no longer representative of the present population (e.g. ASTM), some contain military populations that are not generalizable to the civilian population (e.g. ANSUR; NASA Anthropometric Sourcebook), and others are composed of scattered populations that cannot be compared (Asian women to Canadian men) (e.g. NASA Anthropometric Sourcebook). The civilian American &

European Anthropometric Resource (CAESAR) is a database of three-dimensional body scans of a large civilian population. 3-D scans allow for dimensional extraction straight from the surface scans; however, the extraction process is time consuming and few dimensions are readily available for the population.

2.2.3 Individual Garment Fit: Patterning

Garment patterns are generally two-dimensional blueprints for three-dimensional garments created through flat pattern making or draping methods. Flat pattern making, or pattern drafting, uses body dimensions and an intuitive understanding of the three-dimensional body to generate garment patterns [28]. Alternatively, draping is the process of pinning fabric around a three-dimensional form (i.e body or dress form) to generate a flat pattern, which can then be refined through traditional two-dimensional drafting methods [29]. The success of the garment pattern, specifically achieving the desired fit around the body, is dependent on two factors: (1) the number of body dimensions available and (2) knowledge of the relationship between those body dimensions (i.e. shape).

Draping provides infinite body dimensions and a direct interaction with body shape, making it an ideal method for generating an accurate pattern for an individual [29]. Using only body dimensional data gathered by measuring tapes and calipers is as successful as the number of dimensions available. As detailed in [2], the more dimensions that are added to the garment pattern, the better the garment will conform around body dimensions. A limitation to this method is that relationships must be inferred between dimensions to determine pattern curvature, shape, etc. While more challenging, flat pattern making is often necessary when customized draping is not an option. Skilled pattern makers are capable of making tailored, close-fitting garments through flat drafting; otherwise, fashionable dimensional ease must be added in lieu of body shape knowledge (e.g. women's tunic).

2.2.4 Population Garment Fit: Grading & Sizing Systems

Garment designers translate two-dimensional patterns from a single, base pattern, usually composed of average dimensions, to patterns for a population through grading and the development of a sizing system. Grading is the process of systematically increasing and decreasing base garment dimensions to make smaller and larger sized garments. Sizing systems are designed around the specific set of rules developed to grade base garments. While some dimensions are graded in key increments (e.g. ± 3 cm), other dimensions are graded through

regression coefficients [3]. Additionally, indirect sizing systems can be created by systematically increasing/decreasing gross measurements, such as height and weight; however, this method usually leads to inaccurate garment fit across the population [3]

Sizing systems for the RTW, consumer population rarely satisfy the dimensional needs of the population. To start, 'average' size individuals are non-existent [30]. Certainly, a large percentage of individuals have certain measurements that fall within the 50% range for that measurement, but there is little to no chance that all measurements for an individual will fall within the 50% range [30]. To bypass the improbable average, sizing systems can be developed around the dimensions of a 'fit model', or an individual whose body type and dimensions represent the target population. This approach leads to garment sizes that fit individuals close to that fit model's shape and/or size; however, body shape, proportion, and posture generally change as dimensions change, resulting in garments that don't fit individuals whose dimensions lay at the peripheral of the size system.

To increase the percentage of the population that can be accommodated by a given garment design, designers take one of three approaches: (1) add dimensional ease at areas of the garment where wide, population variability is observed, (2) design the garment with stretch fabric whose strain capabilities match the dimensional variability observed, or (3) design garment with adjustable dimensions through the use of lacing, hooks and eyes, or hook and loop tape [2]. The designer generally chooses the design approach based on the size and variability of the target population as well as the functional and aesthetic demands of that population. While stretch elastane fabrics are acceptable for the design of swimsuits and athletic clothing, consumers generally prefer work attire and outerwear designed with heavier, woven fabrics.

2.2.5 Fit & Sizing for Advanced Functional Garments

To design a successful sizing strategy for advanced functional garments (e.g. SMA-CG), traditional RTW fit and sizing methodologies require modification. Griffin et al. evaluated the effectiveness of the ASTM sizing standard when applied to the placement of ECG electrodes integrated into a shirt. They concluded that RTW is not an effective way to size sensing garments and a more advanced, adjustable or mass-customized sizing system is required for garments with precise sensor placement [25]. Because advanced functional garments require precise placement of actuators/sensors on the body, they usually need to be designed using inextensible fabrics to prevent garment drift and anchor to the body.

Other wearables that are affected by sensor or actuator placement include human exosuits [27], sensing garments [31], and heating/cooling garments [32].

This research seeks to develop methods for quantifying and evaluating anthropometric variability in the North American consumer population within groups specified by different anthropometric dimensions, to inform the development of sizing systems and design strategies that satisfy the needs of advanced functional apparel intended for the consumer market.

2.3 Methods

2.3.1 Data Source: CAESAR

The Civilian American & European Surface Anthropometry Resource (CAESAR) survey provided the foundational data for this study. CAESAR contains 2,391 3-dimensional body scans ($N_{female} = 1264$; $N_{male} = 1,127$) of North American civilians taken from the year 1998 to 2000. CAESAR is also accompanied by 40 pre-measured dimensions for each subject gathered by traditional means, such as measuring tapes and calipers. Dimensions that were not pre-measured could be obtained by manual extraction from each individual body surface scan. The database offered a representative sample of our target population and was used to collect the raw data for this study (North American civilian consumers).

2.3.2 Sizing System Approach

Traditionally, apparel sizing systems are developed by determining key, correlating body dimensions from a large dataset through statistical analyses, such as principal component analysis (PCA) or random decision forest [23]. Only 2 of the 40 CAESAR pre-measured dimensions were relevant to the lower leg; therefore, analyses that require a large dataset were impractical for our data source. Through our knowledge of patternmaking we hypothesized 6 dimensions, shown in Figure 2.2, that could provide the foundational dimensions for a SMA-CG sizing system, once statistically evaluated for covariance. It was impractical to manually extract these dimensions for all 2391 CAESAR scans; therefore, we chose to sample 80 scans.

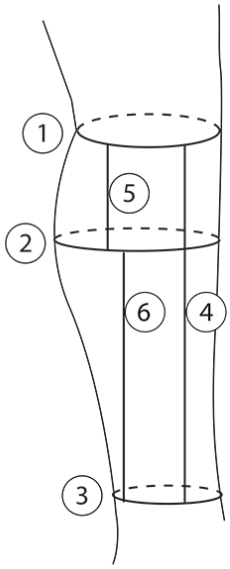

Figure 2.2: **Measurements extracted from CAESAR sample group:** (1) below knee circumference, (2) calf apex circumference, (3) ankle circumference, (4) knee to ankle length, (5) knee to calf length, (6) calf to ankle length

2.3.3 Population Sampling

To provide a representative sample (n = 80) of the full distribution of lower leg dimensions, we sought to determine a predictive variable that would place the CAESAR population in a framework of incrementally increasing, lower body proportion (i.e. smallest leg dimensions to largest leg dimensions). From this framework, we could randomly sample from sub-groups and ensure our sample contained the full breadth of possible dimensions. Determining how to create this framework without having access to specific dimensions was a challenge. With only major body measurements available in the list of 40 pre-measured dimensions (e.g. height, weight), we hypothesized that overall body height would be the greatest influencer of leg lengths, while overall weight would be the greatest influencer of leg circumferences. The calculation for body mass index (BMI) factors in both height and weight, meaning BMI provides implicit predictive power for both measurements. Consequently, BMI was determined to be a suitable organizing dimension for sample collection.

Due to anthropometric dissimilarities, male and female participants were placed in separate groups and arranged by BMI. Descriptive statistics were run for both groups to determine quartiles by BMI, a simple method to place the population into sub-groups. Ten

participants of each sex were randomly sampled from each quartile to provide a representative sample of the CAESAR population.

2.3.4 Data Collection

Figure 2.2 depicts the measurements extracted from CAESAR for each sample body / participant (n = 80). The anatomical markers are the hypothesized key dimensions and were determined by the locations required to pattern a garment that would interface closely with the human leg; those being 1. calf, 2. knee, 3. ankle, and the vertical spacing between the three circumferences (4. knee-to-ankle, 5. knee-to-calf, 6. ankle-to-calf). For this study, calf circumference is located at the apex of the gastrocnemius muscle, knee circumference is located at the bottom-most part of the patella, and ankle circumference is defined as the narrowest point of the leg just above the medial malleolus.

While the ankle circumference was included in the CAESAR pre-measured dimensions, the traditional measurement was gathered low on the foot on top of the medial malleolus. Because this location was not the smallest circumference along the leg, a new ankle measurement was defined and extracted from the surface scan for analysis. Additionally, the leg dimensions gathered varied noticeably between right and left legs of the same participant due to right/left biases and developmental differences; consequently, we used the dimensions from each leg as its own dataset and the new sample group shifted from $n_{participant} = 80$ to $n_{legs} = 160$. Additionally, contours of the sample legs were gathered using cross-sections in both the length and the width directions to evaluate the nature/topography of the dimensions.

2.3.5 Statistical Analysis

A correlational analysis was conducted to determine covariance between the 6 extracted lower body dimensions, specifically length and circumference measurements, to form the framework for a sizing system. Covariance of the lower body was found to be weak; the largest correlation was between measurements 2 and 6 (r = 0.46) and the weakest between measurements 1 and 5 (r = -0.16). Refer to Figure 2.2. Consequently, we redirected our approach and sought to determine a singular dimension that would organize the population into the best possible, or most discrete, size categories. A depiction of perfectly discrete size categories is shown in Figure 2.6. We returned to our hypothesized predictive dimension used for sampling purposes, BMI, and began a statistical analysis to determine if organizing

the population by BMI organized the population in discrete size categories in all, or most lower leg dimensions. An analysis of variance (ANOVA) was run for each of the 6 dimensions gathered to determine if the differences between the mean of each quartile (sub-group) were statistically different. A post hoc analysis was run to determine which specific quartiles were statistically different. A pairwise comparison using ttests with pooled standard deviations with p-values adjusted with the Bonferroni method was used to identify which quartiles were statistically significant (or, which quartiles maintained discrete sub-groups) and which quartiles did not (no evidence of statistically significant differences). While the mean of each quartile would not directly validate a size category, an ANOVA provided strong evidence that the subgroups were statistically different and had potential to become independent size categories upon further analysis.

In response to the results presented below for BMI and to test the relative effectiveness of different predictive variables, the same sample data (n = 80) were reshuffled by other potential predictive dimensions, specifically height, weight, ankle-to-knee length, ankle circumference, calf circumference, and knee circumference. Because height and weight data were available for the full population, statistical quartiles were determined for the full population and the reshuffling resulted in uneven numbers from our original sample in each re-shuffled quartile. The remaining dimensions were only available for the sample (n = 80); therefore, these groups maintained a sample group of 10 of each sex in each quartile. The dimension that had the greatest quantity of statistically significant sub-groups was evaluated through descriptive statistics to determine sub-group variability and overlap.

2.4 Results

2.4.1 Anthropometric Variability: Circumference by BMI

The results of the variability analysis for ankle, calf, ankle, and knee circumferences for men and women when grouped by BMI quartiles are shown in Figure 2.3 (mean ± SD). We can be confident that mens lower limb circumferences are, on average, larger than womens (ankle circumference: $\bar{x}_m = 8.77$ in, $\bar{x}_w = 8.25$ in; calf circumference: $\bar{x}_m = 15.21$ in, $\bar{X}_w = 14.65$ in; knee circumference: $\bar{x}_m = 13.92$ in, $\bar{x}_w = 13.67$ in). The sample range of womens circumferences are generally larger than the sample range of mens circumferences; however, we discovered that an outlier in the female group skews the ranges (ankle circumference: $range_m = 2.98$ in, $range_w = 2.74$ in (with outlier, 4.14 in); calf circumference: $range_m$

= 6.02 in, $range_w$ = 5.5 in (with outlier, 8.67 in), knee circumference: $range_m$ = 4.48 in, $range_w$ = 4.84 (with outlier, 10.44 in)). We decided to keep the outlier data as a good example of possible anthropometric variability; however, if we examine the ranges without the outlier, we see that the range of ankle and calf circumference is larger in men and the range of knee circumference in larger in women.

2.4.2 Anthropometric Variability: Length by BMI

The results of the variability analysis for knee-to-ankle, knee-to-calf, and ankle-to-calf lengths for men and women grouped by BMI quartiles are shown in Figure 2.3 (mean ± SD). We can be confident that mens lower limb lengths are, on average, longer than womens (knee-to-ankle: $\bar{x}_m$ = 12.7 in, $\bar{x}_w$ = 11.39 in, knee-to-calf: $\bar{x}_m$ = 3.49 in, $\bar{x}_w$ = 2.92 in; ankle-to-calf: $\bar{x}_m$ = 9.22 in, $\bar{x}_w$ = 8.48 in) and the sample range of womens lengths are generally the same as the sample range of mens circumferences (knee-to-ankle: $range_m$ = 3.06 in, $range_w$ = 3.1 in; knee-to-calf: $range_m$ = 1.92 in, $range_w$ = 1.92 in). The exception is the ankle-to-calf length where women have a larger range than men (ankle-to-calf: $range_m$ = 3.01 in, $range_w$ = 3.34 in).

2.4.3 Alternative Predictors: Circumference

The best predictive dimension for a single-predictor sizing system would result in the ability to divide the population effectively into groups that overlap as little as possible for the fewest dimensions (see Figure 2.6). To evaluate the effectiveness of BMI as a predictor, an ANOVA was conducted to determine if organizing the CAESAR sample into groups based on BMI would produce statistically independent circumferences (i.e. ankle, calf, knee) between quartile groups. The ANOVA results (see Figure 2.3) show that grouping by BMI does produce at least one independent size between quartiles for both men and women within all three circumferences (ANOVA p-values < 0.001). A pairwise comparison using t-tests adjusted with the Bonferroni method was conducted to specify which quartiles were different from each other. The post-hoc analysis (see Figure 2.3) shows that some groups are significantly different and other are not when organized by BMI; therefore, the same data was reshuffled by other potential predictive dimensions (i.e. (1) height, (2) weight, (3) ankle-to-knee length, (4) ankle circumference, (5) calf circumference, and (6) knee circumference) to determine if organizing by another dimension might produce an organization framework with more discrete quartiles/sizes.

ANOVA results | BMI

	Women mean ± sd	Men mean ± sd	Women mean ± sd	Men mean ± sd	Women mean ± sd	Men mean ± sd
	Ankle Circumference		Calf Circumference		Knee Circumference	
Q1 =	7.77 ± 0.57	8.21 ± 0.54	13.57 ± 0.72	13.98 ± 1.17	12.38 ± 0.56	12.83 ± 0.64
Q2 =	8.16 ± 0.47	8.72 ± 0.38	14.29 ± 0.80	14.98 ± 0.44	13.41 ± 0.60	13.90 ± 0.65
Q3 =	8.17 ± 0.43	8.82 ± 0.36	14.58 ± 0.61	15.53 ± 0.69	13.57 ± 0.71	14.32 ± 0.63
Q4 =	8.91 ± 0.43	9.31 ± 0.66	16.19 ± 1.61	16.34 ± 0.95	15.31 ± 2.25	14.62 ± 0.70
ALL =	8.25 ± 0.75	8.77 ± 0.63	14.65 ± 1.39	15.21 ± 1.20	13.67 ± 1.62	13.92 ± 0.94
ANOVA p-value =	< 0.001	< 0.001	< 0.001	< 0.001	< 0.001	< 0.001
	Knee-to-Ankle Length		Knee-to-Calf Length		Ankle-to-Calf Length	
Q1 =	11.65 ± 0.57	12.78 ± 0.40	3.16 ± 0.29	3.68 ± 0.39	8.49 ± 0.46	9.10 ± 0.55
Q2 =	11.43 ± 1.02	12.46 ± 0.60	3.23 ± 0.28	3.42 ± 0.43	8.21 ± 1.75	9.03 ± 0.51
Q3 =	11.02 ± 0.53	13.03 ± 0.73	2.59 ± 0.41	3.41 ± 0.58	8.43 ± 0.63	9.63 ± 0.62
Q4 =	11.46 ± 0.95	12.54 ± 0.89	2.68 ± 0.45	3.43 ± 0.59	8.78 ± 0.69	9.11 ± 0.89
ALL =	11.39 ± 0.80	12.70 ± 0.69	2.92 ± 0.45	3.49 ± 0.50	8.48 ± 0.75	9.22 ± 0.68
ANOVA p-value =	0.367	0.244	< 0.001	0.577	0.408	0.175

Bonferroni correction

	Women p-value	Men p-value
Ankle	Q1 Q2 Q3 Q2 0.371 Q3 0.343 1.000 Q4 ≤0.001 0.003 0.003	Q1 Q2 Q3 Q2 0.013 Q3 0.002 1.000 Q4 ≤0.001 0.002 0.017
Calf	Q1 Q2 Q3 Q2 0.169 Q3 0.014 1.000 Q4 ≤0.001 0.001 ≤0.001	Q1 Q2 Q3 Q2 0.003 Q3 ≤0.001 0.295 Q4 ≤0.001 ≤0.001 0.023
Knee	Q1 Q2 Q3 Q2 0.068 Q3 0.022 1.000 Q4 ≤0.001 ≤0.001 ≤0.001	Q1 Q2 Q3 Q2 ≤0.001 Q3 ≤0.001 0.269 Q4 ≤0.001 0.006 0.992
	Women p-value	Men p-value
Knee to Ankle	NO STATISTICAL DIFFERENCE	NO STATISTICAL DIFFERENCE
Knee to Calf	Q1 Q2 Q3 Q2 1.00 Q3 0.007 0.002 Q4 0.034 0.012 1.000	NO STATISTICAL DIFFERENCE
Ankle to Calf	NO STATISTICAL DIFFERENCE	NO STATISTICAL DIFFERENCE

Figure 2.3: **ANOVA and descriptive results:** Leg circumferences and lengths grouped by BMI.

The subsequent ANOVA results show that grouping by (1) height and (3) ankle-to-knee length did not produce any discrete circumferential sizes between quartiles for either men and women. Conversely, grouping by (2) weight, (4) ankle circumference, (5) calf circumference, and (6) knee circumference all produced at least one discrete size between quartiles for both men and women within all three circumferences. Of the dimensions that do organize the sample group into discrete circumferential sizes/groups, (4) ankle circumference produced the largest number and most consistent groups of discrete sizes. See Figure 2.4 for results.

2.4.4 Alternate Predictors: Length

An ANOVA was conducted to determine if organizing the CAESAR sample into groups based on BMI would produce sizes with discrete lengths (i.e. knee-to-ankle, knee-to-calf, ankle-to-calf). The ANOVA results (see Figure 2.3) show that grouping by BMI does not form discrete quartiles for the length dimension, with the exception being the knee-to-calf length in females. Consequently, the same data was reshuffled by other potential predictive

Bonferroni correction | Ankle

	Women p-value			Men p-value		
Ankle	Q1	Q2	Q3	Q1	Q2	Q3
Q2	0.049			<0.001		
Q3	0.006	1.000		<0.001	0.001	
Q4	<0.001	<0.001	<0.001	<0.001	<0.001	<0.001
Calf	Q1	Q2	Q3	Q1	Q2	Q3
Q2	0.052			<0.001		
Q3	<0.001	0.076		<0.001	1.000	
Q4	<0.001	<0.001	<0.001	<0.001	0.007	0.024
Knee	Q1	Q2	Q3	Q1	Q2	Q3
Q2	0.054			0.011		
Q3	0.001	1.000		<0.001	1.000	
Q4	<0.001	<0.001	<0.001	<0.001	0.004	0.137

Bonferroni correction | Knee-to-Ankle

	Women p-value			Men p-value		
Knee to Ankle	Q1	Q2	Q3	Q1	Q2	Q3
Q2	0.001			<0.001		
Q3	<0.001	0.003		<0.001	0.009	
Q4	<0.001	<0.001	<0.001	<0.001	<0.001	<0.001
Knee to Calf	NO STATISTICAL DIFFERENCE			NO STATISTICAL DIFFERENCE		
Ankle to Calf	Q1	Q2	Q3	Q1	Q2	Q3
Q2	0.045			0.222		
Q3	0.007	1.000		0.003	0.607	
Q4	<0.001	0.001	0.004	<0.001	0.021	0.944

Figure 2.4: **Post-hoc Bonferroni correction:** (left) Best dimension to organize leg circumferences into discrete groups (ankle circumference); (right) Best dimension to organize leg lengths into discrete groups (knee-to-ankle length).

dimensions (i.e. (1) height, (2) weight, (3) ankle-to-knee length, (4) ankle circumference and the ANOVA was repeated. The subsequent ANOVA results show that arranging by (1) height and (3) ankle-to-knee length do produce at least one discrete size between quartiles for both men and women within all three circumferences, while dimensions 2, 4, 5, and 6 do not. Of the dimensions that do organize the sample group into discrete circumferential sizes/groups, (3) ankle-to-knee length produced the largest number of and most consistent groups of discrete sizes. See Figure 2.4.

2.5 Discussion

2.5.1 Anthropometric Variability: Circumference

The data suggest that men have larger average lower leg circumferences than women and would require generally larger lower leg garments. Additionally, the results imply that male and female groups have different amounts of variability at different points along the leg, suggesting slightly different shapes in addition to scales. At the knee, for example, the range was larger for women than men with and without the outlier data, however, men had greater ranges of ankle and calf circumferences than women when the outlier was removed. The greatest amount of variability for both men and women was observed at the calf, while the ankle fluctuated the least in male and female populations, suggesting the ankle is less

susceptible to fluctuations in response to weight gain or muscle development. Consequently, less circumferential variability may be required at the ankle and more variability may be required at the calf when developing a garment sizing system.

2.5.2 Anthropometric Variability: Length

The range in length from below the knee to the ankle for men and women is similar, however, men have a larger average length. While knee-to-ankle length is only dependent on bone length, the positioning of the calf apex is dependent on gastrocnemius muscle development/placement along the leg. The results suggest that the range of possible calf apex locations is similar for males and females; consequently, we suspect similar trends in gastrocnemius muscle location.

2.5.3 Alternative Predictors: Circumference

The results of the ANOVA and the pairwise comparison using t-tests adjusted with the Bonferroni method suggest that the circumference of the ankle is a key dimension for organizing the population in order of increasing lower leg circumferences (i.e. calf, knee). More research is required to understand anatomically why the ankle is better at organizing the population than other limb circumferences; however, here we are hypothesizing that for every ankle circumference (a bony leg cross section) there is a relatively narrow range of potential growth of the gastrocnemius muscle, which affects the circumferences of both the calf and knee (because the knee circumference is taken below the patella).

To test the statistical results and determine if organizing by ankle circumference could produce discrete sizes, we plotted actual ankle, calf, and knee circumferences (in) and highlighted the range (in) of dimensional variation for each quartile (Figure 2.5). Additionally, we calculated the percent difference between the smallest and largest circumferences in each size/sub-group. Because no statistical difference was detected between Q2 and Q3, we combined Q2 and Q3 and depicted the three new quartiles: Q1 (size small), Q2-Q3 (size medium), and Q4 (size large). Because the sample group of women contained one outlier that skewed the data, we represented the two leg dimensions for that individual with asterisks. Figure 2.5 shows that organizing the sample group by groups/sizes that are statistically different still results in size overlap, suggesting that the dimensional variability in the population is highly complex.

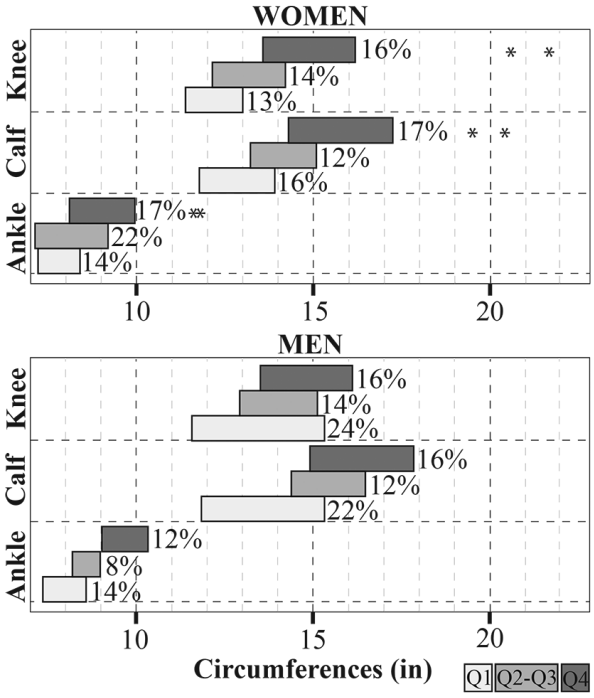

Figure 2.5: **Circumferential variability (in) and percent difference organized by ankle circumference:** (top) women, (center) men.

2.5.4 Alternative Predictors: Length

The results of the ANOVA and the pairwise comparisons suggest that the length between the ankle and the knee is a key dimension for organizing the population in order of increasing leg lengths; however, the dimension only forms discrete groups for itself and for ankle-to-calf length (see Figure 2.4). Because we cannot group the population by two different dimensions at once, we determined that grouping by ankle circumference would produce a sizing system that best meets the functional requirements of our advanced functional garment: SMA-CG. Consequently, we plotted possible length variability within each size group determined in Figure 2.5, still organized by ankle circumference.

Figure 2.7 shows the range of possible length fluctuation for the calf apex and the ankle if the advanced functional garment (i.e. SMA-CG) were placed just below the knee on a human leg. Figure 2.7 suggests that there is a relatively small amount of dimensional fluctuation of both points, and the amount of fluctuation remains consistent across quartiles/sizes for both males and females; exceptions are: (1) the potential fluctuation of calf apexes for Q1 women is smaller than the other groups, and (2) the potential fluctuation of total leg length

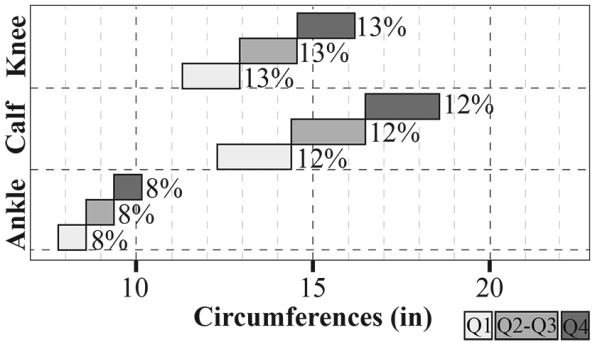

Figure 2.6: **Ideal single-predictor sizing system:** circumferential variability (in) and percent difference.

is smaller for Q1 men than in other groups. Generally, the potential fluctuation of total leg length is larger than the potential fluctuation of calf apex for both men and women in all size groups.

2.6 Conclusions & Future Work

2.6.1 Sizing Strategies for Advanced Functional Garments

To accommodate the anthropometric variability of the North American civilian population, all methods for garment sizing require areas of adjustability (or adjustable dimensions) to prevent the need for an unreasonable number of sizes. Here, we present several sizing strategies and their feasibility.

A one-size-fits-all garment could be manufactured with a wide range of build-in adjustability in the length and width direction; however, this garment would be challenging for the consumer to manipulate, particularly for non-stretch garments. Alternatively, several size options could be made for male and females (e.g. S, M, L men; S, M, L women) with limited, build-in length and circumferential adjustability; however, multi-directional adjustability is still challenging for the general public.

A third alternative is to develop a small size run of garments for men and women, each size with a different, fixed length and limited range of adjustable circumference. The inverse would be to develop a small size run, each size with a different fixed circumference and a limited range of adjustable length. Because circumference is the critical dimension for the functionality of SMA-CG, an adjustable circumference and several fixed lengths would be preferred. We recommend that future researchers take a graded sizing approach

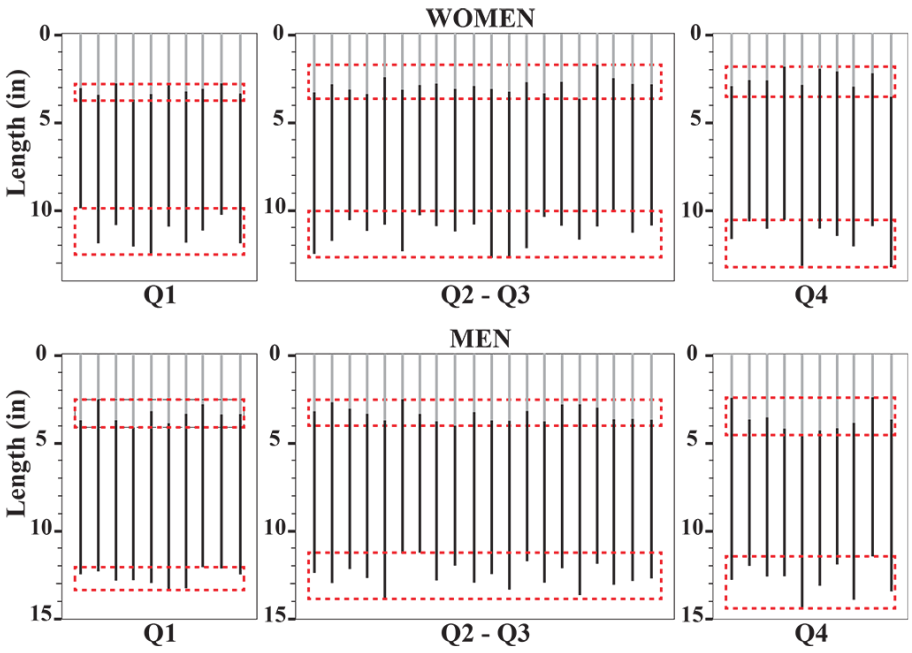

Figure 2.7: **Length variability (in).**

to non-critical dimensions and adjustability approach to dimensions critical for garment functionality. A researchers knowledge of the garments intended function determines the appropriate application of methods.

2.6.2 Design Strategies for Advanced Functional Garments

Methods for Adjustability

To achieve the sizing systems outlined above, methods of adjustability should be considered. Traditional methods of adjustability for non-stretch garments rely heavily on fastening systems. While these methods are native to cut-and-sew manufacturing, familiar to the consumer, inexpensive, and easy to clean with traditional washing methods, discrete fasteners like hooks and eyes and snaps can only be adjusted in steps, are cumbersome to adjust in large amounts, and require strength and/or user dexterity.

Hook and loop tape is a common alternative in medical garments. It is quick to adjust, familiar to the consumer, inexpensive and easy to manufacture, provides continuous adjustability, and can be washed; however, excess material can create stiffness and large overlap, hook tape can scratch and snag surrounding objects, durability and noise can be a

problem, and fine-tuned fit is difficult to achieve.

Lacing can also accommodate a wide range of adjustability. Lacing is familiar to consumers (e.g. athletic shoes), inexpensive, easy to manufacture, provides continuous adjustability, and is easy to clean with traditional washing methods. On the down side, excess lacing can be cumbersome to manage and tensioning can be imprecise.

Ratcheting systems provide an alternative to lacing that maintains the benefits without the excess material or time consuming process. Ratcheting systems (e.g. Boa) provide a quick and precise method for tensioning garments; however, ratcheting systems can be bulky, unfamiliar to consumers, foreign to traditional cut-and-sew manufacturing methods, and difficult to clean through traditional washing.

Managing Adjustability

These methods of adjustability can be manipulated precisely by the wearer to ensure proper fit through various cues. Traditional visual cues (e.g. numbers, notches) are easy for the wearer to follow, low-tech, inexpensive, easy to accomplish through traditional manufacturing, and can be easily washed; however, they require that the wearer premeasure their own body dimensions, which can be time consuming and error-prone. Tension / pressure switches are an alternative that are also easy for the wearer to follow and set correctly without premeasuring; however, electronics add bulk, require a power source, require modification to traditional manufacturing, and can be difficult to wash. Additionally, integrated pressure sensing has many of the same pros and cons as electronic switches. Future researchers should evaluate the pros and cons for each adjustability method and management style appropriate for their wearable application.

2.7 Supplemental Analysis

While the previous analysis reveals challenges to garment population sizing with narrow fit tolerances and design strategies are presented to maneuver around these challenges, the conference manuscript does not present a sizing table for the lower body. This supplemental analysis walks through the process of developing a size chart for the lower leg through supplemental statistical analysis. The purpose of developing this sizing chart is to illuminate the multiplicity of sizes that would be required to accomplish a close-fitting, stiff garment for the North American consumer population without broad, bidirectional adjustability.

2.7.1 Data Source: SizeUSA

SizeUSA served as the data source for this analysis. Access to SizeUSA was acquired subsequent to the original study and provided a larger source of data for the analysis without requiring 3D data extraction. The anthropometric database consists of a spreadsheet of 318 body measurements from 10612 subjects ($N_{female} = 6814$; $N_{male} = 3798$) taken in 2004 with measuring tapes and calipers. Figure 2.8 and Table 2.1 display the dimensions used from SizeUSA. Dimensions 1, 2, 3, and 6 use the same anatomical landmarkers used in the prior CAESAR study, while dimensions 4 and 5 extend to the knee, not the low-knee because the low-knee was not included in the SizeUSA dataset. Ankle girth (7) and knee girth (8) were also included to lay groundwork for a future, lower-body sizing system that extends from the waist to the feet. While left and right legs were used as their own data points in the CAESAR study, this sizing system was build on data from the right leg only to ensure consistent correlation analysis.

Table 2.1: **Comparison of Dimensions used in prior CAESAR study and subsequent SizeUSA study:** Numbers 1-8 correspond with Figure 2.8 [1, 2].

SizeUSA		**CAESAR**	
1	=	1	low-knee girth
2	=	2	calf girth
3	=	3	min-leg girth
4	min-leg-to-knee length	4	min-leg-to-low-knee length
5	calf-to-knee length	5	calf-to-low-knee length
6	=	6	min-leg-to-calf length
7	ankle girth		
8	knee girth		

2.7.2 Sizing System Approaches: Direct, Indirect, and Direct-Indirect

There are three primary methods used to develop sizing systems for wearables. The indirect method uses gross dimensions, commonly stature and weight, while the direct method is based upon key body dimensions to ensure fit at those locations is prioritized [3]. The direct-indirect method is a hybrid of the two approaches and includes both gross and key dimensions in the analysis [3]. The chosen method is highly dependent on the nature of the design, such as desired wearing ease, allowable fit tolerance, fabric properties, and

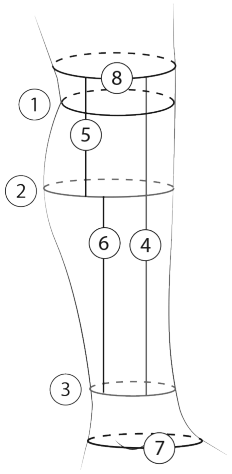

Figure 2.8: **SizeUSA Dimensions:** (1) Low-knee girth, (2) calf girth, (3) minimum-leg girth, ankle girth, (4) minimum-leg-to-knee length, (5) calf-to-knee length, (6) minimum-leg-to-calf length, (7) ankle girth, (8) knee girth were used to data analysis.

percentage of the population accommodated. The lower-body garment requirements for this analysis are defined as followed: (1) 0 cm $\leq$ wearing ease $\leq$ 3 cm, (2) 0 cm $\leq$ fit tolerance $\leq$ 3 cm, (3) high-tension (stiff) fabric, and (4) $\geq$ 95% of the North American consumer population is covered by the size range.

2.7.3 Key Dimensions

At least two direct dimensions are required in the development of a sizing system when small wearing ease, or a close fit is desired. The inclusion of these direct dimensions in the size system prioritize areas where accurate fit is required (e.g. pant waist girth) at the expense of less fit-sensitive regions (e.g. pant knee girth). Previous CAESAR analysis revealed that organizing the North American consumer population into groups of increasing ankle circumference also produces groups of increasing calf and knee circumferences [2]. Alternatively, groups of increasing ankle-to-knee length also produces groups of increasing ankle-to-calf and calf-to-knee lengths [2]. Because both dimensions are critical (and proven to be central) to fit for a conformal, lower-leg garment, ankle circumference and ankle-to-knee length were identified as key, or independent dimensions and served as two direct dimensions for a lower leg sizing system.

Sizing systems that incorporate three dimensions into the analysis have been found to better meet population fit requirements [3]; therefore, a third dimension was sought. While

stature is a common, indirect dimension added to sizing analyses [3], statistical analysis revealed a weak correlation with leg lengths ($r_{thigh-length\&stature} = 0.56$; $r_{ankle-to-calf\&stature} = 0.28$; $r_{calf-to-knee\&stature} = 0.41$) [1]. The breadth of the calf would provide valuable information on the shape of the lower leg garment for garment patterning purposes; however, this dimension was not included in the SizeUSA database. Calf circumference was included in the SizeUSA database and it commonly used as a key dimension for sizing commercial CGs (e.g. Jobst, Medivan, Juzo, Sigvartis) [33]. Consequently, the calf circumference was deemed a valuable contribution to the sizing parameters and was added to the pool of key/independent dimensions used to develop the direct-approach sizing system.

2.7.4 Base Size Dimensions

Summary statistics were calculated for dimensions 1-8 (Figure 2.8. Statistically significant outliers were identified (Q1 - 1.5*IQR; Q3 + 1.5*IQR) and removed from all datasets. The adjusted mean dimensions serve as the 'base' dimensions for the sizing system. See Table 2.2.

Table 2.2: **Sizing System Base Dimensions:** SizeUSA, mean dimensions - statistical outliers [1].

WOMEN		**MEN**	
min-leg girth [cm]	22.77	min-leg girth [cm]	23.87
calf girth [cm]	37.81	calf girth [cm]	38.88
min-leg-to-knee length [cm]	33.28	min-leg-to-knee length [cm]	35.76
ankle girth [cm]	22.80	ankle girth [cm]	27.46
low-knee girth [cm]	36.17	low-knee girth [cm]	36.90
knee girth [cm]	38.73	knee girth [cm]	39.52
min-leg-to-calf length [cm]	38.2	min-leg-to-calf length [cm]	22.41
calf-to-knee length [cm]	11.3	calf-to-knee length [cm]	13.36

2.7.5 Grading

Grading is the process of shifting key/independent and dependent dimensions to make larger and smaller sizes from base dimensions. In a direct-approach sizing system, key/independent dimensions are graded up and down in predetermined size intervals that define garment size categories. The dimensional change in dependent dimensions between size categories

is determined through regression equations. The follow sections outline the process for grading a conformal, low-leg garment.

Key Size Intervals

The size interval, or the standard number by which the mean of the key dimensions are increased and decreased to make smaller and larger sizes, determines the number of sizes in the sizing system. Small size intervals produces a larger number of sizes while large size intervals produce a small number of sizes. While a small size interval (e.g. ± 3 cm) produces a closer fit, the number of sizes required to accommodate the population may be financially and/or logistically unreasonable for manufacturers and retailers [3]. Alternatively, a large size interval (e.g. ± 8 cm) must have large fit tolerances (e.g. women's tunic) to fit a larger portion of the population in just a few sizes, such as small, medium, and large. Because the goal of this research is to develop a sizing system for a snugly-fit leg garment without compliance, a conservative size interval of ± 3 cm was chosen.

Multiple Regression for Dependent Size Intervals

While the key/independent dimensions ((3) min-leg girth, (2) calf girth, (4) min-leg-to-knee length) consistently increase and decrease from the mean in increments of 3 cm, the dependent dimensions (i.e. 1, 5, 6, 7, 8) do not necessarily follow suit. The magnitude and direction that each dependent dimension shift with a 3 cm increase or decrease of each key/independent dimension can be determined through multiple regression equations. Below is a standard multiple regression equation for three independent variables,

$$Y = \beta_0 x_0 + \beta_1 x_1 + \beta_2 x_2 + k \tag{2.1}$$

where Y is any one of the dependent garment dimensions, $\beta_{0,1,2,\ldots n}$ are the regression coefficients, $x_{0,1,2,\ldots n}$ are the independent variable dimensions, and k is the constant, or intercept. To tailor the equation to our variables,

$$Y = \beta_A A + \beta_C C + \beta_L L + k \tag{2.2}$$

A replaces x_0 as the minimum leg girth [cm], C replaces x_1 as the calf girth [cm], and L replaces x_2 as minimum-leg-to-knee length [cm]. The regression equations that result from each dependent dimensions (y-value) and three independent dimensions (x-values) are displayed in Table 2.3.

Table 2.3: **Regression Equations for Dependent Variables** [3]

WOMEN	
ankle girth	$Y = +0.869A + 0.087C - 0.027L + 3.303$
low knee girth	$Y = +0.486A + 0.642C - 0.003L + 1.028$
knee girth	$Y = +0.513A + 0.571C + 0.114L + 1.753$
min-leg-to-calf height	$Y = +0.098A + 0.098C + 0.590L - 3.392$
calf-to-knee height	$Y = -0.098A - 0.098C + 0.410L + 3.392$
MEN	
ankle girth	$Y = +0.849A + 0.015C + 0.086L + 3.749$
low knee girth	$Y = +0.327A + 0.655C + 0.012L + 3.207$
knee girth	$Y = +0.471A + 0.480C + 0.137L + 4.744$
min-leg-to-calf height	$Y = -0.029A + 0.010C + 0.634L + 0.172$
calf-to-knee height	$Y = +0.019A - 0.010C + 0.366L - 0.172$

Consequently, the change in magnitude and direction of each dependent dimension (ΔY) in response to an increase of decrease of independent dimensions A, C, and L is the result of Equations 2.3, 2.4, and 2.5 below,

$$\Delta Y = Y_{A+3} - Y_{base} \tag{2.3}$$

$$\Delta Y = Y_{C+3} - Y_{base} \tag{2.4}$$

$$\Delta Y = Y_{L+3} - Y_{base} \tag{2.5}$$

where Y_{base} is the results of the equations in Table 2.3 with base, or mean dimensions for values A, C, and L and Y_{A+3}, Y_{C+3}, and Y_{L+3} are the results of the same equations with a 3 cm increase of mean dimensions for A, C, or L. Table 2.4 presents the results of the analysis and provide concrete increments for grading or a conformal, low-leg garment.

2.7.6 Population Coverage

To accommodate 95% of the North American consumer population, represented by SizeUSA, a three-dimensional correlation scatterplot was generated to determine the spread and variability of key/independent dimension for men and women [1]. See Figure 2.9. Additionally, the frequency of each key/independent dimension was plotted independently. See Figs. 2.10 and 2.11, which depict the dimensions centered around the mean (*) spread outward in bins

Table 2.4: **Incremental Change in Dependent Dimensions Across Size Intervals:** Refer to Table 2.3 and Equations 2.3, 2.4, and 2.5 for explanation of values.

WOMEN	A	C	L
ankle girth	+2.61	+0.26	−0.08
low-knee girth	+1.46	+1.93	−0.01
knee girth	+1.54	+1.71	+0.34
min-leg-to-calf height	+0.29	+0.29	+1.77
calf-to-knee height	−0.29	−0.29	+1.23
MEN			
ankle girth	+2.55	+0.04	+0.26
low-knee girth	+0.98	+1.97	+0.04
knee girth	+1.41	+1.44	+0.41
min-leg-to-calf height	−0.09	+0.03	+1.90
calf-to-knee height	+0.06	−0.03	+1.01

of 3 cm to represent size intervals. The number of bins in each plot represent the number of sizes required to fit the entire population in that dimension. Figs 2.10 and 2.11 reveal that the majority of men and women can be accommodated in 4-5 sizes if only the minimum leg girth were used to construct the sizing system; however, the length measurement requires up to 7 additional sizes and the calf girth requires up to 9 sizes. To maintain fit in all three key/independent dimensions across the full population could require up to 135-315 uniquely sized garments for women and men.

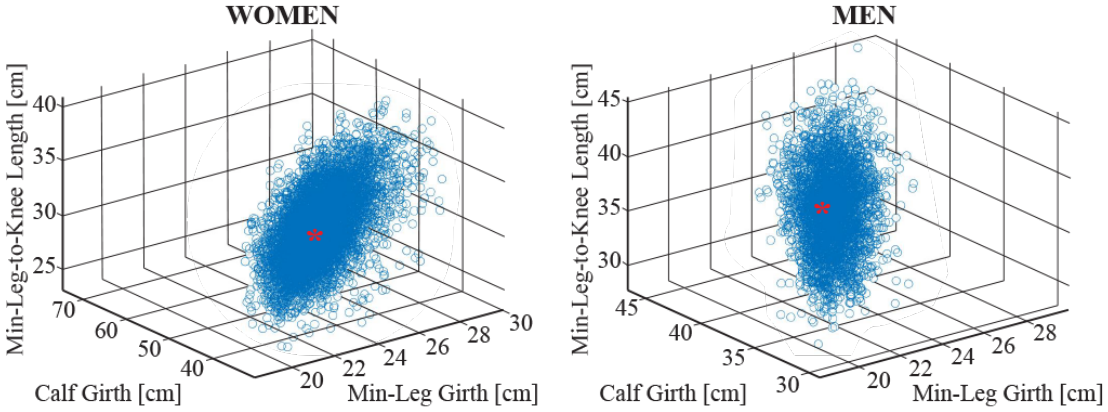

Figure 2.9: **Three-Dimensional Correlation of Key/Independent Dimensions:** (left) women, (right) men with the overlapping mean of the three dimensions represented by *.

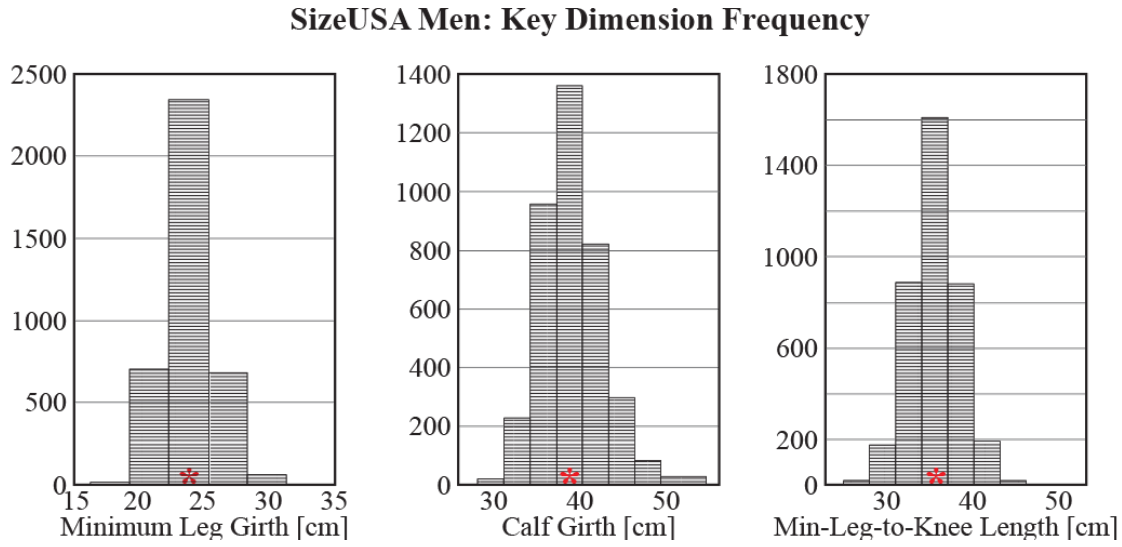

Figure 2.10: **SizeUSA Men, Key Dimension Frequency:** Population dimensions are centered around the mean (*) and arranged in bins of 3 cm intervals.

2.7.7 Sizing System(s)

The number of sizes required in the sizing system were evaluated further by plotting the percentage of the population that falls within each size category for each of the three key dimensions. Because calf circumference is the most variable dimension of the three, this dimension was evaluated independently and the minimum leg girth and minimum leg-to-knee length where evaluated together. Table 2.5 presents the (1) minimum leg girth and (2) minimum leg-to-knee length together. Additionally, the data in Table 2.5 was cropped to approximately 95% of the population to accommodate the largest portion of the group with the fewest number of size categories. The percent of the full population that fit within each size category is listed in each size bin. The result is a system of 13 sizes for women and 14 sizes for men that cover 95% and 97% of the respective population.

Table 2.6 presents an analysis of the calf circumference only for men and women. The table shows that 8 additional sizes are required to maintain fit in the calf for women, making the number of unique sizes increase from 13 to 104. Additionally, Table 2.6 shows that 8 additional sizes are required to maintain calf fit for men, increasing the number of unique sizes required from 14 to 112.

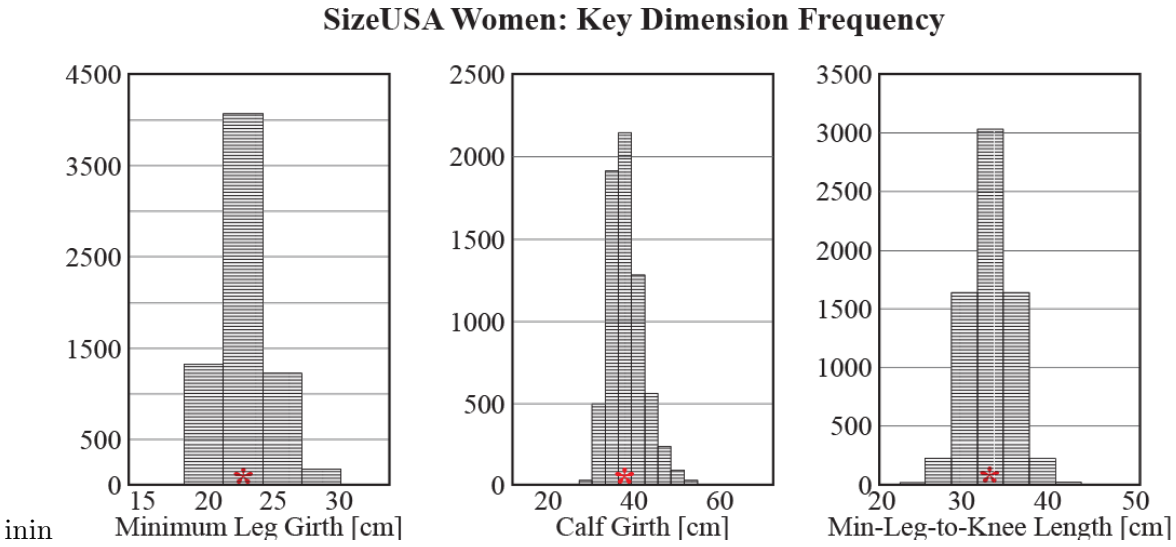

inin

Figure 2.11: **SizeUSA Women, Key Dimension Frequency:** Population dimensions are centered around the mean (*) and arranged in bins of 3 cm intervals.

2.7.8 Discussion & Future work

The sizing system presented in Table 2.5 and Table 2.6 is the first known effort to size and grade a non-compliant, form-fitting garment for the lower leg. Commercially available garments rely on positive ease, fabric compliance, and/or adjustability to accomplish fit, methods that are not appropriate solutions for advanced functional garments that require stiffness and accurate fit. While the logistics of designing, manufacturing, and distributing garments in 104-112 sizes would be challenging, Chapter 4 presents new self-fitting, self-stiffening fabrics that could simplify the challenges presented here.

Table 2.5: **Simplified Sizing System for Leg Garment:** The percentage of the full population that would be accommodated by each length-girth combination in listed in each size bin. Not listed are the 8 additional sub-sizes that are required in each bin to ensure fit in all three key dimensions.

WOMEN						
min-leg-to-knee length [cm]		**26-29**	**29-32**	**32-35**	**35-38**	**38-41**
min-leg girth [cm]	**18-21**	1%	7%	9%	2%	0%
	21-24	2%	14%	27%	15%	2%
	24-27	0%	3%	7%	6%	1%
MEN						
min-leg-to-knee length [cm]		**28-31**	**31-34**	**34-37**	**37-40**	**40-43**
min-leg girth [cm]	**19-22**	1%	6%	7%	3%	0%
	22-25	2%	14%	28%	14%	3%
	25-28	1%	3%	7%	5%	1%

Table 2.6: **Additional Calf Sizes Required to Achieve Population Fit in All Three Key Dimensions:** 8 additional sub-sizes that are required in Table 2.5 to ensure fit in all three key dimensions and the percentage of the population that falls within each size interval.

WOMEN									
calf cir. [cm]	**24-27**	**27-30**	**30-33**	**33-36**	**36-39**	**39-42**	**42-45**	**45-48**	**48-51**
	0%	1%	8%	28%	32%	18%	8%	3%	1%
MEN									
calf cir. [cm]	**25-28**	**28-31**	**31-34**	**34-37**	**37-40**	**40-43**	**43-46**	**46-49**	**49-52**
	0%	1%	7%	26%	36%	21%	7%	2%	1%

Chapter 3

Dynamic Anthropometrics & Sizing for the Lower Body

The following chapter was written for and presented at the 47th International Conference on Environmental Systems in Charleston, South Carolina in 2017 [21]. While the original conference manuscript was written specifically for aerospace applications, passages have been altered to make the text more applicable to other applications.

3.1 Introduction

Medical compression garments (CGs) are worn to treat a variety of health conditions (e.g. cardiovascular, lymphatic, anxiety); therefore, the users groups who interact with these garments are diverse. Some users wear CGs in stationary situations, like bedrest where deep vein thrombosis (DVT) is a concern or during prologued periods of orthostasis. In these instances, proper fit is only required in the one position that the user assumes. Other user groups require compression during periods of activity, like young, active females with postural orthostatic tachycardia syndrome (POTS) or elder adults who experience orthostatic hypotension (OH) upon standing. While pneumatic garments are an option for the former group, inflatable systems are not always appropriate for wearable applications that require mobility due to their large form factor. Undersized CGs are lower profile garments and, thus, enable enhanced mobility; however, these garments are only designed from one set of body dimensions. The repercussion of this one-dimensional design choice is that the CG fits differently as the body changes position and relation to gravity (e.g. standing,

sitting, supine). Because medical pressure is dependent on fit (i.e. the relation of garment dimensions to body dimensions) the patient will receive variable pressure - some not enough to provide effective treatment and some enough to tourniquet the limb.

The following study is centered around the mobility concern for a particular user group - astronauts - who require CGs to prevent orthostatic intolerance (OI) symptoms during reentry, landing, and egress post-space mission. The particular types of garments worn in this instance are referred to as orthostatic intolerance garments (OIG) and are designed through both inflatable (NASA's antigravity suit (AGS)) and undersized methods (Roscosmos's kentavr). The primary goal of these garments is to apply enough pressure to the lower body to maintain mean arterial pressure and ensure enough blood reaches the brain so that the astronaut remains alert during the landing sequence; however, the garment must also allow the astronaut to perform an emergency evacuation if the situation were to arise. While this study presents an extreme example of the need for CGs to maintain consistent medical pressure between postures, the study is relevant to all CGs applications where mobility or multiple working postures is required.

To quantify body variability due to posture change, anthropometrics from 1264 North American women were gathered from the Civilian American & European Surface Anthropometry Resource (CAESAR) database. Women were the ideal subject for this study because women are five times more likely than men to experience OI symptoms post-spaceflight [34]. Four circumferential measurements were collected from a sample of the CAESAR population (n=80) at the ankle, calf, knee, and thigh. A paired t-test was conducted to determine the difference between standing and sitting mean circumferences for each region of the leg. Descriptive statistics were calculated to determine the range of percentage change within the sample statistics. The study concludes that the ankle increases consistently between 0 and 8% for all quartiles and the calf increases consistently between 0 and 6% for all quartiles. The knee was also found to increase in circumference between sitting and standing postures; however, the variable results suggest further research is required. The thigh was found to increase or decrease between postures, suggesting a CAESAR measurement error or physical behavior that is not fully understood. The fundamental value of this anthropometric research is the quantification of postural variability, data which can then be used to design CGs for scenarios where movement is expected (e.g. OIGs).

3.1.1 Research Purpose

For this research, we seek to define the dynamic garment-body relationship, also known as fit, by conducting an evaluation of anthropometric variability and movement-induced dimensional change of the lower body. The study is based around the fact that lower body radii are not fixed dimensions - but rather dynamic dimensions dependent on body posture, composition, and topography. Furthermore, functional pressures exerted on the body are unpredictable if the CG is designed from a series of measurements from a standing posture, yet the garment is used while the user assumes several postures (i.e. seated reentry, standing egress). This shortcoming of undersized CG designs has been found in prior studies evaluating the effectiveness of medical-grade elastic stockings [14, 6, 15]. As shown in Figure 3.1, Wildin et al. found that three medical CGs far exceed the medically recommended pressure range at the knee (labeled popliteal) when the wearer assumes a seated posture [6]. Similar findings were reported by Liu et al. [14, 15].

While this research is applicable to all CG designs, we will focus this analysis on the dimensional change that occurs only in the lower body - the region that directly interacts with the OIG. Consequently, we will explore body variability and dimensional change due to posture in a standing and a seated posture - the seated posture being the astronauts working position maintained during takeoff and landing and the standing position being the original posture assumed when the OIG is donned and the potential posture assumed if the astronaut is required to get out of their seat for an emergency egress.[10]

The aim of this study is to define and quantify body variability to inform the design and development of future OIG technologies. While there are many characteristics of the body that confound uniform and predictable pressure output while wearing undersized CGs, the most critical to the success of OIGs are dimensional changes in leg radii due to postural changes because pressure spikes and tourniquetting can occur, as shown in Figure 3.1.

3.1.2 Population

The literature states 83% of astronauts who return from long duration missions lasting over one month experience cardiovascular deconditioning while in microgravity conditions [35]. Consequently, there is an 83% chance that all astronauts returning from a one month or longer mission have experienced a range of physiological changes that could impact their health during reentry and landing on Earth. Additionally, women are five times more likely to experience OI after exposure to microgravity conditions[34]; therefore, female

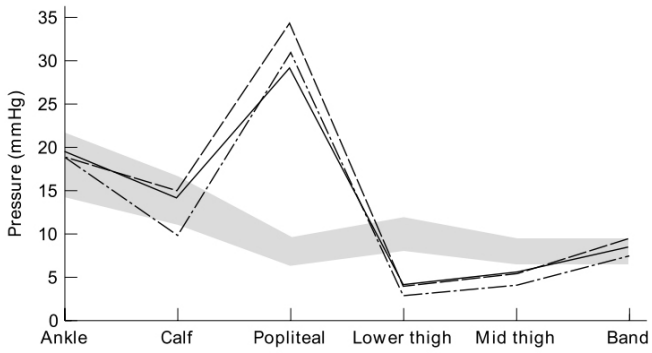

Pressure (mmHg)

Biersdorf	19·3 (14–28·3)	14·3 (9–21)	28·7 (17–89)	4·3 (1·7–8·3)	5·7 (4–7·3)	8·3 (6·7–10·7)
Kendall	19 (10·7–25·3)	10 (6–14·3)	30·3 (8–80·3)	3 (2–6)	4 (2.3–5·3)	7·3 (5·3–12·7)
Brevet	18·7 (12–30·7)	15 (10–18·3)	33·7 (15–100)	4 (3·3–7)	5·3 (4·7–7)	9·3 (8–12·3)

Fig. 4 Median pressure profile in the sitting position with the knee flexed to 90° for Biersdorf (———), Kendall (—·—·) and Brevet (— — —) stockings. The shaded area represents the ± 20 per cent ideal. Values in the panel below are median (interquartile range)

Figure 3.1: **Median pressure profile in the sitting position with the knees flexed at 90 degrees wearing various knit compression stockings.** The shaded region represents the ± 20 per cent ideal. Wildin et al. (1998)[6]

anthropometrics will be the focus of this research. While the cause of heightened female OI is not clear, studies posit that the gender differentiation in orthostatic tolerance could be due to a number of factors, notably a lower center of mass [34, 36] and lower vascular resistance and mean arterial pressure [37, 38] due to a vasodilatory response to estrogen.[36, 39, 40]

3.1.3 Research Questions & Goals

The goal of this study is to quantify movement-induced circumferential dimensional change in the lower body of female astronauts to inform future OIG designs. The primary research questions in this investigation are as follows:

1. What is the mean change in circumference for the ankle, calf, knee, and thigh between a standing and a seated posture for women representative of the female astronaut corps?
2. What is the range of circumferential dimensional change for the ankle, calf, knee, and thigh due to the transition between a standing and a seated posture for women representative of the female astronaut corps?

By evaluating body variability and dimensional fluctuation, we aim to illuminate the complexity of the human form in relation to CGs (i.e. OIGs) and offer quantified data that

could be incorporated into the design process of future OIG designs and technologies.

3.2 Methods

To quantify and evaluate female lower body postural variability, we sought a large database of female anthropometrics to lay the groundworks for this study. The Civilian American & European Surface Anthropometry Resource (CAESAR) contains a collection of individual 3-D body scans ($N_{Women} = 1264$) from which we could extract relevant metrics. To provide structure to our analysis, positive covariance was established between key limb circumferences and a general body measurement (such as, height, weight, or body mass index (BMI)) so that the analysis could be organized around incrementally increasing body dimensions similar to the framework of an apparel size system. A sample of the population ($n = 80$) was randomly selected from the database and five circumferential measurements (ankle, calf, knee, and thigh) were extracted from the 80 body scans. The aim of the anthropometric methodology was to gather sufficient raw data to fully investigate the dimensional variability due to posture within the female population.

3.2.1 Data Source: CAESAR

The Civilian American & European Surface Anthropometry Resource (CAESAR) database was the only available anthropometric database that was appropriate for this study. While the ideal population for this study are military women, anthropometric databases with the dimensions of military personnel (e.g. ANSUR, NASA Anthropometric Sourcebook) do not contain lower body circumferences in the standing and sitting position for women within the same population. Size USA is another large database of civilian measurements that can be easily evaluated statistically; however, Size USA does not include data for subjects in multiple postures - only standing. Consequently, CAESAR was the best source for raw anthropometric data of a consistent female population.

Anthropometrics from 1264 North American women (age 39.82 $\pm$12.12 years, weight 67.81 $\pm$17.10 kg, height 1648 $\pm$76.98 mm; means $\pm$ SD) were gathered from the CAESAR database. CAESAR contains 3-dimensional body scans of men and women in both standing and seated postures taken from the years 1998 to 2000. The database of 3-D scans was accompanied by a spreadsheet that contained 40 additional anthropometric measurements gathered by traditional means (e.g. tape measure and calipers). This study used certain

measurements directly from the CAESAR spreadsheet, like height, weight, thigh circumference, and ankle circumference, and the remaining measurements were extracted from the original surface scans, as specified in the following section on data collection.

3.2.2 Covariance

Limited metrics for the entire population were available in the accompanying CAESAR spreadsheet and only two leg circumference measurement were included - thigh and ankle; therefore, the first step in our methodology was to determine a predictive measurement that would positively correlate with all leg circumferences. Determining a predictive variable that positively correlated with both ankle and thigh circumferences allowed the population to be analyzed in incrementally increasing leg circumferences without having all circumferences for the full population available. Additionally, the two circumference points on the leg were an accurate representation of leg variability; the ankle provided a sample bony joint and the thigh provided a sample soft non-joint. From this analysis of covariance, we can assume that the calf and knee (dimensions not readily available for the entire population) would follow similar relational trends.

Fig 3.2 presents two leg circumferences (ankle and thigh) plotted for correlation with three hypothesized predictive variables height, weight, and body mass index (BMI). The data collected suggests weight (kg) is the strongest predictive variable ($r_{ankle/weight} = 0.747, p < 0.001$; $r_{thigh/weight} = 0.911, p < 0.001$). Consequently, the analysis began by organizing the population numerically by weight.

3.2.3 Intervals

Once a positive correlation was determined between the two leg circumferences (i.e. ankle, thigh) and weight (kg) for CAESAR women (N = 1264), the data were organized numerically by weight (kg) and partitioned into quartiles for analysis, as shown in Figure 3.3. Statistically significant outliers were calculated and any subject over 102.49 kg was removed from the analysis. After removing outliers, the potential population pool was 1169 women. Because the anthropometric study required measurement extraction from the original CAESAR surface data, a sample of 80 participants (20 per quartile) were randomly selected to level the distribution and to provide representative data for the circumferential range within the CAESAR population.

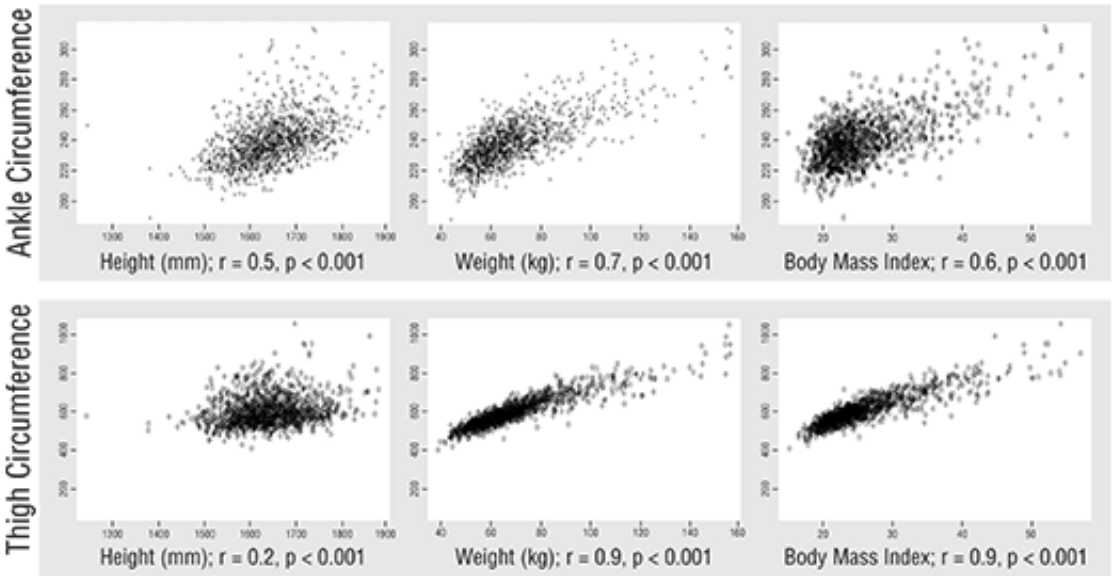

Figure 3.2: **Predictive variables for ankle and thigh circumference (mm):** (1) height, (2) weight, and (3) body mass index; CAESAR, Nwomen = 1264

3.2.4 Data Collection

Four circumferential measurements were gathered from each CAESAR sample (n = 80) from standing and seated scans: (1) ankle, (2) calf, (3) knee, and (4) thigh. See Figure 3.4. For the sake of this study, the circumference of the ankle was defined as the narrowest point of the leg, just above the inferior tibiofibular joint. The circumference of the calf was defined by the apex of the gastrocnemius muscle. The knee circumference was taken in line with the femoral epicondyle and the thigh measurement was taken at the top of the quadricep.

Thigh circumferences (sitting and standing) were gathered during the 1998 - 2000 CAESAR study with traditional measuring tapes and this data for all North American women was used directly from the CAESAR spreadsheet (N = 1264 - outliers). The remaining measurements were manually extracted from each, original CAESAR surface scan (n=80) using ScanWorX software.

The measurements gathered within ScanWorX revealed that the body is highly asymmetrical in nature. Consequently, we used the right and left legs as their own datasets rather than averaging them together to represent a single subject. Clear measurements (i.e. measurements taken from areas without missing or obscured surface data) were gathered

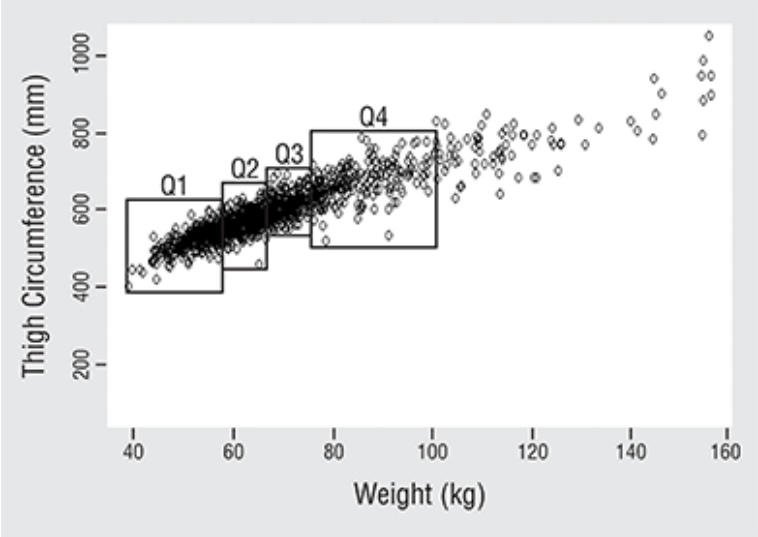

Figure 3.3: **Predictive variables for ankle and thigh circumference (mm):** (1) height, (2) weight, and (3) body mass index; CAESAR, Nwomen = 1264

for 160 knees in a standing posture by autogenerating a transverse surface measurement at the femoral epicondyle, as designated by a CAESAR-placed anatomical marker (12 mm white paper placed directly on the body when scanned). Due to missing surface data at the popliteal fossa in a sitting posture (see Figure 3.5), only 80 knee measurement from a seated posture were gathered (one per scan). The sitting knee circumference was manually extracted within ScanWorX by tracing the circumference with the guidance of a surface plane that intersected the knee crease and patella center. This measurement had the greatest potential for error because the center patella was not marked on the scan and the knee crease marker was often missing due to gaps in surface data, as shown in Figure 3.5. A measurement error was calculated by shifting the approximated anatomical markers up and down 2 cm to simulate misplacement. Due to differing body slopes above and below the approximated landmarker, the measurement could increase up to 6.5% if taken too high or decrease 3.29% if taken too low on the body.

Clear measurements were gathered for 160 calves (sitting and standing) by autogenerating a transverse surface measurement at the apex of the gastrocnemius muscle. While there was not an anatomical marker at the gastrocnemius muscle, ScanWorX appeared to autogenerate the measurement accurately. Potential measurement error was calculated by shifting the approximated landmark up and down 2 cm to simulate misplacement. The

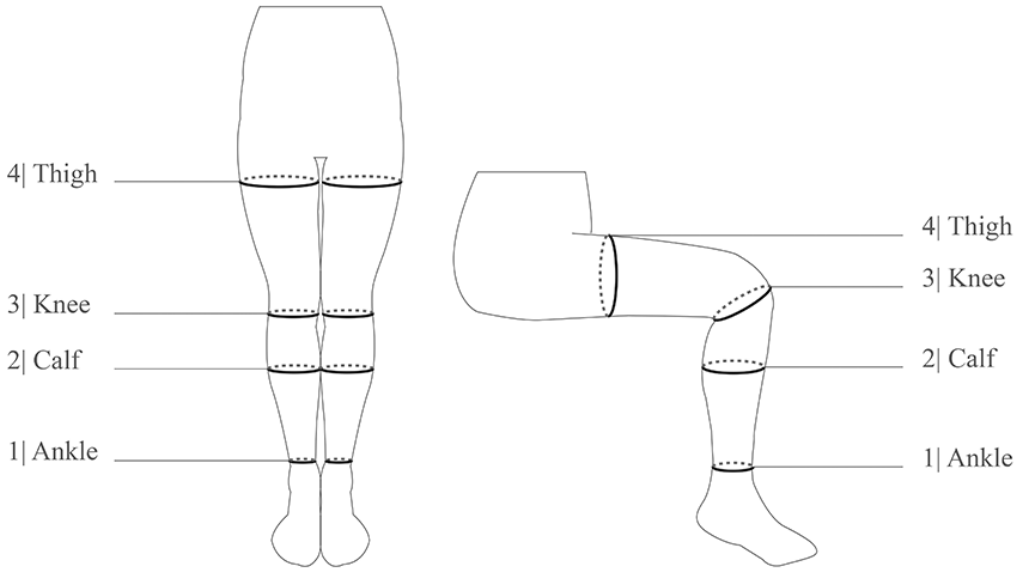

Figure 3.4: **Circumferential measurements taken from the (1) ankle, (2) calf, (3) knee, and (4) thigh from a standing and seated posture.**

measurement error was calculated to be up to -1.41% in either direction standing and -3.79% in either direction sitting if the true apex were misjudged because the body can only slope down above and below the apex point.

Clear measurements were gathered for 160 ankles (sitting and standing). While the ankle circumference was provided for all CAESAR subjects in the spreadsheet and could be easily autogenerated at the malleolus medial anatomical landmarker designed by CAESAR, the measurement was taken from a location low onto the foot. Consequently, these data were not used in our analysis and a new ankle circumference was generated by moving the anatomical marker from the malleolus medial up to the narrowest part of the leg. The potential measurement error was calculated to be up to +4.6% in either direction standing and +4.06% in either direction sitting if the smallest part of the leg were misjudged because the circumference can only increase above and below the smallest leg circumference. Table 3.1 presents a summary table with metrics used in this analysis.

Additionally, cross sections were taken from one randomly selected subject in each quartile to provide a visual analysis of shape change between a standing and a seated posture. The cross sections provide a snapshot of the shape of the body and relative shape change

Figure 3.5: **Missing surface data (red) in a CAESAR scan shown in dark areas.**

Table 3.1: **Number of measurements compiled for each region of the body.**

	ankle (r)	ankle (l)	calf (r)	calf (l)	knee (r)	knee (l)	thigh (r)	thigh (l)
standing	80	80	80	80	80	80	1264	0
sitting	80	80	80	80	0	80	1264	0
total	**160**	**160**	**160**	**160**	**0**	**160**	**1196**	**0**

between posture. See Figure 3.9 along with the results.

3.2.5 Statistical Analysis

Measurements from standing and sitting postures were evaluated for significant difference using a paired t-test. The difference between sitting means and standing means along with their corresponding 95% confidence intervals was determined for each population quartile. Additionally, descriptive statistics were calculated for each of the four measured circumferences of the body (ankle, calf, knee, thigh) to determine the range of change per quartile.

3.3 Results

3.3.1 Mean Circumference Change

The results of the t-test are displayed in Figure 3.7. The findings from the statistical analysis reveal that there is a significant difference between standing and sitting leg circumference in almost all regions of the leg. Figure 3.6 plots the difference in means (mm) between standing and sitting circumferences for each area of the body (ankle, calf, knee, thigh) per quartile. The plot shows that the mean increase in circumference, sitting-to-standing, is greater for the knee than for other parts of the leg. The mean circumferential increase in the calf and the ankle is greater than the thigh, but less than the knee. The mean change in thigh circumference experiences the least amount of change standing-to-sitting than other areas of the leg.

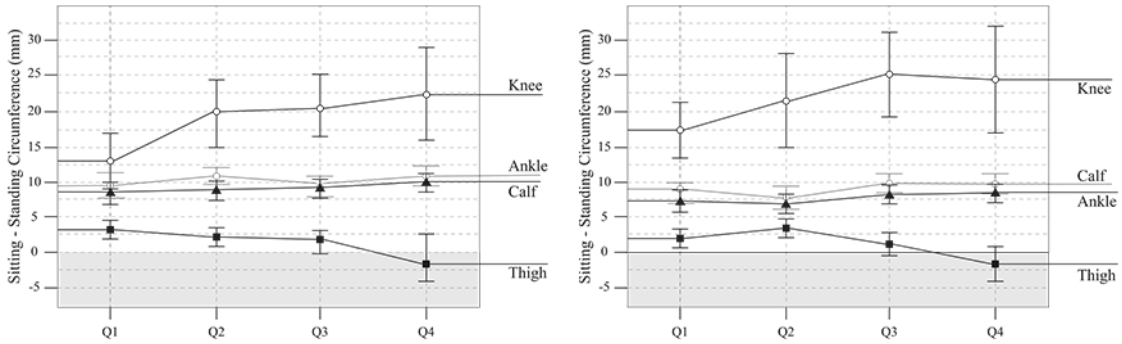

Figure 3.6: **(left) Mean change in circumference with confidence intervals grouped by weight (kg) quartiles, standing to sitting: ankle, calf, knee, thigh; (right) Mean change in circumference reshuffled by body mass index (BMI).**

Secondly, the statistical analysis shows that the significance of change increases from Q1 to Q4 in all regions of the leg, except the thigh. The difference in mean circumferences at the knee, thigh, and ankle increases with incrementally increasing quartile weight. The mean dimensional increase at the calf and ankle is slight while the knee increases more sharply as weight increases. Conversely, the thigh decreases between postures with incrementally increasing quartile weight. To further examine the change in thigh circumference, the data were reshuffled by body mass index (BMI). The results are presented in Figure 3.6. A second t-test was conducted with the data reorganized by BMI. The mean change calculated in thigh quartiles 1 and 4 were found to be statistically significant ($pQ1 < 0.05$; $pQ4 < 0.05$). Conversely, no significant differences were observed in Q2 and Q3 ($pQ2 > 0.05$; $pQ3 >$

0.05).

Difference in Leg Circumferences between Standing and Sitting Postures

	1 | Ankle				2 | Calf				3 | Knee				4 | Thigh			
	Min	Q1	Q3	Max	Min	Q1	Q3	Max	Min	Q1	Q3	Max	Min	Q1	Q3	Max
df =	39	39	39	39	39	39	39	39	19	19	19	19	317	313	322	240
p =	< 0.001	< 0.001	< 0.001	< 0.001	< 0.001	< 0.001	< 0.05	< 0.001	< 0.001	< 0.001	< 0.001	< 0.001	> 0.05	< 0.05	> 0.05	< 0.05
Min 95% CI =	+5.73	+5.54	+7.05	+7.10	+6.87	+6.22	+8.36	+8.29	+13.47	+14.81	+19.31	+16.92	-1.15	+0.39	-2.39	-6.25
$\bar{x}_2 - \bar{x}_1$ =	+7.33	+6.93	+8.26	+8.43	+8.28	+7.80	+9.72	+9.72	+17.31	+21.45	+25.25	+24.51	+0.22	+1.76	-0.66	-3.62
Max 95% CI =	+8.93	+8.33	+9.47	+9.76	+9.69	+9.39	+11.07	+11.15	+21.15	+28.09	+31.18	+32.10	+1.58	+3.13	+1.08	-0.99

$\bar{x}_1$ = sample mean, standing, $\bar{x}_2$ = sample mean, sitting

Figure 3.7: **Difference in leg circumference between a standing and a seated posture in millimeters.**

3.3.2 Range of Circumference Change

The descriptive statistics calculated for the ankle, calf, knee, and thigh within each quartile is summarized in Figure 3.8. This table presents the minimum, maximum, mean, and range of actual circumferential dimensional change in millimeters for each of the four regions of the leg (ankle, calf, knee, thigh). Figure 3.10 plot each dimensional value of change along an axis to draw comparison between the leg regions and quartiles. Figure 3.10 shows that the ankle and calf have the smallest range of actual dimensional change ($range_{ankle} = 17.78$ to 20.57 mm; $range_{calf} = 18.03$ to 18.80 mm). The range of dimensional change in the knee is larger than the ankle and calf, but less than the thigh ($range_{knee} = 29.21$ to 61.98 mm). The plot shows that the thigh experiences the largest amount of actual dimensional change ($range_{thigh} = 69$ to 118 mm). Figure 3.10 a-d represents each quartile separately, while Figure 3.10 e presents a summary of all quartiles for comparison.

In addition to the actual dimensional change in millimeters shown in Figures 3.10, the percentage of change in each of the 5 regions of the lower body (ankle, calf, knee, thigh) were calculated. Figure 3.11 presents a comparison of the range of dimensional fluctuation percentages in each quartile for comparision. From the calculations, we can see that each region has a unique percent range of possible circumferential fluctuation. The calf experiences the least amount of circumferential change (4-6%). The ankle fluctuates between 7% and 8%. The range of percent change in the knee spans from 7% to 13%. Figure 3.11 depicts the thigh as having the highest percentage of dimensional change - from 14 to 17%.

Range of Leg Circumference Change due to Postural Change

	1 | Ankle				2 | Calf				3 | Knee				4 | Thigh			
	Q1	Q2	Q3	Q4	Q1	Q2	Q3	Q4	Q1	Q2	Q3	Q4	Q1	Q2	Q3	Q4
Min. Difference =	-0.76	-1.27	+2.79	-0.76	-2.79	-4.83	0.25	+1.02	+3.05	-0.51	+7.37	-1.27	-35.00	-46.00	-43.00	-60.00
Mean Difference =	+7.32	+6.93	+8.23	+8.43	+8.28	+7.80	+9.72	+9.72	+17.31	+21.45	+25.25	+24.51	+0.22	+1.76	-0.39	-3.62
Max. Difference =	+17.02	+16.00	+19.05	+19.81	+15.24	+16.51	+16.76	+19.81	+32.26	+54.36	+50.04	+60.71	+34.00	+43.00	+50.00	+58.00
Range =	17.78	17.27	16.26	20.57	18.03	+21.34	+16.34	+18.80	29.21	54.86	42.67	61.98	69.00	89.00	93.00	118.00

Figure 3.8: **Range of leg circumference change between a standing and a seated posture in millimeters.**

3.3.3 Nature of Circumference Change

To accompany the statistical results, one randomly selected subject from each quartile was selected to provide a visual representation for circumferential change in each sample region of the leg. The cross-sections were not incorporated into the statistical analysis; however, they provide additional information about the nature of shape change in each region. Figure 3.9 displays a sample cross-section for each region of the body in each quartile.

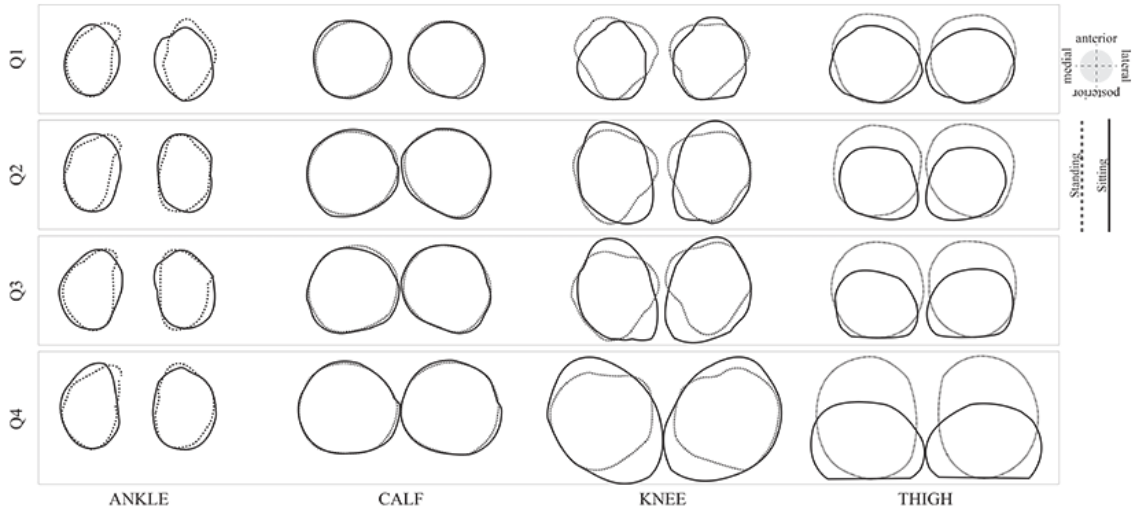

Figure 3.9: **Randomly sampled cross-sections of leg circumferences:** (a) ankle, (b) calf, (c) knee, (d) thigh in standing and sitting postures. Note: cross-sections are not to scale.

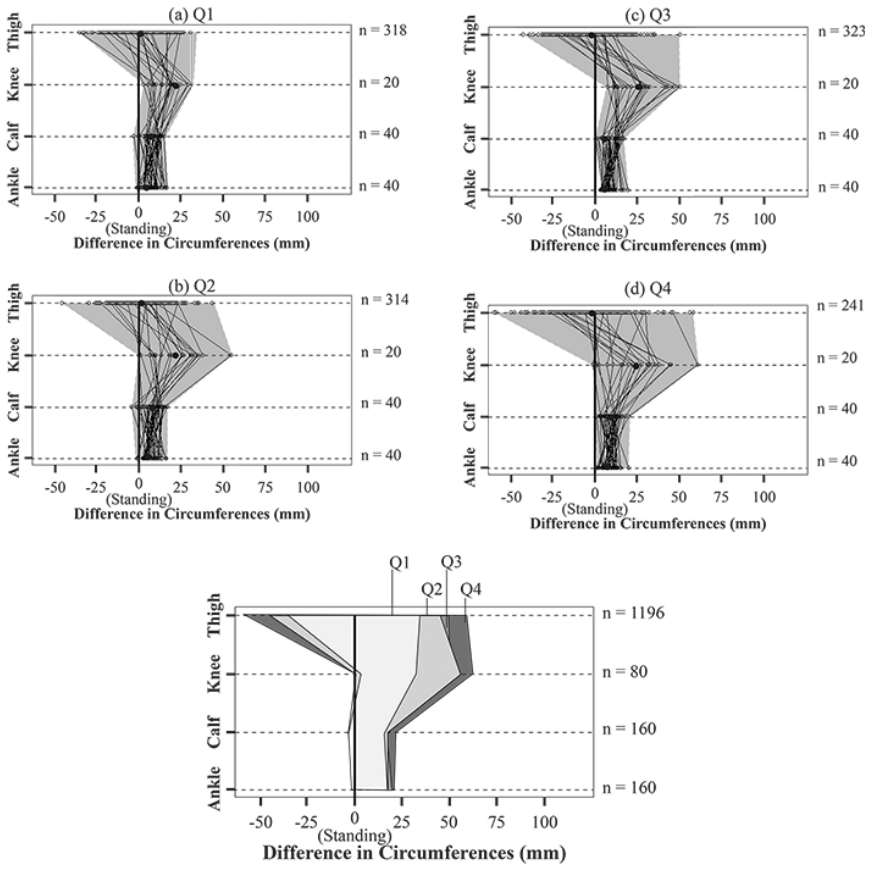

Figure 3.10: **(a-d) Range of circumference change (mm) per quartile; (bottom) Comparison, range of circumference change (mm) per quartile.**

3.4 Discussion

3.4.1 Ankle

A. Mean Circumference Change

While prior studies concluded that there is little to no change in ankle circumference between standing and sitting postures [41], our statistical analysis found that the ankle increases between a standing and a seated posture in all quartiles. The mean change in circumference in the ankle was low (+7.33 to +8.43 mm) compared to other areas of the leg. Figure 3.6 show that the mean change in circumferences standing-to-sitting increases slightly with weight.

B. Range of Circumference Change

Figure 3.10 shows that the possible range of circumferential fluctuation for the ankle is narrow compared to other regions of the leg. While the t-tests show that the actual mean dimensional change in milimeters increases with weight, the percent change between quartiles is narrow - between 7% and 8%. This data suggests that the shape change experienced at the ankle is relatively consistent across all weight categories in females.

C. Nature of Circumference Change

The cross-sections taken at the ankle (shown in Figure 3.9) reinforce the statistical analysis claiming that the circumference of the ankle increases standing-to-sitting. In the standing posture, the cross-sections show that the circumference has a prominent anterior apex at the anterior tibial tendon. In the sitting posture, the circumferences appear to smooth out and become more uniform, most likely a response to a change in joint angle.

3.4.2 Calf

A. Mean Circumference Change

The mean shape change experienced at the calf was found to be lower than that found in a prior study. In 2011, Choi and Ashdown found a mean change of 15.1 mm in the calf region within their sample of 25 females [41]. Our analysis determined a mean change in circumference standing-to-sitting to be between 8.29 to 9.72 mm, suggesting a slight increase in dimensional change with weight.

B. Range of Circumference Change

Like the ankle, the percentage of change in the calf regions was found to be more compact than other areas of the leg. Figure 3.11 shows that the percentage of change was found to be less than the ankle (46%); however, it is unclear if the percentage of change increases or decrease with increased total body weight. It is possible that, like the ankle, the percentage of change in the calf is independent of weight and all females experience a percent change between 4 and 6% in the calf between postures. Additional research is required to determine if there is a relationship between the change in calf circumference and body weight.

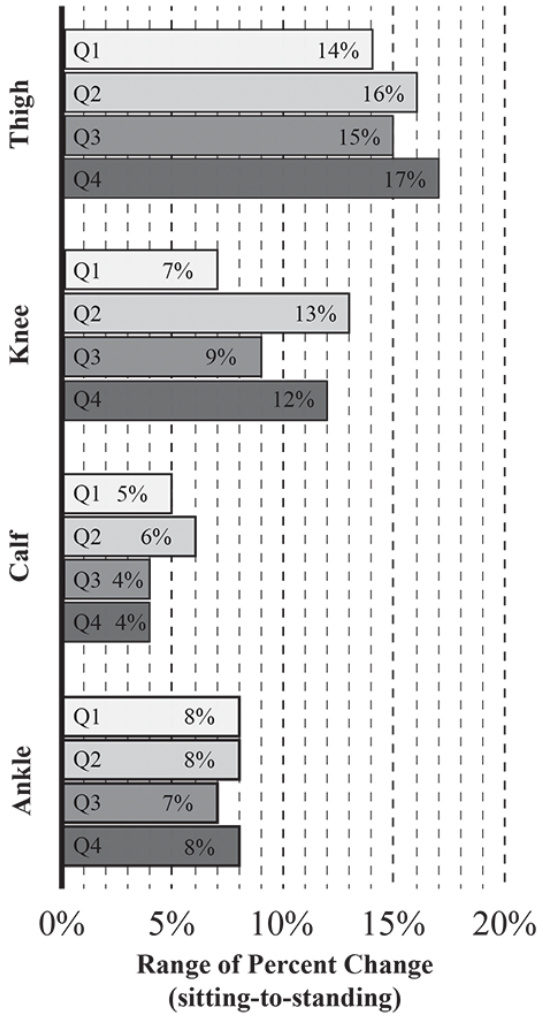

Figure 3.11: **Range of circumference change (%) required to accommodate anthropometric lower body change due to posture.**

C. Nature of Circumference Change

The statistical data support the visual information provided by the sample cross sections taken at the calf (shown in Figure 3.9). The cross sections show little shape change standing-to-sitting and appear cylindrical and uniform in nature.

3.4.3 Knee

A. Mean Circumference Change

The knee experienced a mean change in circumference standing-to-sitting between 17.31 to 25.25 millimeters. This calculation was lower than that reported by prior studies (43.6mm) [41]; however the analysis shows that the knee experienced a higher change between postures than the other three regions of the leg. While the change experience in the third quartile of the knee was greater than the change experienced in the fourth quartile, there does appear to be a general trend of increasing change with increased body weight.

B. Range of Circumference Change

Figure 3.10 confirms that the actual dimensional change standing-to-sitting experienced in the knee was larger in higher weighted quartiles aside from Q3; however Figure 3.11 shows that the range of percent change in each quartile is unpredictable. In this depiction, the data could support an increase in circumference change due to weight if Q2 data were removed. One explanation for the erratic data could be that the shape change at the knee is highly unpredictable. Alternatively, the analysis could reveal that the data extraction method through CAESAR posed challenges with missing surface date. We recommend reevaluating shape change at the knee through alternative 3-D body scans with complete or repaired surface data at the knee or by means of traditional methods, such as measuring tapes.

C. Nature of Circumference Change

The knee cross sections show considerable change in the body in addition to the average 17.31 to 25.25 millimeters to circumference increase (see Figure 3.9). In a standing posture, the knee has a triangular contour with a distinct posterior protrusion at the popliteal fossa. In a sitting position, the knee becomes oblong with a medial-posterior apex at the hamstring tendons. This formation becomes more prominent in larger quartiles.

3.4.4 Thigh

A. Mean Circumference Change

The mean circumference change in the thigh was unique to other parts of the leg in that the dimension was found to decrease between postures a finding that is supported by prior research [41]. Furthermore, the total mean change in thigh circumference was found to be minimal between 1.76 and -3.62 millimeters. The t-tests conducted organized by weight concluded that there was little to no change in quartiles 1 and 3; however, there was found to be a statistically significant increase in Q2 and decrease in Q4. Conversely, the t-test conducted by BMI concluded that there was little to no change in quartiles 2 and 3; however, there was found to be a statistically significant increase in Q1 and decrease in Q4. Because the t-test presented scattered results, we will conclude that there is not likely to be significant change in Q1-Q3 and there is likely a significant decrease in Q4 circumferences between postures.

The trend to decrease with added total weight could be explained by body composition. Higher weighted quartiles have a greater percentage of soft tissue stored in the thighs compared to other regions of the leg [42] a fact that supports the strong correlation found between thigh circumference and weight shown in Figure 3.2. When the body moves from standing to a seated posture, the length from the popliteal fossa to the waist increases as the body hinges at the hip joint[41]. The data suggests that bodies with a higher fat content experience a decrease in circumference as a higher percentage of fatty tissue in the thigh stretches and disperses along a greater surface length of the leg.

B. Range of Circumference Change

While the results of the t-test present the thigh as having the smallest mean dimensional fluctuation, the descriptive statistics present the thigh as having the greatest variability and possible dimensional change. Figure 3.11 shows that the thigh circumference changes between 14% to 17% - the largest percent change of any other regions along the leg. Additionally, unlike the ankle, calf and knee, the full range of percent change in the thigh encompased positive and negative percent changes. Figure 3.12 shows that within Q1, the thigh was seen to increase 6% or decrease 7%. Similarly, Q2 incresed up to 8% or decreased up to 9% and Q3 increases up to 8% and decreased up to 7%. This information is consistent with the statsitical results that concluded that there is possibly no change in dimension in the thigh. Despite the fact that the t-test found a statistically significant decrease in thigh

circumference in Q4, the descriptive statistics show that there is an equal chance that the thigh could increase or decrease 9% in the maximum weight quartile.

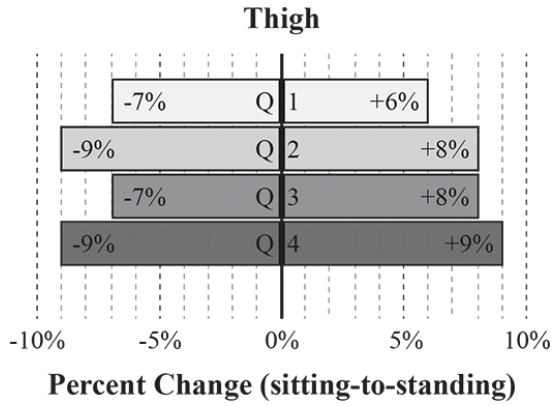

Figure 3.12: **Range of circumference change (%) required for thigh region.**

The results of this data are challenging to interpret. Consultations with anthropometric experts conclude that measurement error must have occurred during the CAESAR collection process. Little information is provided by CAESAR regarding how the measurements were gathered and further analysis must be conducted to clarify results.

C. Nature of Circumference Change

While the mean circumference change in the thigh region was found to be minimal (average 1.76 to -3.62 millimeters), the cross-sections in Figure 3.9 show substantial change in shape. In smaller quartiles, there is little change in contour; however, higher quartiles show a distinct flattening and a widening of thigh. This effect is most likely due to variation in body composition between quartiles. Soft tissue is highly malleable, therefore higher quartiles of greater weight would experience more cross sectional deformation between postures due to gravity.

3.5 Implications

The evaluation and quantification of anthropometric variability of the lower body have implications for all CG designs because garment fit is inextricable from garment function[7]. While undersized OIG designs currently do not have the capability to adapt to the body

and/or maintain consistent pressures between postures, future active OIG designs could accommodate body variability into the functional design process. The results outlined suggest that leg radii are complex and fluctuate non-uniformly from the thigh to the ankle; therefore, active knit fabrics designed for an OIG will require regions of varying functional behaviors. Design requirements for future active OIG that could adapt to lower body circumferential change due to posture are outlined below.

3.5.1 Ankle & Calf Functional Requirements

As summarized in Figure 3.11, the ankle and the calf region will require an active material architecture that provides consistent tension throughout the dimensional range calculated (maximum, 6% at the calf and 8% at the ankle). By adapting to the dimensional change (6% and 8% expansion), an active fabric could guarantee uniform pressure output across postures. A material with 6% expansion at the calf and a second material with 7% expansion at the ankle will likely accommodate women across all weight and BMI spectrums.

3.5.2 Knee Functional Requirements

Functional requirements for the knee region are critical for future OIG designs because increasing radii can transform CGs into a tourniquet causing blood to pool into the feet and calves. The knee region will require different active material architectures depending on weight category. The data suggests that women with lower total weights (39.2 to 57.1 kg) require an active architecture that expands up to 7% at the knee when sitting. Women with higher total weights (75.3 to 102.5 kg) require an active architecture that expands up to 12% at the knee when sitting. The medium weight categories (Q2, 57.2 to 65.0 kg; Q3, 65.0 to 75.3 kg) require an active architecture that expand up to 13% (Q2) and 9% (Q3). Due to the scattered nature of the results of the knee analysis, it is recommended that a follow up study be conducted using traditional measuring tape methods or another method that is capable of accurately and reliably capturing the surface of the popliteal fossa at a 90-degree angle.

3.5.3 Thigh Functional Requirements

The active material requirements for the thigh region are complex and unique from other regions of the leg. Figure 3.12 illustrates that the active material architecture might need

to expand or contract from the target standing circumference. To accommodate the anthropometric requirement of the thigh, an active material designed for the thigh region requires a greater circumferential stroke change than other regions of the leg. The garment would most likely need to be designed to contract more than other regions of the leg upon initial donning. Additionally, when the individual transitions from a standing to a seated posture, the thigh may follow the behavior of other areas of the leg and expand, or it may require additional contraction, an alternative movement to other areas of the leg. This type of modulation of the thigh will require additional research into active OIG controls and sensing capabilities. Like the knee, the thigh region requires the design of several different active architectures according to weight category. Women in lower weight categories (39.23 to 57.14 kg) will potentially require circumferential change up to 14%. Women in higher weight categories (75.29 to 102.49 kg) will potentially require active circumferential change up to 17%. Women in medium weight categories (Q1, 57.15 to 64.96 kg; Q3, 64.97 to 75.28 kg) most likely could be accommodated by the same active material that possesses circumferential fluctuation up to 15% or 16%.

3.6 Limitations & Future Work

3.6.1 Lower Body Length Change Due to Posture

An investigation of length change due to posture was left out of this study because further analysis is required to understand how length change affects the distribution of a looped yarn knit architecture. Generally speaking, an increase in length will decrease the circumference of a circular knit and produce a contraction. Likewise, a decrease in length will increase the circumference and produce an expansion. Because the human leg experiences complex and uneven length change - the back of the leg contracts and the front of the leg expands standing-to-sitting [41] - further analysis is required to determine how much this bidirectional length change affects fabric tension and corresponding pressure output. Even though we attempted to separate out length in this investigation, the analysis of body circumferential change revealed the interconnectivity of length and width. This interconnectivity was most apparent in the thigh where circumference sometimes decreased due to an increased length and stretching of soft tissue along the thigh as both knee and hip joints transitioned into 90 degree angles.

3.6.2 Body Composition

Body composition was also left out of the quantitative investigation because fMRIs were not available for the CAESAR population; however, we can deduce relative composition through paired knowledge of anatomy with CAESAR anatomical landmarkers. It appears that body composition and muscle activity (contraction, relaxation) combined with the bodys range of motion produced the circumferential shape change evaluated in this paper. Areas with a higher percentage of fatty deposits (e.g. thigh) appeared to undergo more shape change. Areas with a higher percentage of muscle (e.g. calf) appeared to undergo less shape change. Areas with a higher percentage of bone and ligaments (e.g. knee, ankle) appeared to experience a shape change that was dependent on the degree and nature of joint flexion, or displacement of hard tissues. Additionally, research shows that pressure can be higher than expected in areas of hard tissue and lower than expected in areas of soft tissue [14]. Subsequent studies should evaluate the effects of body composition on pressure output on a larger population to determine how and if an active OIG could build in isolated regions with more or less contraction to counteract uneven distribution due to body composition (e.g. shin bone versus gastrocnemius muscle).

3.6.3 Body Topography

The majority of CG designers calculate pressure on the body through mathematical formulas that assume each body cross section has a consistent radius and a uniform circumference [7]. The cross-sectional samples collected from one randomly selected CAESAR scan in each quartile (see Figure 3.9) reveal that the bodys topography is highly variable in nature and that variable topography changes with posture. It is currently unclear how this circumferential non-uniformity affects pressure output on the body and further investigation is required. It is likely that body topography and body composition are related - hard protrusion (e.g. medial posterior knee, anterior ankle) could produce higher pressure spikes than soft protrusions (e.g. medial and lateral posterior thigh).

3.6.4 Exposure to Weightlessness & Lower Body Volume Loss

Each of these anthropometric concerns - dimensional, compositional, and topographical - is compounded by individual variability, such as age, fitness level, hydration level, etc. The most important individual variable for astronauts is exposure to weightlessness. In 1977

Hoffler et al. released Inflight Lower Limb Volume Measurements as part of the Apollo-Soyuz Test Project Medical Report [43]. In the study, researchers from the Johnson Space Center determined that astronauts lose leg volume during exposure to weightlessness (i.e. around 1 liter per leg) [43]. Volume loss in the legs is directly tied to limb circumference and would undoubtedly change the pressure output of an OIG. Additionally, the location of volume loss is non-uniform (i.e. increased volume loss in the thigh compared to the lower leg) and the amount of volume loss is dependent on period of exposure to zero gravity [43]. In 2000, LeBlanc et al. released an article called Muscle Volume, MRI Relaxation Times (T2), and Body Composition After Spaceflight that quantified the percentage of volume loss for specific muscle groups as well as general body composition (i.e. bone mineral, fat, lean body mass) for the limbs over short (17 day) and long (16-28 weeks) duration space missions [44]. Studies by Hoffler et al. and LeBlanc et al. both attempt to predict the complex anthropometric changes that occur in space. While neither of these studies incorporated the anthropometrics of female astronauts, the incorporation of inflight lower body anthropometrics, specifically tracking volume loss through time, into OIG design and development will be critical for future work and success.

Lower limb volume loss is further complicated by the pooling of blood that occurs in the limbs as astronauts are reexposed to gravity during reentry and landing on Earth. Further research is required to understand the anthropometric changes that occur when exposed to weightlessness and subsequently reexposed to gravity; however, a successful OIG would be able to anticipate and adapt to those physiological changes to fully protect from OI upon mission return. It is recommended that studies be conducted during future space missions to quantify body dimensional change due to exposure to weightlessness. It is also recommended that anthropometrics from female astronauts be collected during such future studies since they are disproportionately affected by OI [36]. This research is intended to improve OIG design for astronauts whose tasks require mobility (i.e. changes in posture). The fundamental value of this anthropometric research is to highlight that human geometry changes during movement; therefore, garments (e.g. OIGs) that are used during scenarios where movement is expected must be capable of adapting to the body in order to provide consistent garment performance. While this research poses more questions than solutions regarding the human bodys relationship to CGs, the study is a step forward in quantifying anthropometric variability and change to inform and improve future OIG design and research.

Chapter 4

Active-Contracting Fabrics for On-Body Compression

On-body compression is widely used throughout consumer, medical, athletic, and aerospace settings to anchor clothing to the body, regulate health, maintain range of motion and preserve a low-profile form. Active-contracting fabrics have the ability to expand on-body compression technologies, which are presently limited to pneumatic and undersized garments. While pneumatic garments are dynamic and easy to don/doff, they impede mobility and have a larger form-factor. Alternatively, undersized garments enable mobility and slim, rather then enlarge the shape of the body; however, they are not dynamic and can be difficult to don/doff. This research evaluates a novel active-contracting fabric, contractile SMA knitted actuator fabrics, to characterize actuation forces, approximate on-body compression capabilities, and evaluate the potential on-body compression applications that could benefit from this technology.

4.1 Introduction

On-body compression has a wide range of applications, spanning from medical to sport to consumer. Low-level compression is widely prescribed by medical practitioners to treat an array of cardiovascular, lymphatic, and anxiety-related disorders. Many cardiovascular disorders are managed with daily-use, gradient compression garments (CG) that apply higher distal pressures and lower proximal pressures to the legs. Such disorders include postural orthostatic tacycardia syndrome (POTS) (30-40 mmHg [45]), orthostatic hypotension

(OH) (25-40 mmHg [46, 47]), orthostatic intolerance (OI) (40-80 mmHg [48]), and deep vein thrombosis (DVT) (130-200 mmHg, foot; 40-50 mmHg, calf [49]). Gradient and intermittent compression (max,50 mmHg) is recommend to treat lymphedema, a condition which requires frequent physical manipulation of lymph fluid [50, 51]. Likewise, intermittent and varying levels of compression around the torso and shoulders have been found to reduce the symptoms of sensory processing disorders, including generalized anxiety disorder (GAD) [52, 53], autism spectrum disorder (ASD) [54], and attention deficit hyperactivity disorder (ADHD) [55, 56]; however, pressure quantity and duration are highly subjective and individual in nature [57].

In addition to wide medical use, low-level compression is crucial in everyday clothing to hold garments to the body at anatomical anchor points, such as the waist, feet, and shoulders. Examples include waistbands, hat bands, belts, shoe tops, bras straps, and suspenders. Increased levels of compression are desired to achieve aesthetic body shaping and provide physical support (e.g. spanx, bras). Compression clothing is also purchased by the general public for sport and recreation when close-fit and mobility are prioritized. While designed for a particular use-case, athletic clothing has become increasingly integrated into everyday fashion trends (e.g. 'athleisure') [58].

While the magnitude of pressure across applications varies drastically ($<$ 18 mmHg clothing [59, 60], 300 mmHg tourniquet [61]), all on-body compression is presently accomplished either through (1) inflation or (2) garment reduction (i.e. cinching and/or stretch fabrics). Each technology has pros and cons that make them more or less suitable for a given application. This work presents the current state of both technologies and proposes a novel, alternative: active-contracting fabrics. Active-contracting fabrics could provide a form-fitting and dynamic market alternative to commercially available pneumatic and undersized garments. This research investigates the force capabilities of a type of active-contracting fabric, contractile shape memory alloy (SMA) knitted actuator fabrics, and provides an on-body compression approximation, given population anthropometrics.

4.1.1 Compression Garments (CG)

Compression therapy is typically administered through CGs, which are worn articles of clothing that apply positive pressure to the body either through garment reduction (e.g. knit shapewear) or through garment inflation (e.g. blood pressure cuff). The following sections describe the common medical and commercial use-cases for each type of CG and

outline their technical mode of functionality.

4.1.2 Pneumatic Garments

Pneumatic CGs have historically been used when precise control of pressure quantity and duration is required. Examples include orthostatic intolerance garments (OIG), like the anti-gravity suit (AGS) used by astronauts and military pilots [62]. Additionally, lymphedema is generally treated with pneumatic garments because they can apply rhythmic pressures to the body by strategically inflating and deflating chambers inside the garment [51]. Modern tourniquets used in surgery are also pneumatic and allow surgeons to monitor the level of pressure being applied as well as the rate that pressure is released [63]. Finally, pneumatic CGs are commonly used post-surgery to reduce the risk of DVT because they allow for dynamic, intermittent compression therapies that reduce venous stasis and increases blood flow. [49]

The "ballooning" behavior of inflatables, translate to uneven pressures when these bladders are wrapped around the body [11, 64]. While tension in the bladder walls are equal throughout, the shape of the bladder is dissimilar from the topography of the body. Consequently, circumferential wrapping translates higher forces to the body at the center, most distended area of the bladder and little-to-no forces are at the edges where the bladder lifts away from the body surface.

In addition to pressure distribution, garments that balloon out from the body are not conducive to movement, especially around joints that require large range of motion [12]. In order to accomplish knee flexion, the materials overlaying the front of the knee require extension, while the materials overlying the back of the knee require contraction. When wrapped in a stiff, bulky bladder, the knee can accomplish neither and mobility is inhibited. Additionally, pneumatic garments deflate with movement [12] and must be tethered to an air supply. To work around these mobility challenges, pneumatic CGs are either designed with cut-out regions around the knees (e.g. NASAs antigravity suit), a solution that can results in severe edema [10] or these garments are limited to stationary uses (e.g. post-surgery bedrest).

While inflatables present usability challenges, pneumatic CGs are the only commercially available compression technology that are dynamic, meaning pressure exerted on the body can be changed by adding or releasing air into the garment bladders. Dynamic function is crucial for many medical conditions (lymphedema, DVT) and the ability to change pressures

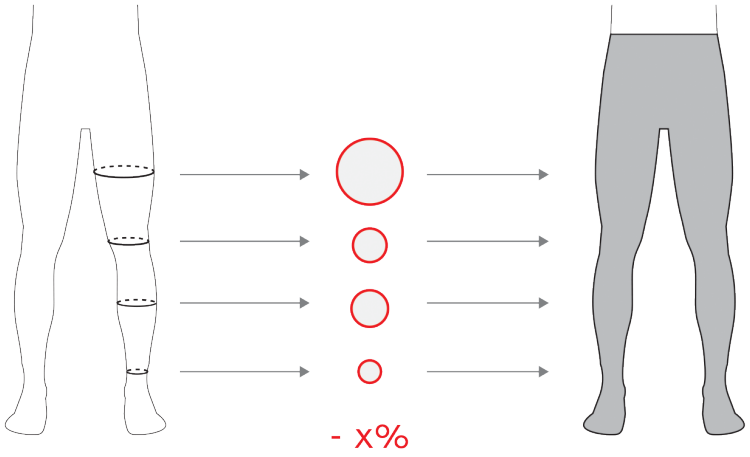

Figure 4.1: **Undersized CG Design Process:** (1) CG designers begin by gathering key circumference measurements. (2) Depending on the desired pressure (p) and limb radius (r), the fabric tensile properties (T) are manipulated through strain ($T = p * r$). Increased strain increases fabric tensions and reduced strain reduces fabric tension. (3) Consequently, the CG is made by circumferentially reducing garment dimensions in relation to body dimensions ($-x\%$) to achieve desired fabric strain (i.e. tension), which exerts pressure on the body relative to body radius (p = T/r) [7].

allows for easy don/doff desired in medical, sport and consumer applications.

4.1.3 Undersized and Cinched Garments

Undersized, skin-tight CGs are an alternative technology that have typically been designed using stretch knits (fabrics made of interlooping yarns) with rubber or elastane (e.g. Lycra spandex) yarns to provide compression [65]; however, these garments could also be made with wovens or non-wovens if adjustable closures, like lacing or straps, are tightened post-don. As shown in Fig. 4.1, undersized, stretch CGs are designed to function through pattern reduction. Circumferential limb dimensions are gathered in a standing posture. Garment dimensions are reduced so that tensile stress increases as the garment stretches over the body [7]. Consequently, the shape of the body in relation to the garment determines the magnitude of pressure exerted on the body [14]. This design strategy can be represented mathematically by merging Laplace's law (Equation 4.1) with a simple hoop stress formula (Equation 4.2),

$$p = \frac{t\sigma_\theta}{r} \tag{4.1}$$

$$\sigma_\theta = \frac{F}{tw} \tag{4.2}$$

where pressure (p, [Pa]) is represented in terms of fabric thickness (t, [m]), hoop stress (σ_θ) and cylindrical radius (r, [m]), while hoop stress is represented in terms of force ($F, [N]$), fabric thickness, and fabric width (w, [m]). Substituting Equation 4.1 into 4.2, we derive the following relation.

$$p = \frac{T}{r}; T = \frac{F}{w} \tag{4.3}$$

Equation 4.3 is commonly used in CG design to determine the fabric tension range that is required to exert the appropriate pressure range on a particular set of limb dimensions. This tension range further informs the percent reduction of garment dimensions in relation to body dimensions, or garment design [7]. For instance, if low-leg circumferences range from 20-50 cm and the target medical pressure range is 30-40 mmHg (4 - 5 kPa), then a fabric that reaches tension between 160 and 320 N/m is required ($0.03m * 5333Pa = 160N/m$; $0.08m * 4000Pa = 320N/m$). Through traditional tensile testing, a designer can then determine the fabric strain percent (displacement) that is required to achieve the desired tension range. Most medical-grade compression fabrics are designed to maintain high forces and strain moderately (e.g. 50%), while fabrics used for low-compression sports leggings strain as much as 150-200% with small tensile forces. Consequently, the tensile properties of the chosen fabric paired with the dimensions of the body determine the achievable range of on-body compression. Furthermore, pressures (within the given range) can be tailored by the designer by increasing or decreased fabric strain when pulled over the body by respectively decreasing or increasing garment dimensions [7].

Undersized CGs offer superior mobility, reduced metabolic cost, and user discretion compared to pneumatic CGs, making them more suitable for individuals who require daily compression and are not restricted to bedrest or otherwise stationary condition [12, 65]. Undersized CGs are frequently used by those with POTs, a condition which predominantly affects young, otherwise healthy females, and those with OH, a condition which impacts elderly adults who often strive to maintain independence and mobility. While preferred for their mobility and form-fitting nature, undersized CGs are not capable of exerting controllable or dynamic compression[17]. Undersized CGs at high pressures are difficult to don/doff because they are designed with both large dimensional reduction and high fabric tension (i.e. stiff and small), leading to patient non-compliance. [66]. Additionally, as depicted in Fig. 4.2, large variations in pressure are caused by irregular body topography (i.e. peaks and valleys), irregular body composition (i.e. rigid shin bone vs compliant calf) and dimensional fluctuations due to posture and/or fluid shift [6, 15]. Despite these functional

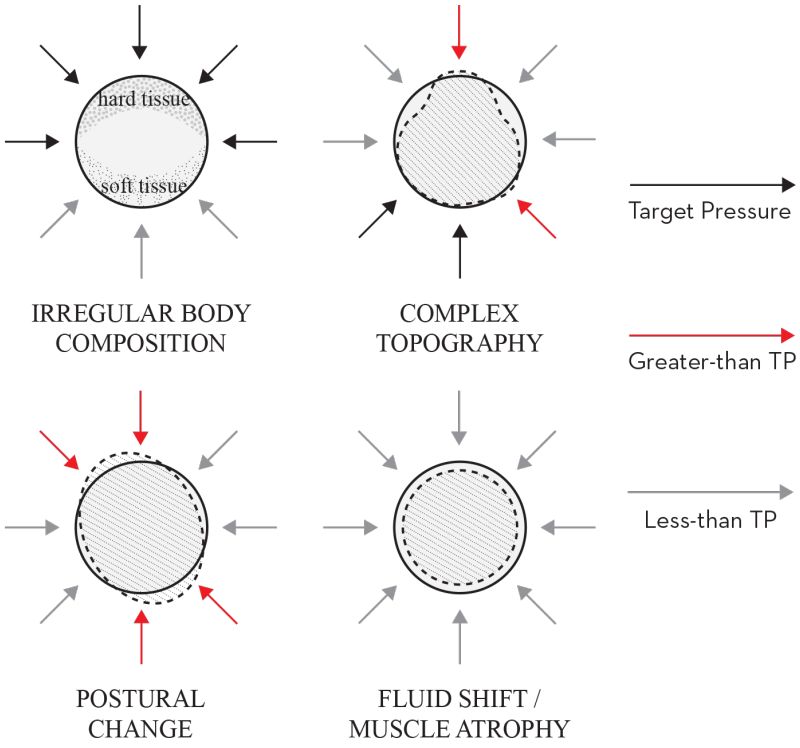

Figure 4.2: **Challenges with Undersized CG Pressure Distribution:** Factors such as (1) irregular body composition, such as soft and hard tissues, (2) complex body topography, (3) postural change, and (4) fluid shift and muscle atrophy can produce greater-than or less-than target pressures throughout wear of CGs.

flaws, undersized CGs are widely used for their simplicity and user discretion.

4.2 Contracting SMA Knitted Actuator Fabrics

Active-contracting fabrics are a new field of research that could advance the capabilities of CG design, allowing garments to contract on demand. This technology has applications spanning from aerospace (orthostatic intolerance garments, vertical loading garments) to terrestrial medical (lymphedema garments, compression stockings) to general consumer (shapewear, shoe tops). This section describes the design and functionality of a novel active-contracting fabric: contractile shape memory alloy (SMA) knitted actuator fabric.

4.2.1 Shape Memory Alloy (SMA)

Shape memory alloy (SMA) is a shape memory material (SMM), meaning it is capable of recovering a remembered shape after deformation with a change in a particular stimulus. This shape memory ability occurs because the material's internal structure is linked to, or coupled with, an external condition, such as light, pH, temperature, or magnetic field. SMA is characterized by thermomechanical or magnetomechanical coupling, meaning either temperature or magnetic field induces transformation. Nickel titanium alloys, or nitinol (NiTi), are a type of SMA that exhibit high recovery strains (6-8%) and high recovery stress (500-900 MPa) in response to changes in temperature, making them excellent thermomechanical actuators [8]. Consequently, NiTi is the particular type of SMA considered for this research.

SMA (i.e. NiTi) alternatives between a stable, high-temperature austenite phase, characterized by a cubic crystal structure, and a variable, low-temperature martensite phase, characterized by a monoclinic crystal structure [20]. Martensite variant include twinned (stress-free) and detwinned (stressed) monoclinic crystal states [20]. Due to the oscillation between cubic and monoclinic crystal structures, SMA exhibits both superelasticity and the shape memory effect. Superelasticity refers to the material's ability to respond elastically to stress while in an actuated (austenite) state, meaning stress-induced deformation is reversible. Alternatively, shape memory is the ability to fully recover unactuated (martensite) deformation once the material reaches its austenite finish temperature (A_f). The austenetic, "remembered" shape of any SMA is determined by its thermomechanical history. SMA can be trained to remember a particular formation through binding and heat-treatment [67]. The temperature range, duration of exposure, and quenching methods are all factors that effect the end behavior of the heat-treated specimen [67].

SMA actuator wire, or shape memory wire, is either sold as-drawn or heat-treated. As-drawn wire has not been shape-set, or heat-treated to remember any particular formation, while heat-treated wire has been trained to remember a straight formation. Flexinol (Dynalloy, Inc.) is a common, commercially available SMA actuator wire that is heat-treated and is available in a variety of transition temperatures (A_f =70°, 90°, 170°). Both as-drawn and heat-treated actuator wire can be (re)trained through shape setting.

The temperature ranges that trigger a response from SMA (martensite start M_s, martensite finish M_f, austenite start A_s, austenite finish A_f) are primarily dependent on material composition, specifically the ratio of nickel to titanium and the presence of additives, such as hydrogen, carbon, oxygen, and nitrogen [8]. NiTi is generally equiatomic, containing

50% nickel and 50% titanium [68]. Higher percentages of nickel produce SMA with a lower transformation temperature (A_f) [68]. Post-fabrication heat-treatments increase A_f due to nickel precipitation; consequently, A_f is easily raised post-manufacturing, but cannot be lowered.

4.2.2 Knitted Fabrics

Knit fabrics have the potential to create large, complex actuations across their surface because of the variety of structures that can be created with interlocking loops and the shape change that occurs when these loops are subject to tension [69]. Knitting can be divided into two general architectures: (1) weft knitting, which is a process in which an individual yarn is fed into one or more needles in a crosswise (lateral) fashion and (2) warp knitting which is a process in which a multiplicity of yarns are fed into one or more needles in a lengthwise (vertical) fashion [70]. While warp knits are more stable architectures, weft knits have the most mechanical stretch, a structural characteristic that can be leveraged in the design of active-contracting fabrics [71].

Two weft knit structures have been found to contract when fabricated with SMA wires: (1) the garter knit and (2) the stockinette, or jersey knit [72]. As shown in Fig. 4.3, the garter knit is composed of alternating courses of loop and purl stitches, which are defined by the orientation of their loop ridges. By alternating orientation, the garter knit is a balanced structure that produces planar contraction with incorporated active materials [18]. By contrast, the stockinette knit, or jersey knit, is composed of repeating knit stitches, making it an unbalanced structure that contracts and also curls in on itself without axial forces. This study evaluates stockinette (jersey) and garter knits for their contractile abilities; however other, unexplored knitted structures could also produce contraction and require further investigation.

4.2.3 Geometric Design Parameters

Previous work has identified key geometric design parameters that inform actuation contraction performance of contractile SMA knitted actuator fabrics, those being (1) wire diameter and (2) knit index [4]. The knit index (k_i), similar to the spring index (C), is a non-dimensional parameter developed and defined by [4] as the ratio between the enclosed loop area when the martensitic knit is under load (A_l, m) and the wire diameter (d):

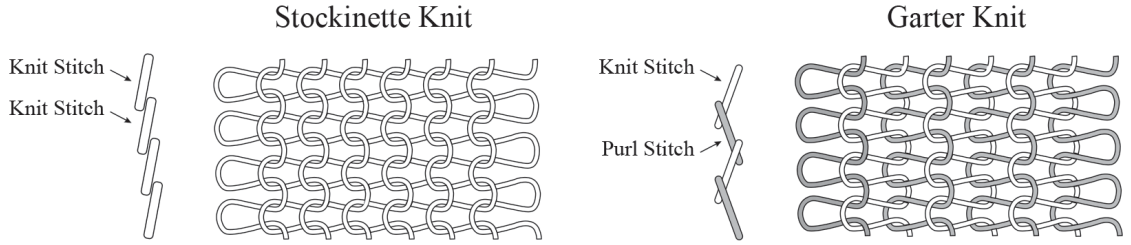

Figure 4.3: **Stockinette (Jersey) and Garter Knit Structures:** (left) Stockinette, or jersey, knitted structures are composed of successive rows of knit stitches, which are oriented with the peaks of each stitch facing the same side of the fabric. (right) Garter knitted structures are composed of alternating knit and purl stitches, meaning the peaks of each row of knitted loops face the reverse side of the fabric.

$$k_i = \frac{A_{l,m}}{d^2}[4] \tag{4.4}$$

Consequently, a high knit index (e.g. 138) describes an open-structure knit with large loops, whereas a low knit index (e.g. 38) describes a high-density knit with small, closely-packed loops.

Traditional force-displacement characterization has been conducted across a range of knits with systematically modified wire diameters and knit indices [4]. The results of this characterization show that increasing the wire diameter results in increased maximum mechanical work performance (i.e. displacement (δ) of an applied load (F_{app})). Additionally, increasing the knit index also increases %-actuation contraction at maximum work load ($F_{\hat{W}}$). In addition to approximating the on-body compression potential of contractile SMA knitted actuator fabrics, this research aims to expand prior force-displacement work to determine the effects of both geometric design parameters, identified by [4], on displacement-controlled actuation force.

4.3 Experimental Characterization

Actuation contraction of each contractile SMA knitted actuator fabric, hereafter referred to as active-contracting fabric was evaluated through a thermal blocked force test. The aim of this experimental characterization was to determine the displacement-controlled, blocked force response to increased temperatures. Because an active-contracting fabric CG would be composed of fabrics stretched and wrapped around a body, a displacement-controlled

test simulates a condition in which active-contracting fabrics are wrapped around the body at various strain levels and then actuated by a change in temperature.

Fig. 4.4 presents thermal blocked force (displacement-control) testing method in relation to cyclic heat cool (force-control) testing method conducted by [4]. Both test methods can be framed through common SMA superelastic curves that depict the behavior of austenetic SMA with incrementally increasing load (red line) and martensitic SMA with incrementally increasing load (blue line). While testing conducted by [4] evaluated the shape memory behavior of SMA knits under fixed applied loads and free displacement, this research evaluates the shape memory behavior of SMA knits under fixed displacements to characterize force change behavior. Graphically, thermal blocked force tests (displacement-control), blocked at lengths L_1, L_2, and L_3 are depicted by the vertical black arrows between $M_{L,1}$ and $A_{L,1}$, $M_{L,2}$ and $A_{L,2}$, and $M_{L,3}$ and $A_{L,3}$. Alternatively, prior cyclic heat-cool testing (force-control) can be depicted by the gray, horizontal arrows between A_{L_2} and M_{L_3}. Because the frictional qualities of both testing conditions are different, the martensite and austenite values deviate from classic superelastic curve; however, by conducting thermal force blocked tests at multiple lengths, we can see if displacement controlled knits follow the same general behavioral trends represented by superelastic curves. The following sections detail the testing setup and the experimental testing procedure.

4.3.1 SMA Knit Manufacturing

Active-contracting fabrics were manufactured with varying geometric design parameters (i.e. SMA wire diameter and knit index), according to [4], to capture a range of actuation performance. Additionally, each geometric design was applied to a stockinette and a garter knit so that performance between knit structures could be compared. Ten active-contracting fabrics, as detailed in Appendix 4.1, were fabricated in 15 course by 15 wale samples. These dimensions were chosen to mitigate boundary effects and ensure actuation force performance was attributable to the systematic varying of knitted structure and geometric design parameters [4].

All fabricated contractile SMA knitted actuators (garter and stockinette knits) were composed of Flexinol ®wire ($A_f = 90°C$ Dynalloy, Inc) in either 0.127, 0.203, or 0.381 mm diameter. The smaller diameter wires (0.127 mm, 0.203 mm) were knit on a Taitexma TH-860 manual knitting machine and the larger diameter (0.381 mm) on a Taitextma TH-260 machine. The TH-860 is composed of 200 latch needles with a standard needle spacing

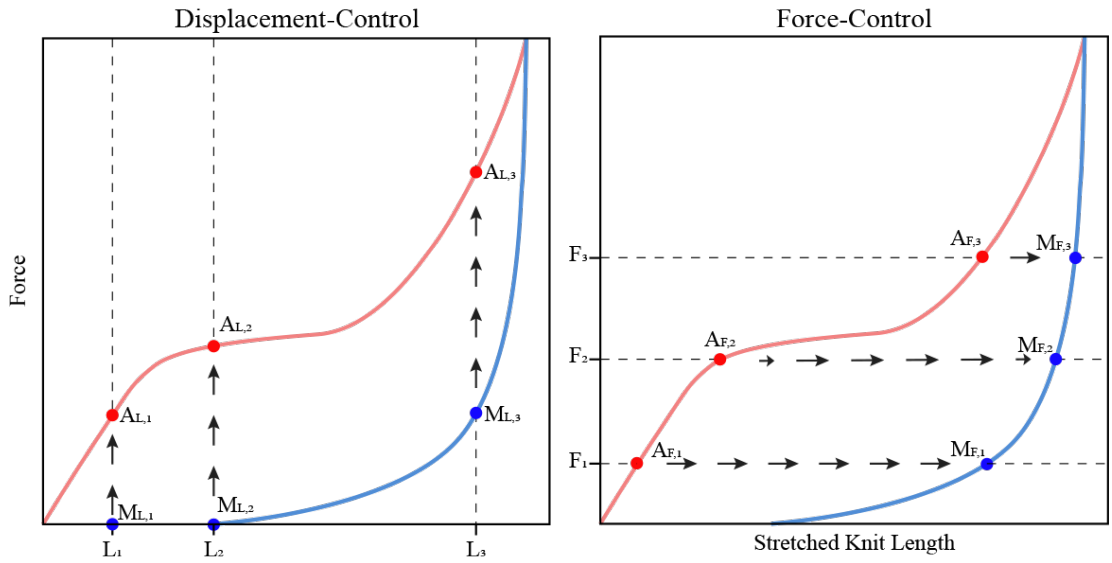

Figure 4.4: **Displacement-Control versus Force-Control Testing:** Hypothetical SMA knit curves are shown for illustrative purposes only. Displacement-control (thermal blocked force) tests evaluate the change in force between austensite and martensite phases when a specimen is fixed, or blocked, at a certain length. The force differential between $M_{L,1}$ and $A_{L,1}$ when blocked at length L_1 depicts the actuation force due to the shape memory effect. The actuation force varies based on length, as shown at L_1 (two arrows), L_2 (three arrows), and L_3 (four arrows). Force-control (cyclic heat-cool [4] tests evaluate the change in stretched knit length between austenite and martensite phases when a specimen is constrained by an applied load. The stretched length differential between $M_{L,1}$ and $A_{L,1}$ when constrained by F_1 depicts the actuation displacement due to the shape memory effect.

of 4.5 mm (standard gauge). The TH-260 is composed of 114 latch needles with a wide spacing of 9 mm. This wider needle spacing (larger gauge) was chosen for the 0.381 mm wire because it increased the imposed material bend radius. If knit on 4.5 mm needle bed, the 0.381 mm wire would experience concentrated stress points at the apex of each knitted loop due to a small bend radius inappropriate for the wire diameter. The change in knit index was accomplished by altering a machine setting which controls the length of wire fed into each knitted loop.

After fabricating 10 sample knits (see Table 4.1), each knit was loaded with their unique maximum work load, determined by [4] and exposed to 15 thermal cycles that transitioned from 20°C to 120°C over 40 minutes to stabilize performance hysteresis before characterization testing [8].

Table 4.1: **Specifications for Knitted SMA Actuator Samples Tested.**

knit type	diameter [mm]	knit index [mm/mm]	strain [%]	length [mm]
garter	0.127	124	0	36
			15	41
			30	47
			45	52
stocking	0.127	124	0	40
			15	46
			60	52
garter	0.203	138	0	16
			15	18
			30	20
			45	23
stocking	0.203	138	0	15
			15	17
			30	20
			45	22
garter	0.203	39	0	54
			15	62
			30	70
			45	78
stocking	0.203	39	0	54
			15	62
			30	70
			45	78
garter	0.381	124	0	101
			15	116
			30	132
stocking	0.381	124	0	102
			15	117
			30	132
			45	142
garter	0.381	64	0	50
			15	57
			30	65
			45	73
stocking	0.381	64	0	42
			15	48
			30	55
			45	61

4.3.2 Test Setup

Thermal blocked force tests were conducted with a custom, uniaxial tensile testing machine housed inside a thermal chamber (Cincinnati Sub Zero). A linear encoder (200 CPI, US Digital) collected displacement data while a 5-lb load cell (M34, Honeywell) collected force data. Multiple thermocouples were place inside the thermal chamber to gather temperature data in parallel with forces and displacements. To ensure even tension across the knitted loops during displacement, split rings (3/8" zinc-plated steel) were looped through the first and last loop of each knitted wale and subsequently loaded onto a rod that anchored the knit to the tensile machine. See Fig. 4.5.

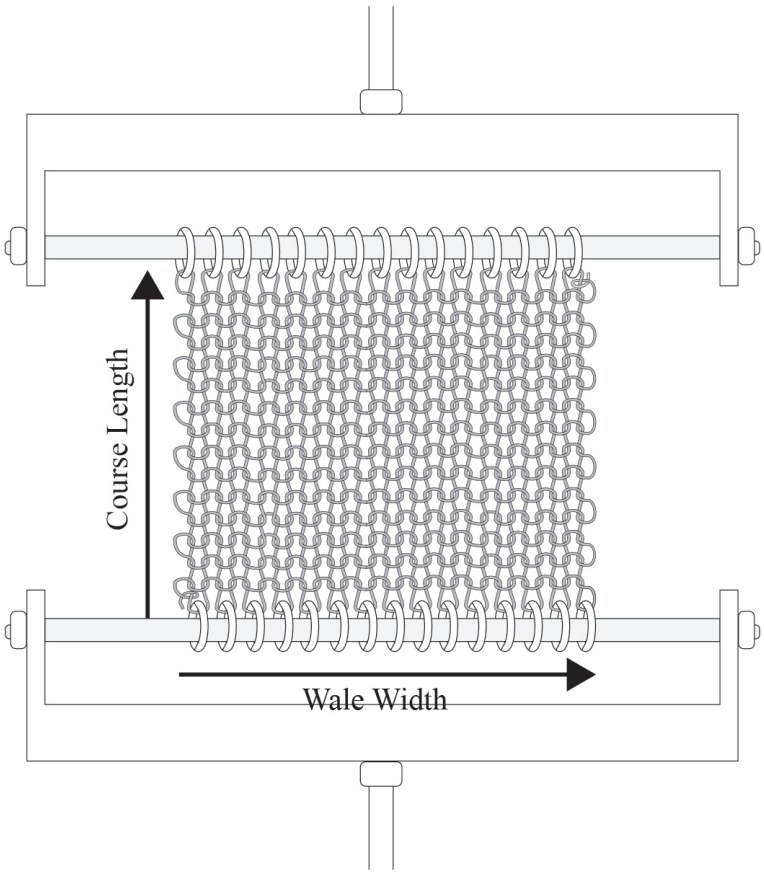

Figure 4.5: **Knit Sample Diagram:** Each knitted sample was composed of 15 knitted courses and 15 knitted wales. The first and last loop in each wale was held in place by a small split ring, which served at the attachment point to the tensile testing rig. Here, the length refers to the distance along increasing knit courses. Width refers to the distance along increasing knit wales.

4.3.3 Test Procedure

The thermal blocked force test was conducted by loading the knit sample into the tensile machine in ambient environmental conditions. Because the loops of a knitted structure shift in relation load and orientation, the best 'origin' length was to approximate a martensite free length (i.e. no load, $M_{L,2}$, Fig. 4.4). To locate the martensite free length, the knit sample was displaced until the load cell began to flicker between no-load and a slight-load reading. The distance between the two fixtures was then locked to prevent further displacement. This length at which the martensitic sample did not exert tension force was labeled the '0% strain' length. A limitation to this method is that martensite variants (i.e. twinned, detwinned) are were not identified in knitted SMA samples, potentially causing length discrepancies between samples. Detwinned, or partially detwinned samples would results in increased, or exaggerated martensite free length. Detwinning could occur during the mechanical knitting process or post-manufacture handling.

Once loaded in the tensile machine and blocked in length, the knit sample was exposed to thermal cycles (20°C $\rightarrow$ 120°C) to induce phase-change. The chamber was heated to 120°C over 10 minutes. The knit sample soaked for 15 minutes to ensure the specimen had reached A_f. The chamber was then cooled to 20°C over 10 minutes and remained cool for an additional 5 minute martensite soaking period. The thermal cycle, depicted in Fig. 4.6, was repeated three times for each blocked length.

After conducting a thermal blocked force test on the knit sample at 0% strain, the sample was further displaced and tested at 15%, 30%, and, 45% strain. While the choice of strain % from 0 was designed to cover the full range of potential strain (from no-strain to max-strain), some samples were not capable of reaching 45% strain while others could have been displaced above 45% strain. The choice to begin testing at low strains and gradually increase to higher strains was chosen to prevent plastic martensite deformation that would permanently shift performance curves to the right. Because each knit was pre-cycled at a low load before testing to stabilize performance hysteresis (see Section 4.3.1), performance drift was not likely to occur throughout testing. Table 4.1 presents a summary of samples tested along with blocked lengths.

4.3.4 Experimental Results

The results of the thermal blocked force tests for 10 active-contracting fabrics at multiple lengths were first evaluated in terms of their force-temperature relationship. Figs 4.7 and

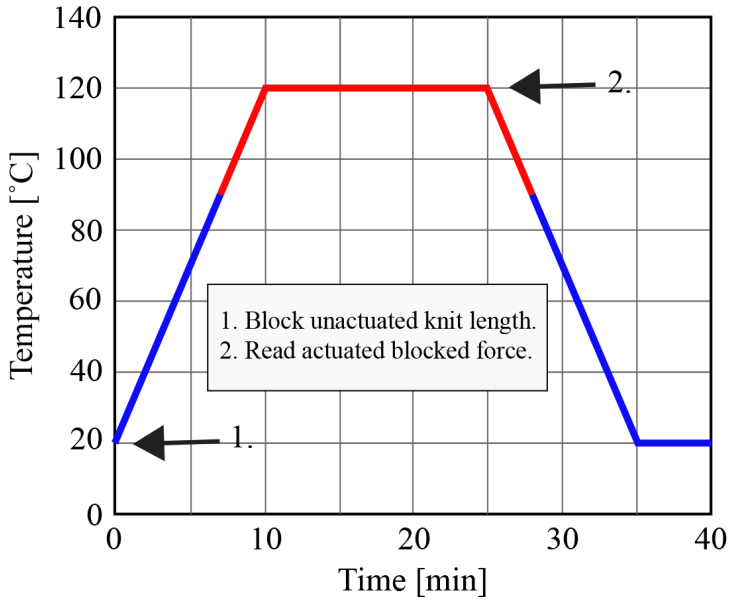

Figure 4.6: **Thermal Blocking Force Test Procedure:** (1) The test sample was placed between the tensile fixtures and locked at a desired length in ambient environmental conditions (martensite). The surrounding environmental chamber was heated to 120°C over 10 minutes and followed by a 15 minute austenite soak. The the force at A_f was collected at the end of the soak (2) and the chamber was cooled back 20°C over 10 minutes. After a 5 minute M_f soak, the cycle was repeated two additional times.

4.8 depicts a clear force response to controlled changes in temperature for all 10 knit architectures. The force path of each knit at 0% strain is depicted in light gray, while subsequent stretch lengths are depicted in successively darker tones. Garter knits are positioned on the left with their equivalent stockinette parter positioned on the right. Arrows are used to depict the cyclical direction of the force-temperature path. Certain knits (usually those at higher strain) deviated from their cyclic path upon initial actuation. In these cases, the initial pre-tension at ambient loading is depicted as a solid dot and a dashed line traces the path before merging with the repeated trajectory.

Maximum actuation forces from the force-temperature plots depicted in Figs. 4.7 and 4.8 (austenite force - martensite force) are further evaluated in terms of knit type (stockinette, garter) and geometric design parameters (wire diameter, knit index). Fig. 4.9 presents the actuation force of each knit sample in relation to varying (A) wire diameter and (B) knit index. The correlation plots shows a clear increase in actuation force with an increase in wire diameter. Additionally, garter knits (•) generally have larger actuation forces than

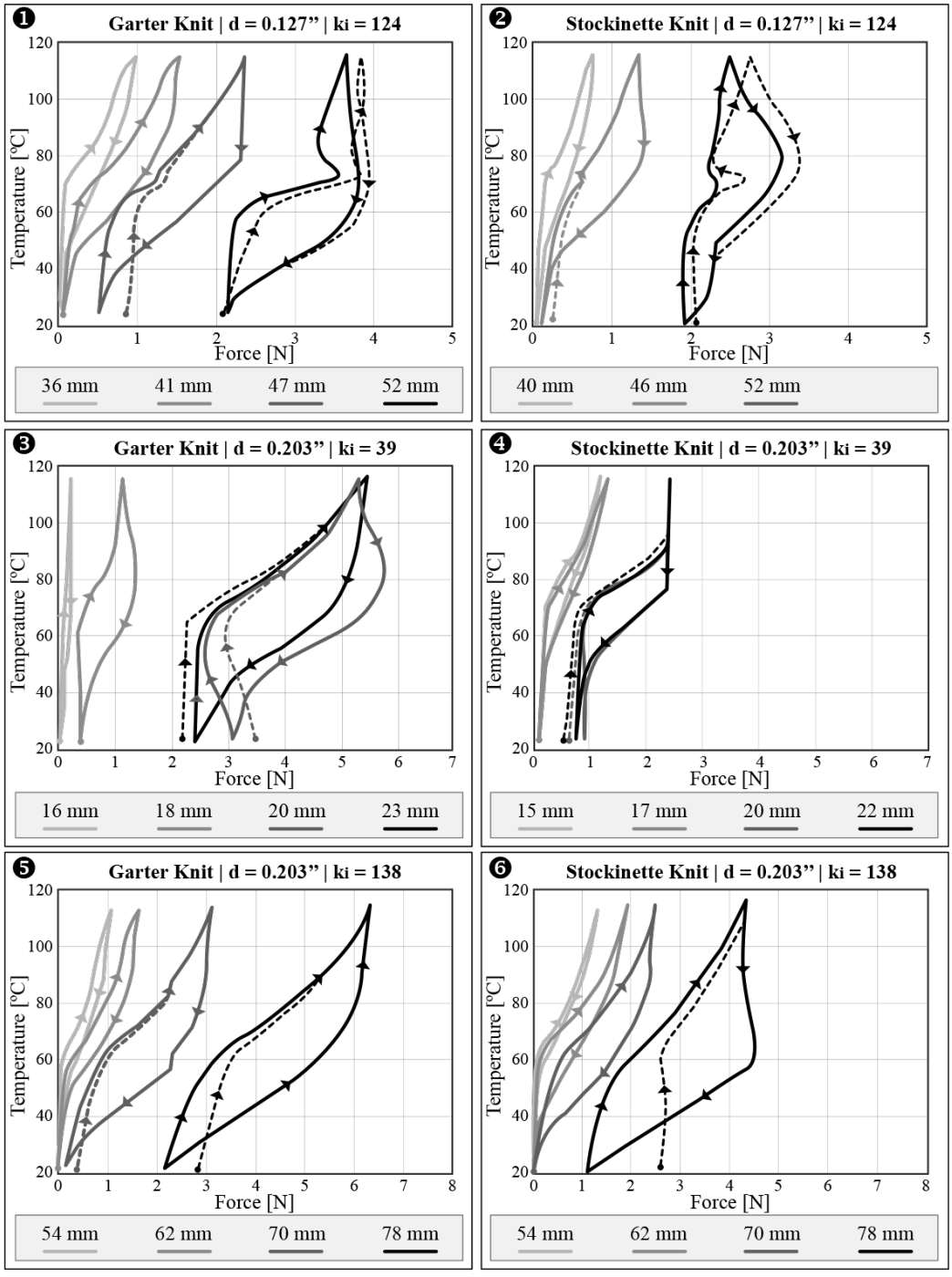

Figure 4.7: **Temperature-Force Relationship of Active-Contracting Fabrics at Different Blocked Lengths [mm]:** Samples 1-6. See next page for samples 7-10. Arrows represent direction of cyclic heat-cool path. Dot (•) represents starting martensite tension and dashed line (- -) represents initial path before merging with solid, cyclic path.

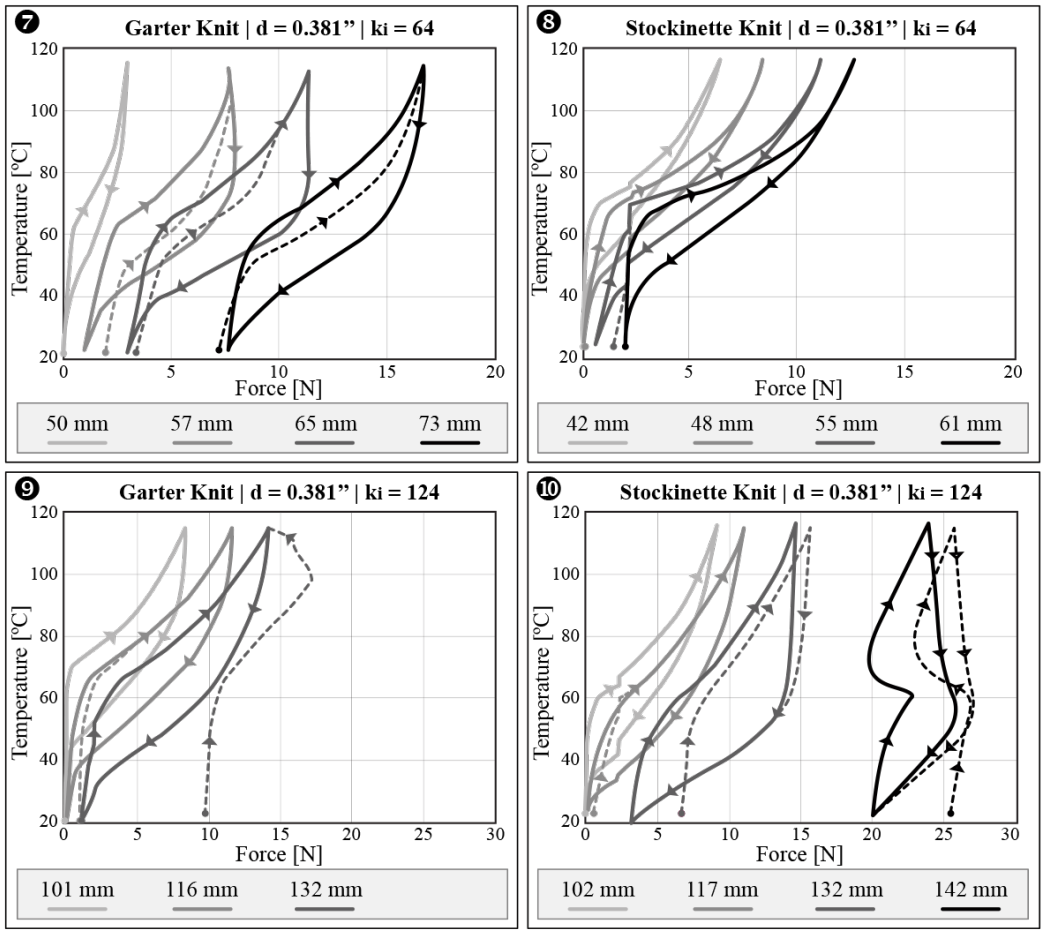

Figure 4.8: **Temperature-Force Relationship of Active-Contracting Fabrics at Different Blocked Lengths [mm]:** Samples 7-10. See previous page for samples 1-6. Arrows represent direction of cyclic heat-cool path. Dot (•) represents starting martensite tension and dashed line (- -) represents initial path before merging with solid, cyclic path.

their stockinette knit (o) counterparts, with the exception of one comparison (d = 0.381, k_i = 64) where a greater stockinette length was achieved (stockinette max length = 142 mm; garter max length = 132 mm). It is likely that if the knits were both strained to the same length, the garter would reach a slightly higher actuation force, a trend that is observed in other sample comparisons strained to the same length.

The significance of knit index is evaluated in Fig. 4.9B. While the results initially look scattered, arrows are added to show that, between knits of the same wire diameter, increasing the knit index appears to increase the actuation force. A major limitation to this preliminary analysis is that only two wire diameters (0.381 mm; 0.203 mm) have modified

knit indices (124, 64; 138, 39). Furthermore, only two knit indices are included for comparison. To fully evaluate the relationship between knit index and actuation force, it is recommended that several wire diameters are knit into 3-5 different knit indices for testing.

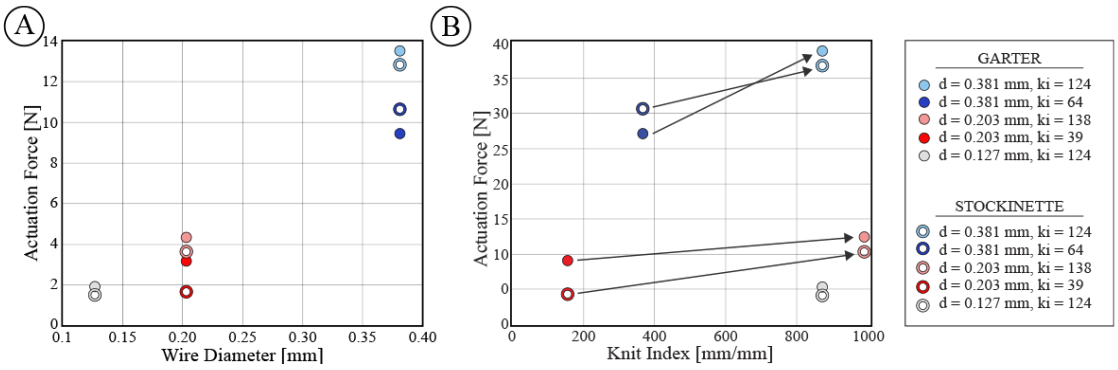

Figure 4.9: **Effects of Wire Diameter and Knit Index on Actuation Force:** (A) Actuation force (austenite force - martensite force) increases linearly with increasing wire diameter. (B) Actuation force appears to increase with an increase in knit index for a given wire diameter; however, more variation in knit index per wire diameter is needed to evaluate this relationship.

While the previous analysis only considers the maximum actuation force of each knit at a given length, the significance of knit length strain (as depicted in Fig. 4.4) is further evaluated in Figs. 4.10 and 4.11. Here, the minimum and maximum observed forces at each blocked length for all knit samples are mapped. The amalgamation of blocked tests show fragments of material curves that resemble traditional SMA superelastic curves. These curves generally exhibit minimal hysteresis at low forces, increased hysteresis at medium forces, and maximum hysteresis before austenite and martensite curves merge. The results show that martensite pre-tensioning enables contractile SMA knitted actuator fabrics to reach their maximum actuation forces, as well as add to the total applied force.

4.3.5 Dimensional Scaling

To determine the implications of the thermal blocked force test results, a preliminary study was conducted to determine the effects of scaling on active-contracting fabric actuation force. One knit (garter, d = 0.203 mm, k_i = 138 mm/mm) was fabricated in three different dimensions: (1) 15 courses by 15 wales (sample size), (2) 30 courses by 15 wales, and (3) 15 courses by 30 wales. The dimensions of each knit are depicted in Fig. 4.12. Each knit was characterized by thermal blocked force testing at 0% strain, as described in Section

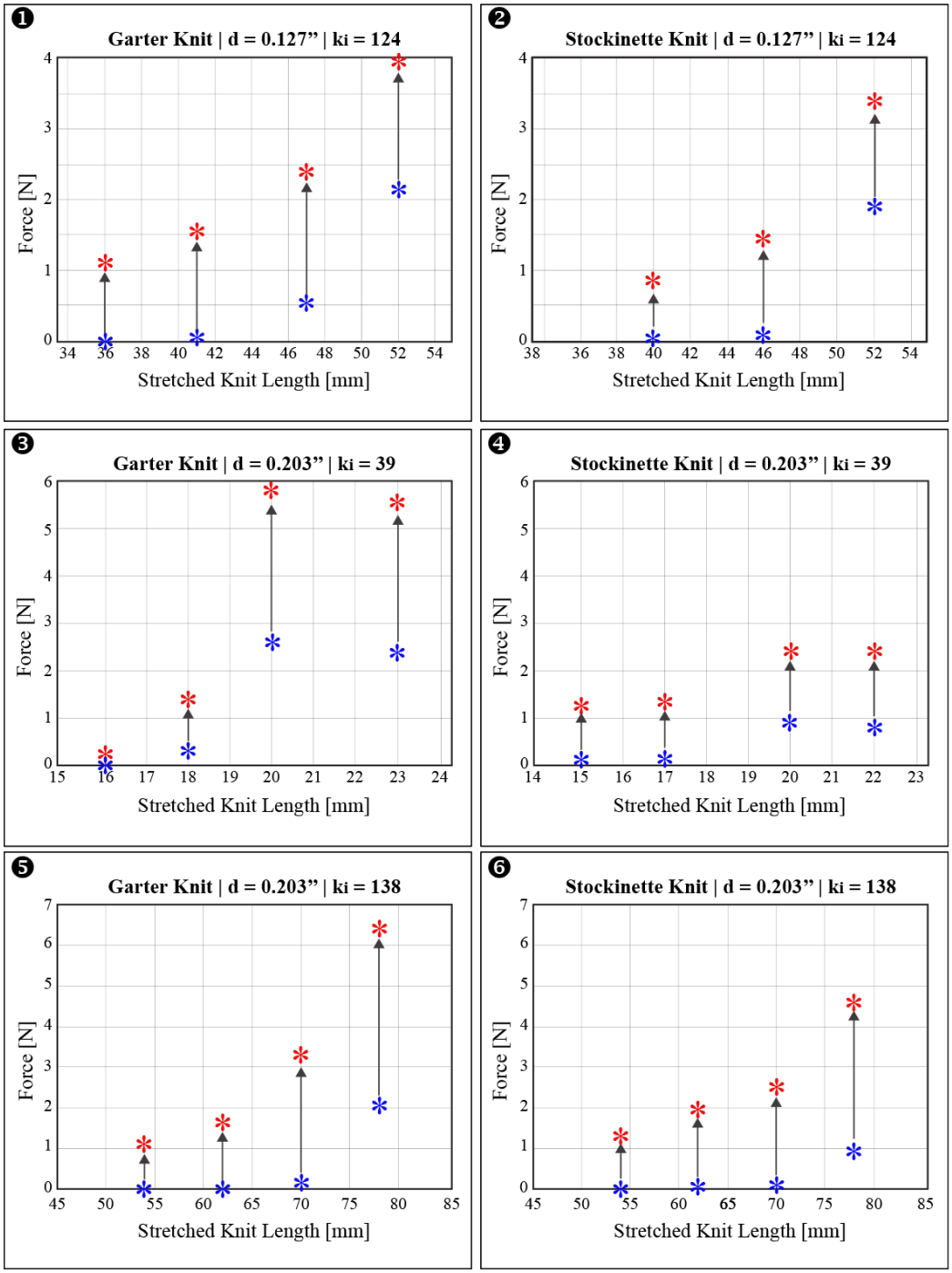

Figure 4.10: **Minimum Martensite and Maximum Austenite Oberved Force Per Fabric Length:** Samples 1-6. See next page for samples 7-10. Red asterisk represents the maximum force observed at a given length. Blue asterisk represents the minimum force observed at a given length. The upward arrow represents the force path between martensite (blue) and aurtenite (red) forces.

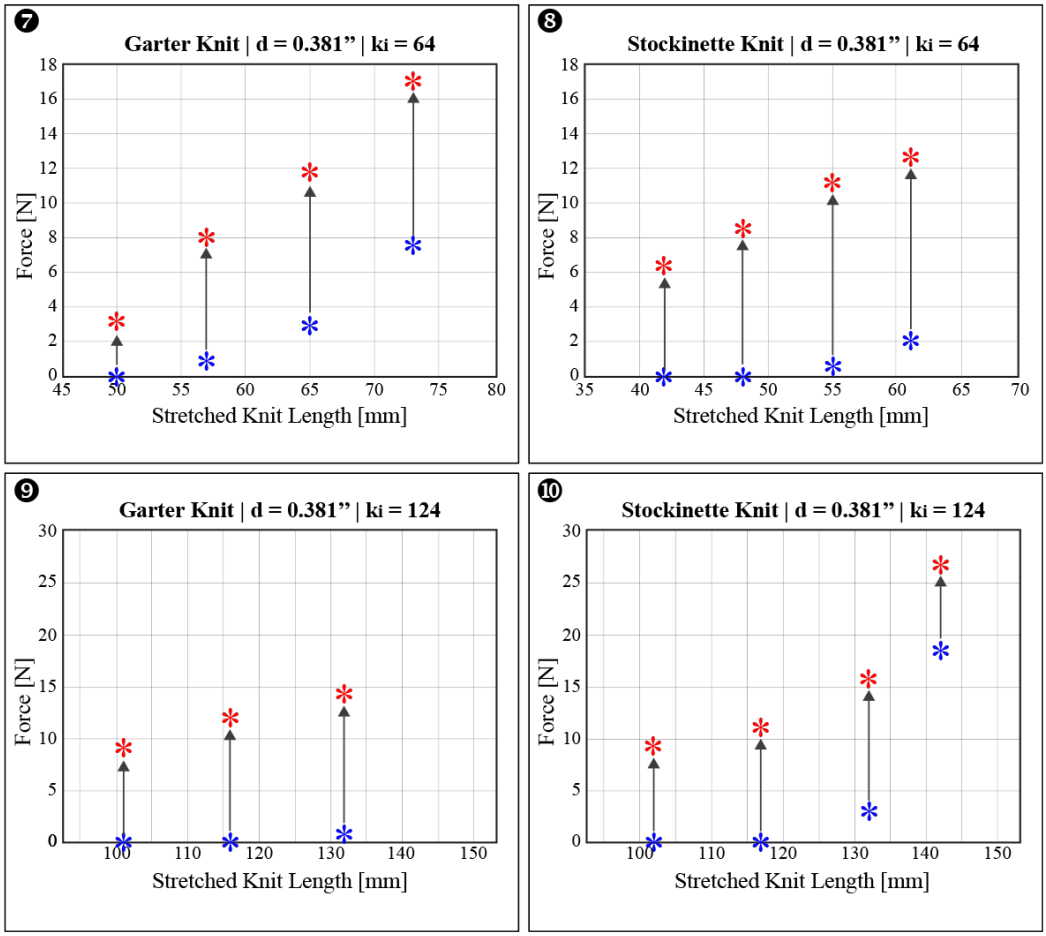

Figure 4.11: **Minimum Martensite and Maximum Austenite Oberved Force Per Fabric Length:** Samples 7-10. See previous page for samples 1-6. Red asterisk represents the maximum force observed at a given length. Blue asterisk represents the minimum force observed at a given length. The upward arrow represents the force path between martensite (blue) and aurtenite (red) forces.

4.3.3. Fig. 4.12 depicts the effects of scaling on actuation force. When knitted wales were doubled, the actuation force increased over 100%; however, doubled courses resulted in the same actuation force as the sample knit (15 courses by 15 wales). An analogy can be made to passive spring forces arranged in series or parallel. Adding springs (knit loops) in series (knit courses) does not increase forces; however, adding springs (knit loops) in parallel (knit wales) does increase forces.

As depicted in Fig. 4.13, contractile SMA knitted actuator fabric must be oriented with increased wales along the height of limbs and increased courses spanning the circumference of the limbs to apply circumferential compression. This orientation results in scaled forces as the garment becomes longer (i.e. ankle height vs thigh height); however, adding courses to increase the circumference does not increase actuation forces. A simple analogy can be made to spring architectures, which scale force in parallel, but not in series.

While the actuation forces observed during sample testing (15 courses by 15 wales) remain constant when courses are added or subtracted to wrap around changing body circumferences, adding and subtracting courses are critical to manipulating garment dimension in relation to body dimension; Adding or subtracting loops courses modifies the amount of strain that is required to wrap that fabric around the body. Consequently, while adding knitted courses of active material does not, in itself, increase actuation force, circumferential length manipulation of a garment is crucial in tailoring actuation forces.

The number of knitted courses used to make a CG ($\#_g$) can determined by Equations 4.5 and 4.6,

$$\frac{\#_s}{l_{ss}} = \frac{\#_g}{l_c} \tag{4.5}$$

$$\#_g = \frac{l_c * 15}{l_{ss}} \tag{4.6}$$

where the body circumference length (l_c) and the number of courses needed to make the strained garment ($\#_g$) are directly proportional to the length of the strained sample (l_{ss}) and the number of knitted courses used to make that sample ($\#_s = 15$).

4.4 Implications for Wearable Compression Applications

The following sections discuss the implications of the previous tests on CGs designed for the lower body with active-contracting fabrics. The evaluation proceeds with an approximation of maximum on-body compression capabilities as well as the suitability of active-contracting fabrics for on-body compression applications.

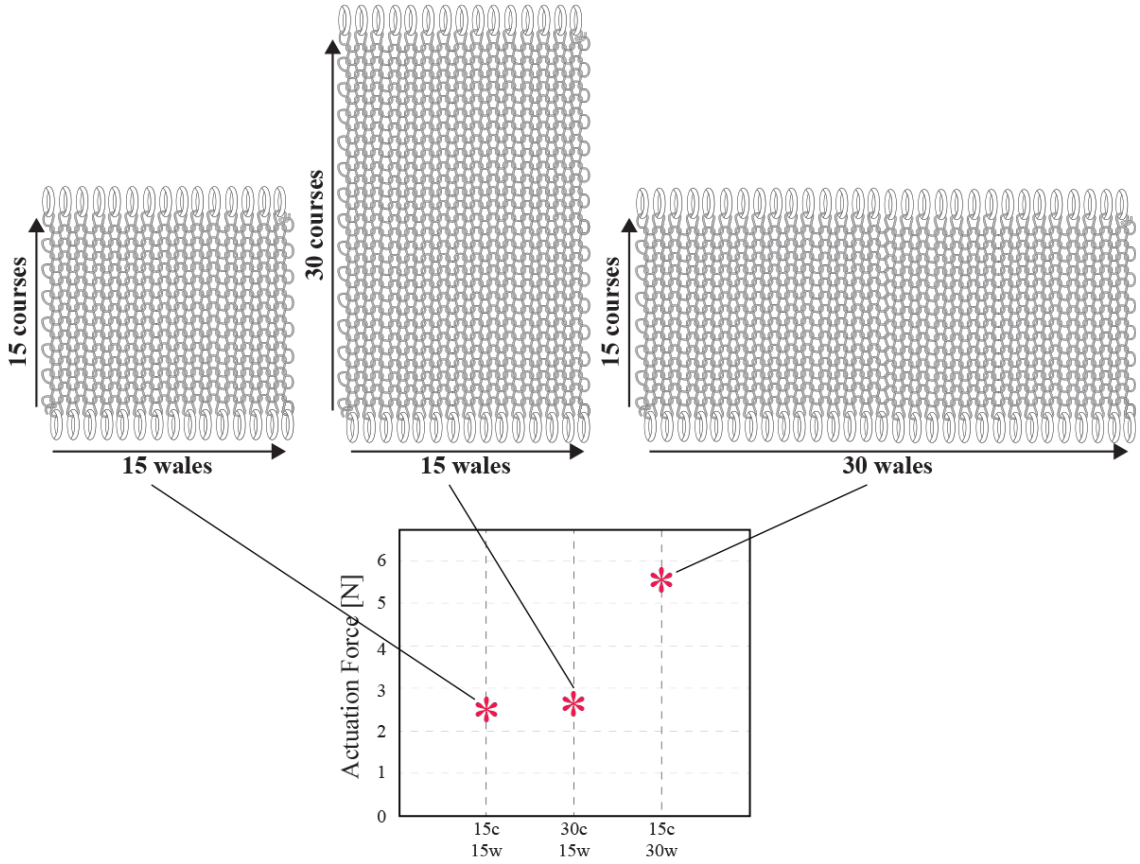

Figure 4.12: **Scaling Active-Contracting Fabrics:** One active contracting fabric architecture (garter, d = 0.203 mm, k_i = 138 mm/mm) was evaluated in terms of changing loop dimension. The blocked force at 0% strain of a 15 course by 15 wale knit (sample dimensions) was approximately equivalent to the blocked force at 0% strain of a 30 course by 15 wale knit. Alternatively, the blocked force of a 15 course by 30 wale knit was over twice that of the other knits. These results suggest that actuation forces scale in wale width, but not in course length.

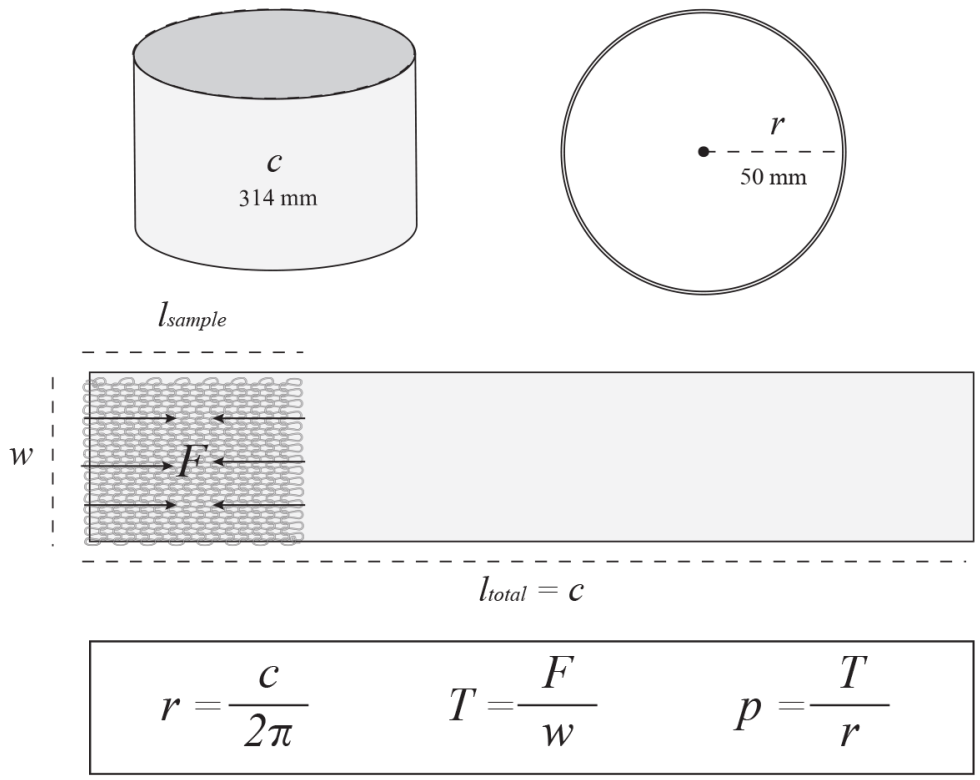

Figure 4.13: **Garment Pressure Calculation:** Garment pressure (p) [Pa = N/m^2]can be approximated by fabric unit tension (T) [N/m] per cylindric radius (r) [m]. Because active-contracting fabric forces do not scales in the course length, the ratio of the observed force and width of the 15 course by 15 wale sample at a given strain are used to calculate fabric unit tension.

4.4.1 Approximate On-Body Pressure Capabilities

To translate maximum actuation force data from active-contracting fabrics into approximate on-body compression data, the undersized CG equations are used (Equations 4.2, 4.1, and 4.3). While prior research has found that mathematical approximations of on-body pressure are not accurate because they assume rigid bodies and perfect cylinders when the body is in fact compliant and non-uniform in topography [6, 73, 74], these equations provide estimations that are useful in the design process. Furthermore, Equations 4.2, 4.1, and 4.3 are standard regulation in the design of commercial CGs [75]. The use of these equations for active-contracting fabric CG pressure calculation is depicted in Fig. 4.13. The range of limb radii used in these calculations were collected from SizeUSA data and span from 0.04 m (minimum leg circumference) to 0.17 m (maximum hip circumference). As shown

in Table 4.2, the unit tension (T) [N/m] of each fabric sample (actuated and unactuated) was determined through the ratio of observed force (at maximum actuation strain) [N] and wale width [m].

Table 4.2: **Fabric Unit Tensions Values for Actuated and Unactuated Samples:** .

structure	**d [mm]**	k_i $[\frac{mm}{mm}]$	F_M **[N]**	F_A **[N]**	**w [mm]**	T_M $[\frac{N}{m}]$	T_A $[\frac{N}{m}]$
garter	0.127	124	2.15	3.95	32	67	123
stocking	0.127	124	1.90	3.45	30	63	115
garter	0.203	138	2.05	6.45	48	43	134
stocking	0.203	138	0.95	4.60	45	21	102
garter	0.203	39	2.60	5.75	67	39	86
stocking	0.203	39	0.80	2.55	60	13	43
garter	0.381	124	0.80	14.40	83	10	173
stocking	0.381	124	3.00	26.95	75	40	359
garter	0.381	64	7.60	17.05	100	76	171
stocking	0.381	64	2.05	12.70	105	20	121

As shown in Fig. 4.14, the results of the calculation show that active-contracting fabrics are capable of reaching unit tension between 43 and 359 N/m when actuated at their maximum force length. When this range of unit tension values are evaluated in terms of changing body radii, the maximum actuation pressures range from 15 mmHg (2 kPa) at the mean hip circumference (men, SizeUSA) to 65 mmHg (9 kPa) at the mean minimum leg circumference (women, SizeUSA). One knit (stockinette, d = 0.381 mm, K_i = 124) is noticeably higher in both unit tension and pressure values than other knits because, compared to other knit made of high-force 0.381 mm wire, the blocked length was at a point in the material curve where a sharp rise and merging of austenite and martensite curves can occur, as shown in Fig. 4.4, L_3 and Fig. 4.11, plot 10. Because the maximum force length of this knit has very little actuation contraction, as shown in Fig. 4.11, plot 10, the results can be presented without this sample; in this case, the maximum unit tension values range from 43 to 173 N/m and maximum pressures of 8 mmHg at the mean hip circumference (men, SizeUSA) and 30 mmHg at the average minimum leg circumference (women, SizeUSA).

While Equation 4.3 does not factor in body complexities outlined in Fig. 4.2, the results of the mathematical approximation of on-body pressure provide information about

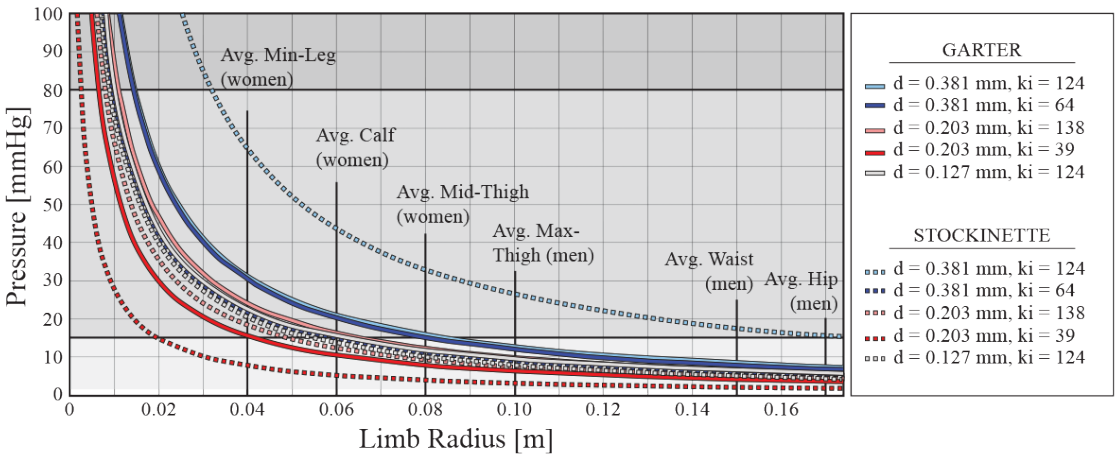

Figure 4.14: **Approximated On-Body Compression Achievable with Contractile SMA Knitted Actuator Fabrics at Maximum Force Potential:** Pressure has an inverse and non-linear relationship with changing body radius. Average body dimensions gathered from SizeUSA are depicted to show how much pressure could be exerted around those circumferences. While 30-60 mmHg is achievable on minimum leg circumferences, less than 15 mmHg are achievable on largest areas of the lower body, like hip girth.

the range of applications that may be suitable for contracting SMA knitted actuator fabrics. Consumer and sports applications that require compressive forces under 15 mmHg are well met by the breadth of single-layer knitted architectures that are evaluated here. Additionally, certain medical applications that require low-levels of medical pressure (i.e. 15-30 mmHg) on the lower-legs (possibly POTS and OH) could benefit from this technology without significant development. Other medical applications (OI, DVT, lymphedema) that require higher medical pressures could reach higher forces by further increasing wire diameter, increasing knit index, and/or layering active-contracting fabrics. While Section 4.3.5: Dimensional Scaling depicts the effects of scaling active-contracting fabrics in the x- and y-axes, it is common for fabrics to be scaled in the z-axis (layering) in CG design [76, 77]. Additionally, prior work has found that scaling in the z-axis approximately doubles active-contracting force potential [78]. Consequently, the results show that a double-layered system could produce pressures between 15 and 65 mmHg from the mean hip circumference (men, Size USA) to the minimum-leg circumference (women, SizeUSA), respectively. This calculation assumes a maximum active-contracting fabric unit tension of 173 N/m (actuated). Furthermore, a three-layers system could produce between 23 and 97 mmHg.

A significant advantage to an active-contracting fabric approach to CGS design is that

unactuated garments, even those that are designed with up to three layers, will not exert over 10 mmHg on the body. This calculation assumes a maximum active-contracting fabric unit tension of 76 N/m (unactuated). The ability of fully functional fabrics to transition from less than 10 mmHg to 97 mmHg on the body through a change in temperature is unprecedented and compels further exploration into applications from aerospce orthostatic intolerance garments to commercially available, medical compression garments.

4.5 Conclusion & Future Work

On-body compression is desired for medical, sport, and general consumer use. Current pneumatic and undersized CG technologies have several functional limitations that demand further development. Active-contracting fabrics, specifically contractile SMA knitted actuator fabrics, could provide low-profile, dynamic compression to satisfy this technology gap.

This work evaluated active-contracting fabrics in terms of their displacement-controlled actuation force capabilities. To observe a breadth of performance (i.e. actuation contraction), geometric parameters identified in [4] were systematically modified. The results conclude that increased wire diameter increases actuation force. Additionally, higher actuation forces were observed at higher strains, suggesting future active-contracting CGs will require pre-tensioning (i.e. pulled snugly to the body) to achieve maximum potential pressures.

Furthermore, the pressure performance active-contracting fabrics was approximated through the Law of Laplace and common hoop stress equations. The analysis estimated that maximum pressure of 30-65 mmHg are achievable on minimum leg circumferences (average woman, SizeUSA), while maximum pressures were calculated 15 mmHg around the hips (average man, SizeUSA) due to larger cylindrical radii. These approximated values suggest that active-contracting knits could be used in the design of low-pressure, consumer apparel ($<$ 15 mmHg) and low-pressure, medical compression socks (15-30 mmHg, knee high). If these fabrics are doubled, maximum pressures between 60 and 130 mmHg could be observed. More research should be conducted to determine the effects of layered fabrics on actuation forces. Additionally, further scaling testing with strained fabrics is required to understand how this configuration increases actuation forces.

Future work will investigate methods to increase actuation forces of active-contracting fabrics in an attempt to reduce system mass to one layer. Additionally, SMA materials

should be developed to actuate a lower temperatures, specifically at ambient or slightly above skin temperature. Finally, systems-level work will be conducted to build active-contracting CG prototypes which can be evaluated with pressure sensors. The following chapter discusses this future work in detail and provided an in depth discussion of future systems design using active-contracting fabrics characterized here.

Chapter 5

High-Displacement Fabrics for Self-Fitting, Self-Stiffening Wearables

The design and development of self-fitting, self-stiffening wearables was a collaborative research effort with Kevin Eschen, Ph.D. candidate within the University of Minnesota's Mechanical Engineering Department. The initial research was compiled as a conference manuscript, Active-Contracting, Variable-Stiffness Fabrics for Self-Fitting Wearables [22], presented at the 2018 ASME Conference on Smart Materials, Adaptive Structures, and Intelligent Systems (SMASIS) in San Antonio, Texas. Sections on research motivation, anthropometric analysis, and garment manufacturing are included here to frame our collaborative work within this thesis work. Figures created and sections written by K. Eschen, such as the background on SMA knitted actuator fabrics and prototype validation, will simply be referenced in this text. At the end of the chapter is supplemental analysis that evaluates the implications of self-fitting garments for consumer population fit challenges.

5.1 Introduction

Self-fitting is the ability of a wearable, garment or body-mounted object to recover the exact shape and size of the human body. Self-fitting is highly desirable for wearable applications, ranging from medical and recreational health monitoring to wearable robotics and haptic feedback, because it enables complex devices to achieve accurate body proximity, which

is often required for functionality. While garments designed with compliant fabrics can easily accomplish accurate fit for a range of body shapes and sizes, integrated actuators and sensors require fabric stiffness to prevent drift and deflection from the body surface. This paper merges smart materials and structures research with anthropometric analysis and functional apparel methodologies to present a novel, functionally gradient self-fitting garment designed to address the challenge of achieving accurate individual and population fit.

This fully functional garment, constructed with contractile SMA knitted actuator fabrics, exhibits tunable percent actuation contraction between 4-50%, exerts minimal on-body pressure ($\leq$ 10 mmHg) and can be designed to actuate with body heat. The primary challenge in the development of the proposed garment is to design a functionally gradient system that does not exert significant pressure on part of the leg and/or remain oversized in others. Our research presents a new methodology for the design of contractile SMA knitted actuator garments and concludes with statistical analysis of garment performance evaluated through three-dimensional marker tracking.

5.2 Anthropometry & Garment Fit

Garment fit is defined as the relationship between garment dimensions and body dimensions [23]; consequently, the design of a self-fitting garment necessitates an investigation of the garment-body interface. Anthropometry, or the study of the size and shape of the human body [79], provides the foundation for fit analysis. The following sections map the challenges of achieving fit with current anthropometric resources and apparel design methodologies.

5.2.1 Anthropometry of the Lower Extremities

While garments are ubiquitous and methods for producing mass garments are well established, fit challenges are pervasive in the consumer market. Fit challenges are further magnified in the design and distribution of advanced functional apparel [2]. As shown in Figure 5.1, using anthropometrics as the basis of garment patterns is a challenge in terms of intra- and inter-subject variability. Cross-sections taken from CAESAR body scans show that the human leg is highly irregular in form, specifically, not cylindrical, from the ankle to the knee. Furthermore, these non-cylindrical cross-sections are not consistent across the population. Common measured body dimensions (e.g. lengths, circumferences) available in most anthropometric databases used in the apparel industry (e.g. SizeUSA [1]) do not

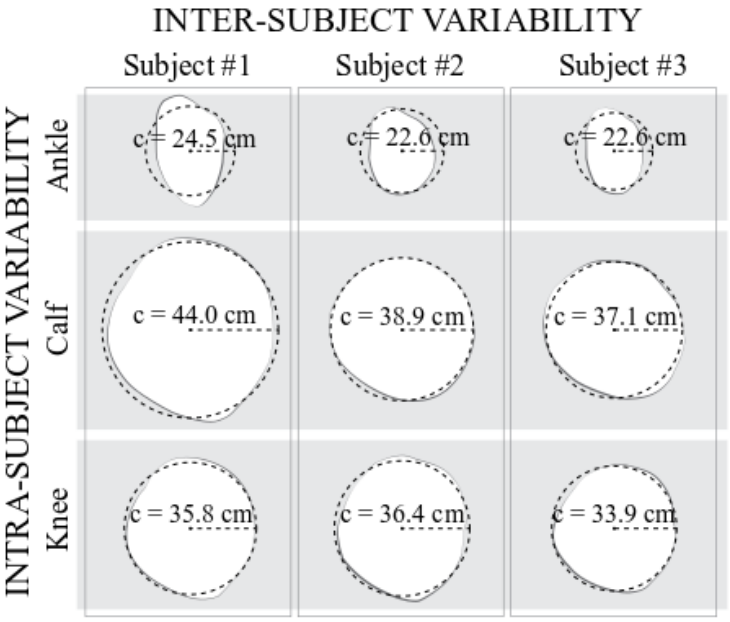

Figure 5.1: **Inter- and Intra-Subject Anthropometric Variability:** Cross-sections taken from randomly selected male subjects from the Civilian American & European Surface Anthropometry Resource.

provide topographical or morphological data. Consequently, apparel designers make stylish simplifications to body shape and size that are discussed further in Section 4.2.2. Advanced databases (e.g. ANSUR II, CAESAR) incorporate three-dimensional data to enable complex analysis of body volume and morphology; however, body scanning is rarely used in the industrial production of garments because the technology is time-consuming and costly [2]. New methods of automation that enable rapid response need to be conceptualized before body-scanning can enable mass-customization of wearables. [80].

Additionally, the dimensional variability within the population is complex without considering topographical differences [2]. As shown in Figure 5.2, the apparel industry generally achieves population fit by determining correlations between key body dimensions. These key dimensions are determined through statistical methods, such as principal component analysis (PCA), cluster analysis, or decision tree analysis [81]. Even amongst dimensions with a high correlation (hip dimensions, waist dimensions; $r = 0.89$) [81], technical garment designers are only able to pattern garments to fit a small portion of the population, as depicted by the solid-line, boxed size categories (e.g. small, medium, large, etc.) in Figure 3.2. The unboxed circles in Figure 3.2 represent the vast portion of the population that

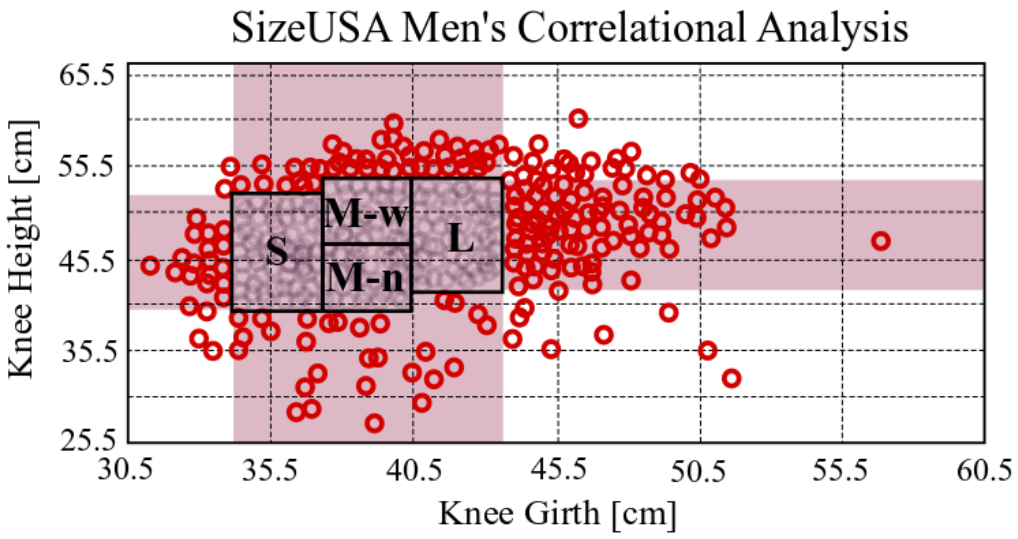

Figure 5.2: **Sizing for Apparel Market:** Mass produced garments are designed to fit the public by forcing a correlation between two or more body dimensions and blocking out sizes categories (e.g. small (S), medium-narrow (M-n), medium-wide (M-w), large (L)), as depicted by the solid black boxes. This method results in major portions of the population un-fit, as depicted by the red points outside of the chosen size categories. [1]

remains unaccommodated, or unfit by the identified size categories. Strategies to improve fit for an individual as well as for a population are discussed in the following section.

5.2.2 Garment Fit

To accommodate anthropometric variability, apparel designers traditionally take one of four approaches. (1) Garments can be designed with compliant fabrics using elastane fibers such as in leggings or leotards. These stretch garments are generally designed with undersized dimensions, called negative ease, so that the garment stretches around the body to achieve a close fit in each size group. The range of dimensional variability that can be accommodated in each size group is dependent on the strain properties of the fabric chosen. (2) Another method is to design garments with non-compliant fabrics and produce a large number of sizes; however, this option is prohibitively complex in terms of both production and purchasing logistics. (3) A frequently used alternative is to increase garment dimensions so that the garment is slightly oversized. The amount of added garment dimension, called positive

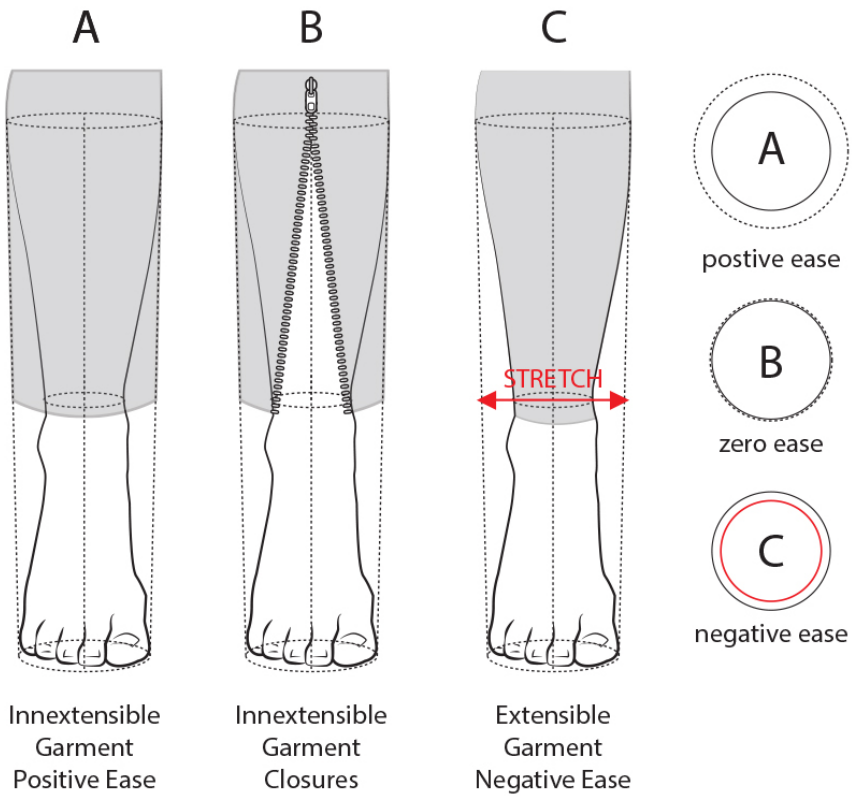

Figure 5.3: **Garment Don/Doff Design Logistics:** (A) Inextensible garments must be designed with positive ease to traverse the foot, or (B) inextensible garment must be designed with closures (e.g. zipper) that can open for don/doff and close to achieve fit. (c) Fitted garments can also be made with extensible fabrics that strain to traverse the foot. These garments are designed with negative ease to ensure fit.

ease, determines the amount of anthropometric dimensional variability a garment can accommodate. Consequently, oversized t-shirts designed in three sizes may fit a larger portion of the population than a fitted dress shirt in six sizes due to the amount of garment ease that is aesthetically desired in that garment. (4) Another, frequently used alternative is to incorporate adjustable closures (e.g. lacing, hooks, snaps) into a non-compliant or limited-compliance garment [2]. While all approaches are suitable for general consumer garments with only mobility, comfort, and aesthetic requirements, garments with enhanced functionality (e.g. wearables with actuators or sensors) often require complex size-adjustability mechanisms to achieve a close fit when garment stiffness is required [2].

In addition to enabling adjustability, closures are critical design features to facilitate don/doff without garment dimensional compliance or positive garment ease. As shown in

Figure 5.3, while the ankle opening of a pair of stretch leggings can strain as the foot passes through (Figure 5.3C), a pair of non-compliant dress trousers must be designed with added dimension, called positive ease, to enable don/doff (Figure 5.3A). If a pair of trousers are designed to fit tightly around the ankle, there must also be a side closure (e.g. zipper, snaps) that can be released as the foot passes through and refastened to achieve fit (Figure 5.3B).

Alternatively, we propose the use of active-contracting, variable-stiffness fabrics as a new design approach to achieve fit and stiffness without the use of closures. As shown in Figure 5.4, the ideal design is compliant and oversized in circumference until the garment has been donned. Once around the body, the garment contracts and stiffens fully self-powered with body heat. Percent actuation contraction is designed to achieve fitting to body dimensions without surpassing pressures of 10 mmHg, which is common garment pressure (e.g. socks) and below minimum medical pressures ($\geq$ 18 mmHg) [59].

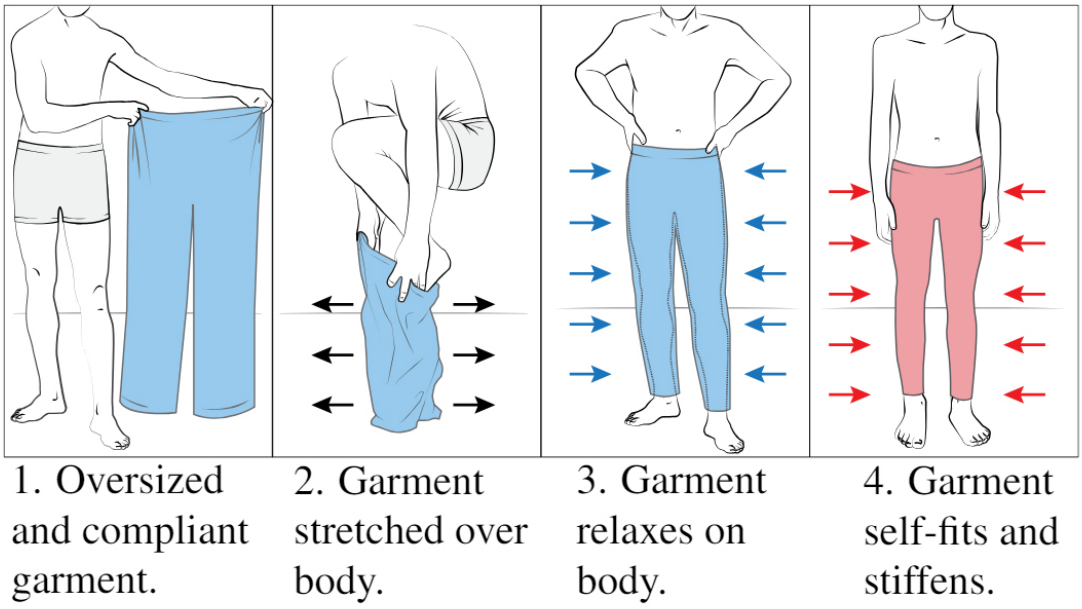

Figure 5.4: **Proposed Self-Fitting Garment:** (1) The proposed garment is compliant and oversized before don. (2) During the donning process, the compliant garment is stretched out further as it is pulled over the limbs. (3) Once on the body and free of external forces, the garment slightly relaxes around its new form (4) The garment then warms to skin temperature, which causes contraction and stiffening. To doff, the garment would either need to be cooled or designed with release mechanisms.

5.3 Active-Contracting Fabrics

Active-contracting fabrics are common fabric structures (e.g. Figure 5.5 wovens, non-wovens, and knits) that strategically incorporate shape memory materials (SMM) to enable one-, two- or even three-dimensional contraction upon actuation. SMMs are materials that change microstructural composition in response to change in magnitude of a particular stimuli, such as temperature, light, pH, magnetic field, etc. This physical coupling enables tailorable, repeatable change in mechanical structure in response to that stimulus [82]. Examples of active materials include shape memory polymers (SMP), shape memory alloys (SMA), piezoelectric polymers and ceramics, and dielectric elastomers.

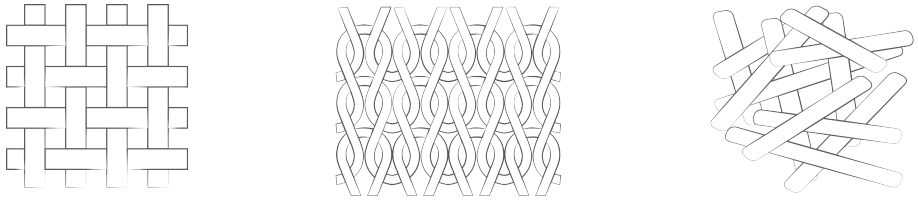

Figure 5.5: **Generic Fabric Structures:** (left) Woven fabric; (center) Knit fabric; (right) Non-woven fabric.

This research focuses on contractile SMA knitted actuator fabrics, an active-contracting fabric developed by Dr. Julianna Abel during her Ph.D. work at the University of Michigan composed of knitted SMA wires [18]. SMA is an alloy that exhibits thermomechanical or magnetomechanical coupling, meaning its internal structure, and thus, external shape, changes in response to fluctuation either in temperature or magnetic field. This work focuses on nickel titanium alloys, or nitinol, SMA that exhibits thermomechanical coupling behavior. Nitinol is commercially available, biocompatible, and possesses higher recovery stress (500-900 MPa) and transformation strain (6-8 %) compared to other commercially available alloys (e.g. CuZnAl, CuAlNi) [8]. Throughout the chapter, all future discussion of SMA refers specifically to nitinol.

As shown in Figure 5.6, SMA oscillates between a stiff austenite phase and a less-stiff martensite phase according to the magnitude of the temperature stimulus. This characteristic phase-change behavior enables SMA to exhibit both a shape memory effect (SME) and a superelastic effect (SE). Shape memory effect (Fig 5.6 (left)) refers to the material's ability to recover deformation when heated above a material-specific transformation temperature, or austenite finish (A_f) temperature. The transition temperatures (martensite

start (M_s), martensite finish (M_f), austenite start (A_s), austenite finish (A_f)) are dependent on manufacturing process variables, such as ratio of nickel to titanium, additives, and heat treatments. As shown in Fig 5.6 (right), the superelastic effect refers to the ability of austenetic SMA to experience stress-induced martensite (SIM) when applied stress reaches a critical, material-specific threshold.

The original SMA formation (# 1 in Figure 5.6) is a product of heat treatments, a process called shape-setting. Some commercially available SMA is sold as-drawn, meaning it has only been cold-worked into a form (e.g. wire) and has no shape memory abilities. As-drawn SMA can be purchased and shape-set into custom formations, such as springs or hinges, by clamping the SMA in the desired shape with a steel mold and heating the material to high temperatures (e.g. 400 - 550°C) [8]. Alternatively, SMA can be purchased already shape-set, or heat-treated, in a straight formation (e.g. Flexinol ®, Dynalloy, Inc.). Heat-treated wire can be trained again through shape-setting procedures; however, each additional heat treatments increase the transformation temperature, specifically A_f, of the SMA specimen.

Contractile SMA knitted actuator fabrics rely on the SME to transition from an elongated, compliant knitted fabric to a contracted, stiff knitted fabric. As shown in Figure 5.7, traditional weft knit architectures can be engineered to produce contraction if the original form of the SMA wire is straight. The shape-set wire is deformed into an interlaced loop formation while in a less-stiff, martensite phase to form a weft knit. Upon heating to A_f, the SMA wires attempt to straighten, causing planar contraction up to 40% along the length of the knitted wales [4]. The magnitude of this contraction is determined by two primary geometric design parameters: (1) the SMA wire diameter (d) and (2) the knit index (k_i), defined as the ratio of the squared wire diameter and the area within each knitted loop while under an applied load and in the martensite state ($k_i = \frac{A_{l,m}}{d^2}$) [4]. In 2017, K. Eschen & J. Abel used these two geometric design parameters for contractile SMA knitted actuator design to map changes in force-displacement behavior and calculated percent actuation contraction (ζ) [4]. Table 5.1 presents summary data from this manuscript that was referenced for the design and manufacture of our self-fitting, self-stiffening lower body garment.

For further information on the mechanical performance of contractile SMA knitted actuator fabrics, refer to K. Eschen's work, specifically [4] and Section 3: SMA Knitted Actuator Fabrics in [22].

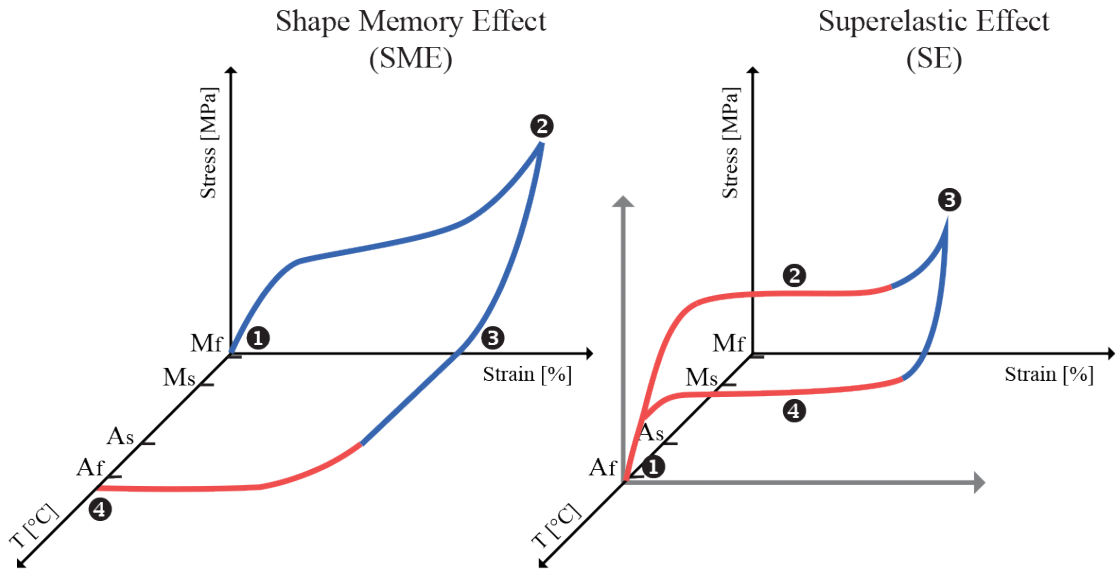

Figure 5.6: **SMA shape memory and superelastic behaviors:** SME (left): (1) Twinned, martensitic SMA (2) deforms with applied stresses. (3) Only a small amount of the original shape is recovered and the detwinned SMA remains partially deformed when applied stresses are released. Upon heating above the material-specific austenite finish temperature (A_f), (4) the original shape is completely recovered. SE (right): (1) Stiff, austenetic SMA behaves elastically until (2) applied stresses reach some critical threshold, resulting in (3) stress induced martensite (SIM). Upon unloading (4), the material returns to austenite and plateaus before returning to (1). [8]

5.4 Self-Fitting SMA Knitted Garment Design

The design of a SMA knitted garment merges anthropometric, functional apparel, and active materials and structures research. The following sections describe the methods used to define the performance requirements and design the ideal contractile garment using SMA knitted fabrics.

5.4.1 Anthropometric Analysis

The first step to design a self-fitting garment is to map the body-garment relationship. Prior research has shown that contractile SMA knitted actuators exhibit tunable functional performance through the systematic modification of geometric design parameters, specifically wire diameter and knit index [4]. Before we determined suitable knit geometries to achieve self-fit, the body-garment relationship was mapped. We began by gathering dimensional

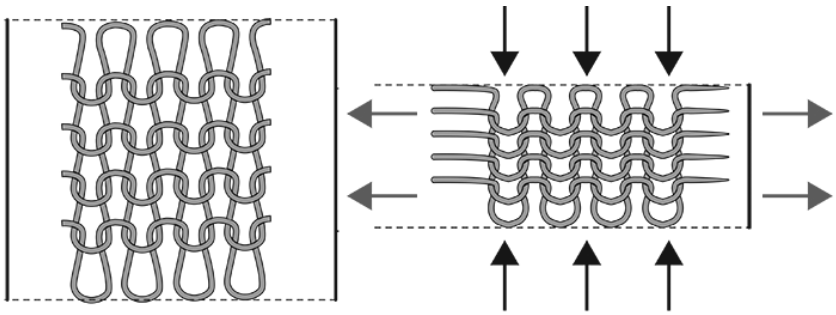

Figure 5.7: **SMA Knitted Actuator Fabric:** (left) Woven fabric; (center) Knit fabric; (right) Non-woven fabric.

data from one male participant. Marks were placed on the participant's right leg from the ankle to the mid thigh in 2 cm increments. At each incremental mark, a circumferential measurement was taken with a standard apparel measuring tape. A subset of these lower-body measurements is displayed in Figure 5.8. Once circumferential measurements had been gathered, we sought to define the performance requirements of the self-fitting garment. For an inextensible garment, the minimum garment dimension required at the base of a pant leg to enable don/doff (i.e. traverse the foot) is the calf dimension plus 2.5 cm of positive ease [9]. This recommended added garment dimension means that the garment circumference around the ankle should be equal to the garment dimension around the calf. Additionally, the garment dimension around the knee must be equal to the garment dimensions around the calf to enable the garment to traverse the calf. We modified the garment pattern slightly by adding a 7 cm taper from the knee to the ankle, a common, slimming pattern alteration. Figure 5.8 displays the required leg sleeve outlined around the participant's leg.

The required functional performance of the self-fitting garment is consequently defined as the percentual difference between the garment dimensions and the body dimensions. Figure 5.8 displays the required %-actuation contraction as defined by the garment-body interface. As shown in Figure 5.10, the garment begins in an oversized, compliant state (Figure 5.10 ①) with key dimensions displayed in Figure 5.9. When donned, force is applied to the garment as it is pulled over the body (Figure 5.10 ②). Martensite relaxation occurs when the wearer releases the garment, now surrounding the body (Figure 5.10 ③). When actuated through body heat or other means, the garment contracts until it hits the reduced dimensions of the body, at which point interfacial pressure builds according to SMA knit's specific austenite curve. (Figure 5.10 ④). The primary challenge in the development of the proposed garment is to design a functionally gradient system that does not exert significant

Table 5.1: **Actuation contraction behavior of contractile SMA knitted actuator fabrics:** According to Eschen & Abel [4], %-actuation contraction of contractile SMA knitted actuator fabric is dependent on two geometric design parameters: (1) SMA wire diameter and (2) the knit index, defined as the ratio of the squared wire diameter and the area within each knitted loop, while under an applied load and in the martensite state ($k_i = \frac{A_{l,m}}{d^2}$)[4]. Below is a summary of finding from [4] used in the design of self-fitting, self-stiffening wearables.

diameter [mm]	knit index [mm/mm]	actuation contraction [%]
0.127	125	35
0.152	134	32
0.203	138	40
0.203	130	37
0.203	98	22
0.203	85	20
0.203	53	8
0.203	39	5
0.254	71	19
0.254	33	4
0.305	72	14
0.305	31	3
0.381	124	35
0.381	105	27
0.381	64	14

pressure on part of the leg and/or remain oversized in others.

5.4.2 Garment Design Criteria

The design of a contractile SMA knitted garment, tuned to the dimensional requirements of the body, was accomplished through a clear set of required/exclusionary criteria. Three main criteria are performance, comfort, and manufacturability, which will be discussed among the secondary design criteria (weight, ridge distance, and cost) in the following sections. The design process is presented with the example of the self-fitting leg garment for the participant's anthropometry, however the language is kept intentionally general as the design process can be applied for any participant and body region.

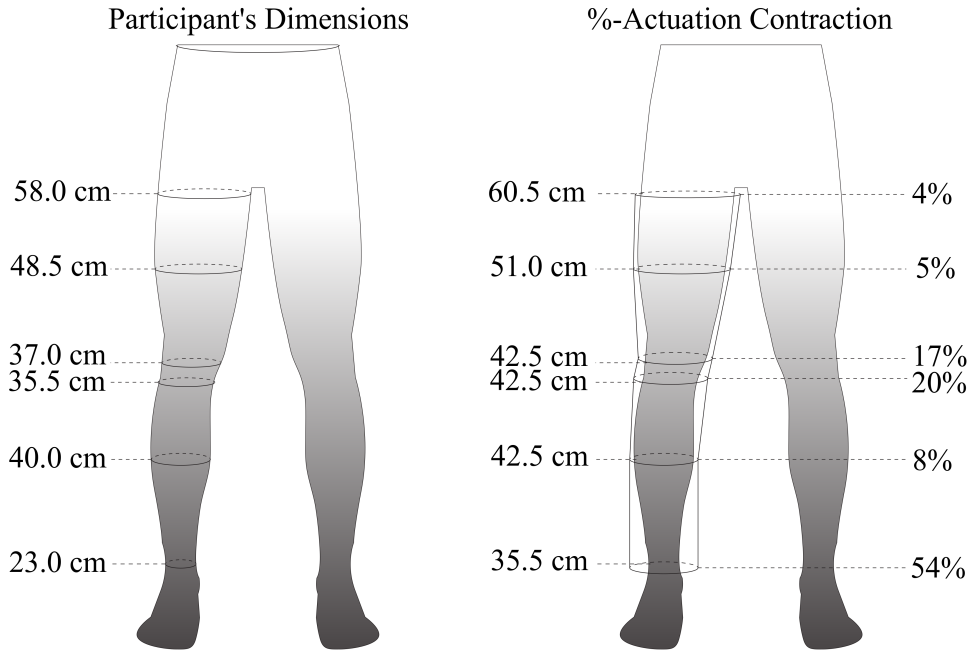

Figure 5.8: **Anthropometric Analysis for a Lower Body Garment:** (left) Circumferential measurements were taken in 2 cm increments along the length of the participant's right leg. Abbreviated dimensions are displayed here. (right) The circumferential measurements were increased to enable garment don/doff according to [9] and the percent difference between the garment and body measurements were calculated.

Performance

The required %-actuation contraction ($\zeta_{n,req}$) at each of the 27 circumferential measurements was calculated by determining the percent difference

$$\zeta_{n,req} = \frac{c_{n,garment} - c_{n,body}}{c_{n,garment}} \tag{5.1}$$

between the body's circumferences ($c_{n,body}$) and the circumferences of the pre-determined don-able/doff-able garment ($C_{n,garment}$), as shown in Figure 5.9 .

Each of the 27 circumferential measurements was matched with multiple SMA knits with comparable %-actuation contraction [4]. While contractile SMA knitted actuators with slightly higher nominal %-actuation contraction (+5%) are acceptable as they are not predicted to exceed the pressure limits, fabrics with slightly lower %-actuation contraction (-1%) were immediately excluded from the selection because they do not accomplish fit.

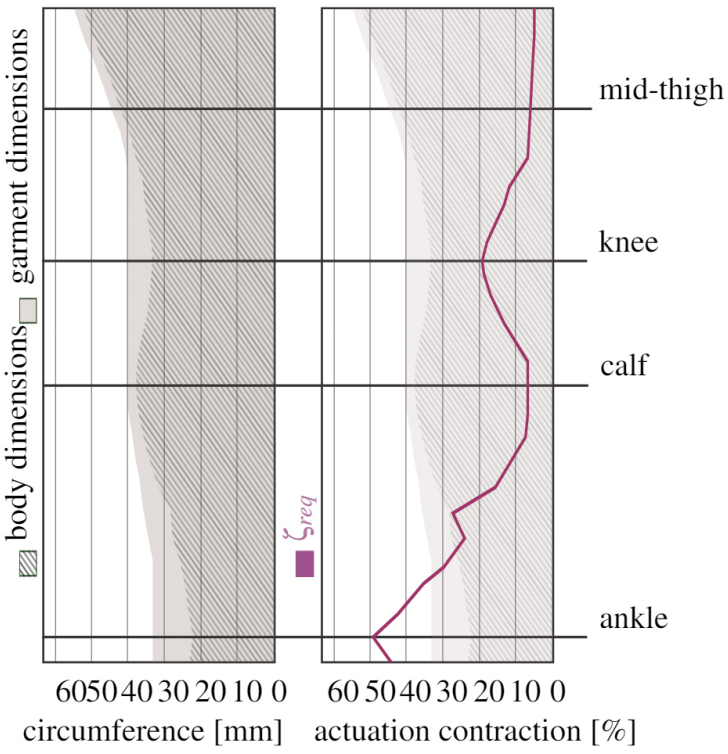

Figure 5.9: **Fit and Performance Requirements for Self-Fitting Garment:** Garment ease is greatest around the ankle and knee due to donning logistics and, consequently, require greater contraction to achieve fit.

5.4.3 Comfort

A successful self-fitting garment achieves fit without generating substantial pressure on the wearer's body, an objective that clearly distinguishes this research from medical applications that exert therapeutic pressures ($\geq$ 18 mmHg or 2400 Pa) [59]; however, pressures that are not substantial (i.e. pressures below the pressures exerted by socks, 1333 Pa) were deemed appropriate for this design. The pressure exerted by the self-fitting garment is calculated for each n-th circumferential measurement assuming rigid bodies. The hoop stress (σ_θ)

$$\sigma_\theta = \frac{F}{tw} \tag{5.2}$$

and the circumferential pressure (p)

$$p = \frac{\sigma_\theta t}{r} \tag{5.3}$$

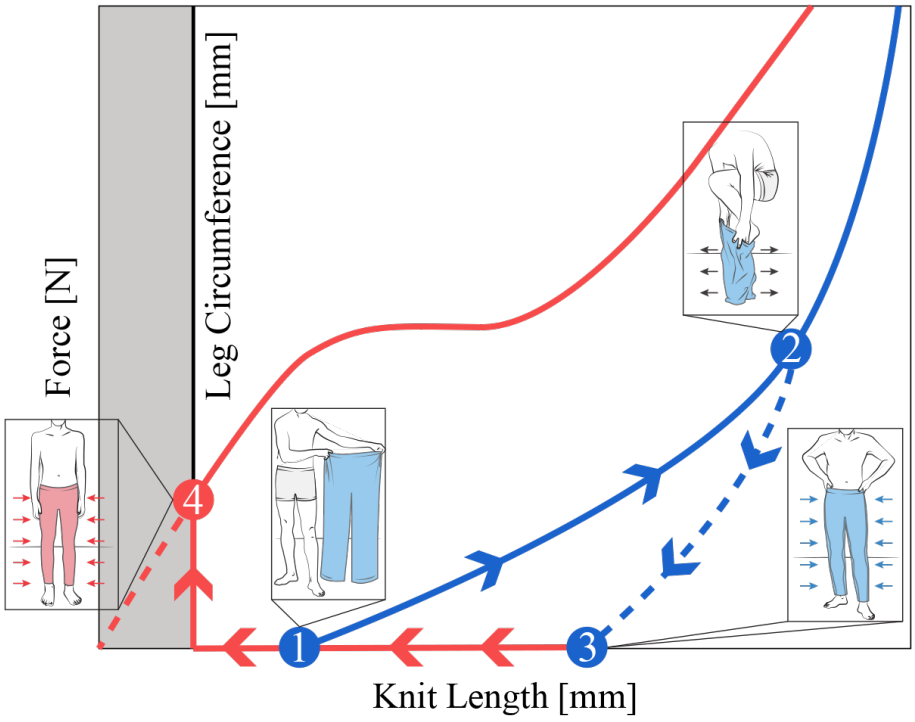

Figure 5.10: **Self-fitting Garment Operation:** The fully-martensitic garment is compliant and oversized (1). Upon doning, small forces are exerted on the garment, which cause further garment dimensional expansion (2). Upon release, the garment contracts into its martensite relaxed state and recovers some of the extension from the donning process (3). Heating (body or external source) causes the garment circumference and the leg circumference to equate (4). Additional contractile ability of the garment results in a generation of forces and pressure on the leg, which are to be minimized in the design.

are expressed through the fabric thickness (t), the limb radius (r), the fabric width (w), and the tensile force (F). Substituting Equation 5.2 into Equation 5.3 results in

$$p = \frac{F/w}{r} \tag{5.4}$$

an expression that relates the circumferential pressure (p) and the tensile force (F). Using the defined critical pressure ($p_{crit} = 1333Pa$), the width of the circumferential measurement ($w = 0.02m$), and rearranging Equation 5.4

$$F_{crit} = P_{crit}wr = (1333Pa)(0.02m)r \tag{5.5}$$

provides the critical force (F_{crit}), dependent on limb radius (r).

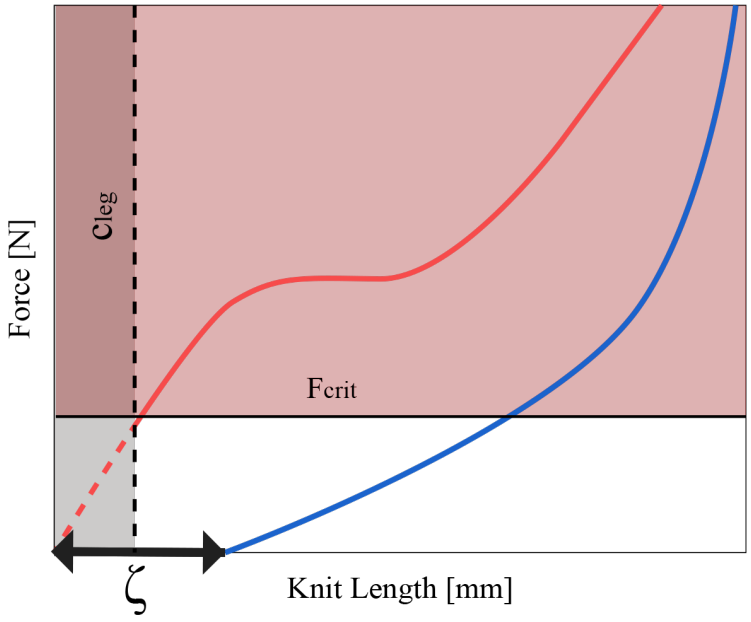

Figure 5.11: **Maximum Pressure Calculations:** Pressure on the body is determined by the relationship between force per fabric width and body radius (Equation 5.4). Consequently, the critical force (F_{crit}) at which pressure reaches 1333 Pa) is determined by the dynamic garment-body interaction and is unique to each SMA knit + body region combination (Equation 5.5).

Implementation of Equation 5.5 is presented in Figure 5.2. While the original force-length profiles gathered from characterization by [4] presented data for 15 course by 15 wales knits, this data is scaled up for garment design, which will be discussed in Section 4.4.4. The critical force (Equation 5.5) at which the exerted pressure reaches 1333 Pa at the particular region's radius is marked by the horizontal line. Forces above F_{crit} enter the realm of medical pressure garments. Consequently, any knit whose $c_{n,body}$ and austenite curve intersect occurred above the F_{crit} line was eliminated as a possibility for the n-th circumferential measurement.

5.4.4 Manufacturability

We considered each circumferential measurement and paired contractile SMA knitted actuators in terms of adjacent pairings with the goal of building a unified garment structure. We observed that certain knits were unsuitable neighbors due to extreme differences in wire diameter that could threaten the structural integrity of the manufactured garment. Consequently, we selectively excluded any knits whose wire diameter was greater than 0.1 mm

its adjacent wire diameter.

5.4.5 Additional Design Criteria

The previous design metrics thoroughly cover the known design space; however, if there were additional options remaining, supplementary criteria, specifically, comfort, weight, and cost, would be used. Specifically, we consider the impacts of loop size on touch comfort to mitigate sensations of point pressure [83]. With this data, knits with large knit indexes and large wire diameters at regions with heightened tactile acuity (e.g. mid-shin, front mid-thigh) can be mitigated. While further development is require to improve the wearer experience, we further consider comfort by prioritizing SMA knits with lighter weights. Finally, if there are comparable fabrics that could be used for the same region, the lowest priced fabric architecture should be chosen. See K. Eschen's analysis in [22] for more information.

5.4.6 Garment Manufacturing

Once a suitable contractile SMA knitted actuator fabric had been chosen for each circumference, we began the manufacturing process. Traditionally, knitted patterns are generated by knitting a sample swatch with the chosen yarn and loop size. The number of wales and courses within a 2.5 cm $\times$ 2.5 cm square are counted and these dimensions are scaled to achieve a knit pattern with desired dimensions. Once knit according to the pattern specifications, traditional yarn knit panels are washed, blocked, and steamed to relax the yarns into their new form. Finally, each garment panel is joined through a crochet, graft, or mattress stitch. Because our contractile SMA knitted actuator fabrics oscillate between different course-wise lengths with a change in temperature, we modified this process to fit our dynamic design. The following sections describe our design process and the methods that deviate from traditional knit manufacturing practices.

5.4.7 Course Mapping

We began the garment design process by scaling the 15 course by 15 wale contractile SMA knitted actuator data gathered from previous force-length characterization [4] to calculate knitted course requirements for each unique body circumference and SMA knit combination. Each of the 27 results are depicted in Appendix A. The plots include the austenite and martensite force-length curves scaled up to the body circumference measurement. Both

the circumferential measurements ($c_{n,body}$) and the force at which garment pressure reaches 1333 Pa (F_{crit}) are included in the plots.

The number of knitted courses is determined through this scaling process and was adjusted slightly to ensure that the intersection between the body circumference and the austenite curves did not surpass F_{crit}. Additionally, we made adjustments if the body circumference line was to the right of the base of the martensite curve. In application, this means that the garment would begin compliant, but would already fit, or conform around the body region in the martensite state. In a commercial/consumer setting, this adjustment would not be necessary; however, for the purposes of a proof-of-concept prototype, we aim for the self-fitting capability to be visible. Because there will be some degree of martensite relaxation, as depicted in point 2 of Figure 5.10, we adjusted the austenitic loop number until the body circumference reached the minimum martensite knit length *or* F_{crit}, depending on which point was reached first.

5.4.8 Knit Pattern Generation

Once the number of courses had been determined for each of the 27 circumferential measurements of the body, the knit pattens, which provide detailed blueprints for knitted garment construction, were generated. Typically, circular garments such as socks, pants, or sleeves can be knit in the round, a technique which eliminates the need for joining seams. Circular knitting is not an option for self-fitting garments because the loops must be oriented in the circumferential direction to achieve the desired actuation contraction. Consequently, we designed our self-fitting garment as multiple flat knitted panels, each with a unique knit pattern, with joining seams.

Figure 5.12 depicts the full garment pattern with each of the 27 circumferential measurements indicated by a dotted line. Circumferential measurements that were paired with the same contractile SMA knit actuator fabric as their neighbor were grouped together to simplify the knit pattern. These groupings formed discrete regions depicted in Figure 5.12. Once the discrete regions had been established, a shape was drawn around the edges of the regions to define the perimeter of the knit panel, indicated by a bold outline.

The 11 knit panels defined in Figure 5.12 are described further in Appendix B, which presents detailed knit patterns. At this point, the number of wales required to fill out each of the discrete regions was determined by evaluating contractile SMA knitted actuator fabric samples while fully martensitic and simply counting the number of wales within a

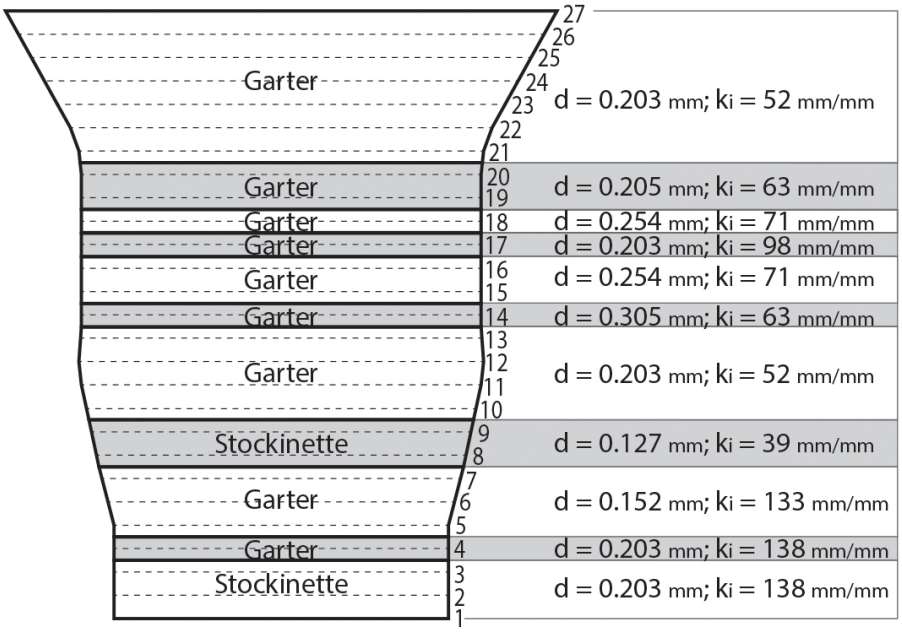

Figure 5.12: **Garment Pattern:** Each body circumferential measurement, represented by a dotted line, is grouped with neighboring circumferences that require identical knit architectures. Eleven knit panels, outlined in black, make up the full garment design. See Appendix B for detailed patterns.

2 cm length (i.e. the minimum knitted panel width) and scaling to the required panel width. Because the perimeters of the knit panels are not always straight (for example, some are curved or diagonal), we employed a knitting technique call shaping, which involves selectively adding or dropping latch needles along the needle bed to respectively increase or decrease the width of the knit panel. In addition to filling in the required courses and wales to satisfy the functional requirements of the 11 panels, careful shaping was included in the knit patterns to smooth transitions and improve garment shape.

5.4.9 Knitting

The 11 knit panels were knit on a Taitexma TH-860 knitting machine with SMA wire (Dynalloy Flexinol ®, $A_f = 90°C$) according to the pattern specification in Appendix B. In order to knit panels with edge shaping as one piece, loops would need to be added on one end of the knit panel and subtracted at the other end. Through experimentation, we discovered that the process of subtracting, or doubling over loops results in fabric curling

upon actuation. In contrast, the process of adding, or spreading out loops results in further contraction upon actuation. Consequently, we sought to knit all edge conditions the same way and restrict our manufacturing process to include added loops only. To accomplish this design restriction, we split certain knit pattens in half and joined them vertically at the front and the back, while knit patterns that do not require edge shaping were knit in one piece and joined in the back only.

5.4.10 Thermal Blocking

As with fiber yarn knitting, contractile SMA knitted actuator fabrics require a post-knit step that allows the SMA monofilament to settle into its new architecture. Fiber yarn knits are generally washed, stretched, and pinned into their intended shape and exposed to steam, a process called blocking. The combination of applied force, heat, and water coaxes the yarn to relax into a new shape. Similarly, contractile SMA knitted actuator fabrics require thermal blocking, specifically a small applied load (50 g) and exposure to several thermal cycles ($20°C \rightarrow 120°C$), to settle into their intended length and width dimensions. Consequently, each knit panel was loaded with 50 grams, scaled according to the number of wales in the panel, and exposed to 5 cycles of thermal transition.

5.4.11 Knit Garment Assembly

Once the knit panels had been fabricated and thermally blocked, the panels were joined with a common crochet joining stitch to achieve the original garment design depicted in Figure 5.12. The final prototype, in a compliant, oversized state, is shown in Figure 5.13.

5.5 Results & Performance Validation

K. Eschen developed a garment performance validation method using three-dimensional marker tracking [22]. Markers were placed down the front and side of the garment to track relative changes in knitted loops. Two 5.0MP CMOS cameras with 1.4/17 mm lenses gathered visual data that was then interpreted with a Correlated Solutions VIC-3D image correlation software. The garment was validated on a plaster replica of a leg that could withstand the required high actuation temperatures. The garment was actuated with two heat guns, one on either side of the leg. Figure 5.14 presents the results of the validation effort along with the previously defined required actuation (ζ_{req}). Both the average ($\bar{\zeta}$) and

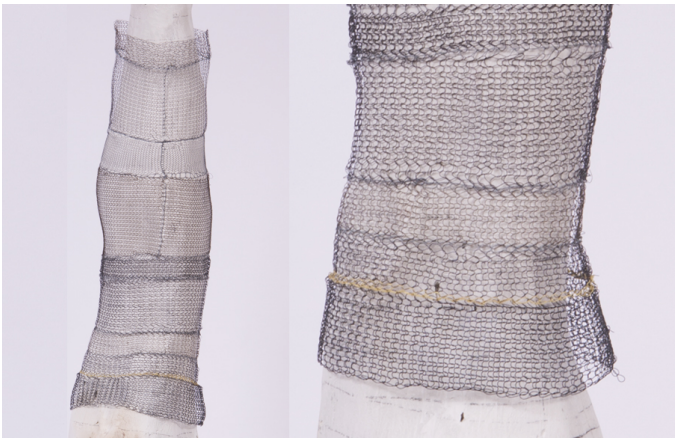

Figure 5.13: **Active-Contracting, Variable-Stiffness SMA Knit Garment Prototype in an Unactuated State:** (left) Front view, full garment. (right) Side view, thigh closeup. The prototype garment was knit according to the specifications in Appendix B.

the maximum ($\hat{\zeta}$) observed actuation performances are included because the drape of the martensitic garment was highly variable (i.e. like clothing). Consequently, $\hat{\zeta}$ is the closest representation of actual garment actuation-contraction. One point between the calf and the ankle experienced no actuation contraction because the martensitic garment was already fitted in that region. This area of pre-fit impacted the actuation contraction performance of surrounding areas. This outcome does not negatively impact the functionality of the design; however, more knitted loops should be added to this section so that full actuation contraction potential is visible. For more details on the validation results led by K. Eschen can be found in [22].

5.6 Conclusions

This paper presents the design process, manufacturing and experimental validation of an active-contracting, variable-stiffness garment for the lower extremities using contractile SMA knitted actuators. Anthropometric data was collected from a single male participant to provide the basis for this proof-of-concept prototype design. The participant's leg was measured circumferentially in n increments of 2 cm widths between the ankle and the thigh. Using standard garment design methodologies, the required dimensional ease to enable don/doff of a standard, non-stretch pant was calculated at each circumferential measurement. The dimensional difference between garment and body provided the required

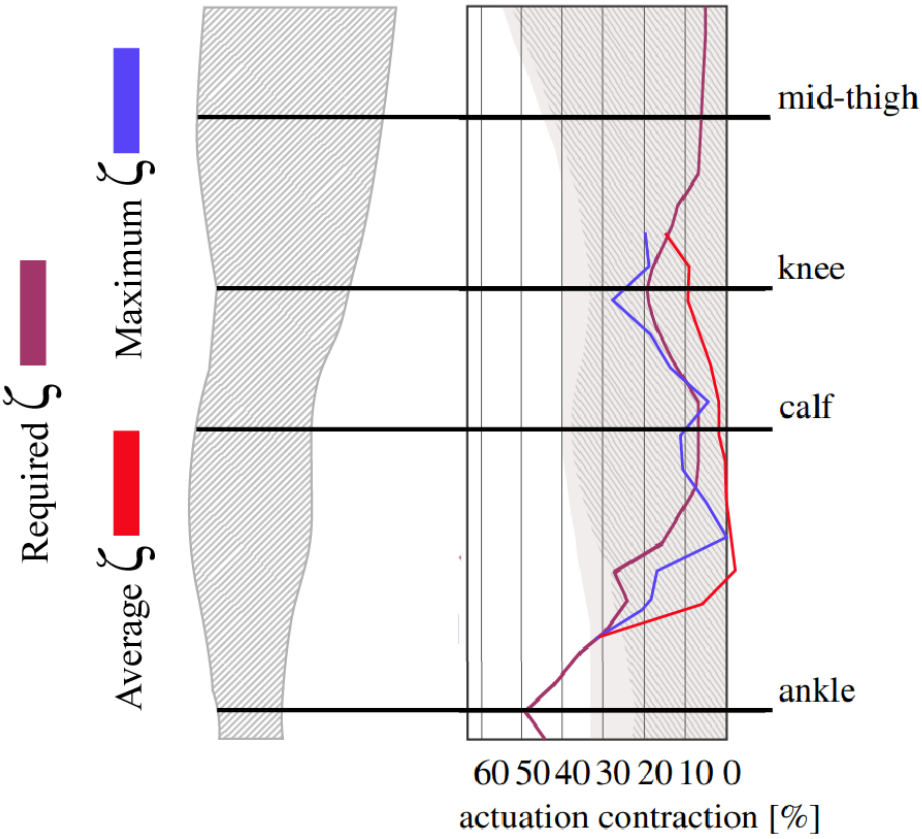

Figure 5.14: **Actuation Contraction Requirements vs Experimental Findings:** The observed average contraction ($\bar{\zeta}$) deviated from the observed maximum contraction ($\hat{\zeta}$) because of high martensite variability inherent to fabric drape. Consequently, $\hat{\zeta}$ is the closest representation of actual garment actuation-contraction.

%-actuation contractions for the self-fitting garment. Contractile SMA knitted actuators that accomplish the actuation requirements were selected for each defined circumferential measurement. The complete design requirements are in descending order of importance: performance, comfort, and manufacturability. The active-contracting variable-stiffness garment was manufactured on a Taitexma-series knitting machine in separate knitted panels that met the design requirements of the individual segment and subsequently joined with a standard crochet stitch.

The performance validation conducted by K. Eschen and detailed in [22] present complete self-fitting (i.e. the convergence of garment dimensions to leg dimensions) through optical measurement of fabric surface deformations (3D Marker Tracking).

For the first time, a fully-functional, self-fitting, and self-stiffening garment was designed, manufactured, and experimentally validated. Future implementations of this design will utilize SMA material that achieves self-fitting upon heating to the participant's skin temperature ($T_{skin} \approx 32°C$) resulting in a self-powered, self-fitting garment. Through the design of a functionally gradient, self-fitting garment, this research addresses the challenges of achieving individual and population fit by establishing new garment design methodologies with active materials.

5.7 Self-Fitting Garments for Population Fit

As shown in the previous analysis, active-contracting fabrics have the ability to self-fit to the body (i.e. up to 40% actuation contraction) and self-stiffen around their new form. Chapter 2 presented a complex sizing system for a non-compliant, form-fitting low-leg garment (104 sizes, women; 112 sizes, men). This section seeks to merge the two analyses and present the implications of self-fitting, self-stiffening fabrics on population fit challenges.

Active-contracting fabric could reduce the number of sizes required for a stiff, fitted garment by merging circumferential sizes. At this phase in development, active-contracting fabrics are not designed to alter length of garments; therefore, the 5 length categories for men and women cannot be eliminated. The goal of this analysis is to identify which of the 104 to 112 unique sizes for males and females can be eliminated by reducing sub-sizes required in maintain circumferential fit.

5.7.1 Minimum Leg Circumference

Previous anthropometric analysis determined that three unique minimum leg circumferences sizes are required for men and women to maintain fit within 3 cm of 95% of the North American consumer population. The design methodology from [22] was employed by pairing anthropometric data with actuation contraction data from [4] to determine garment design criteria. Specifically, the SizeUSA database was evaluated to determine the percent difference between the calf circumference and the minimum leg circumference. If the minimum leg circumference (i.e. just above the ankle) were designed to be the same dimension as the calf, then the garment could be easily donned [28]. Consequently, garment actuation contraction in the ankle region is defined by the percent difference between the calf circumference and the minimum leg circumference.

For SizeUSA men, group 1 (minimum ankle circumference = 19-22 cm) actuation contraction requirements ranged from 27-48%, group 2 (minimum ankle circumference = 22-25 cm) actuation contraction requirements ranged from 28-47%, and group 3 (minimum ankle circumference = 25-28 cm) actuation contraction requirements ranged from 24-47%. The mean actuation contraction requirements for all groups was 29%. When added to the percentage of dimensional variability within each size group due to the ±3 cm size interval (group 1, 14%, group 2, 12%, group 3, 11%), the total required actuation contraction required to fit each size group ranged from 59-62%.

For SizeUSA women, the required actuation contraction around the ankle region was higher. Like the men, women had three distinct minimum leg circumference sizes in 3 cm intervals: group 1 (18 - 21 cm), group 2 (21-24 cm), and group 3 (24-27 cm). The percentage of variability within each size interval was 14%, 12%, and 11%, respectively. Anthropometric analysis was conduction to determine the percent difference between calf and minimum leg circumferences in each group, which would then define garment actuation contraction requirements. The range in group 1 was found to be 28-52%, group 2 19-56%, and group 3 24-27%. Consequently, the total required actuation contraction around the ankle region in an active-contracting garment for women was 64-68%. Table 5.2 provides a summary of this data.

Table 5.2: **Actuation Contraction (ζ) Requirements:** Minimum leg circumference. [1]

WOMEN				
Min-Leg circumference [cm]	Size Variability	ζ	Mean ζ	Total ζ
18-21	14%	28-52%	40%	66%
21-24	12%	19-56%	40%	68%
24-27	11%	19-53%	40%	64%
MEN				
Min-Leg circumference [cm]	Size Variability	ζ	Mean ζ	Total ζ
19-22	14%	27-48%	39%	62%
22-25	12%	28-47%	39%	59%
25-28	11%	24-47%	38%	58%

Active-contracting fabrics are presently only capable of contracting up to 40% of their original length; therefore, active-contracting fabrics are not able to reduce the three unique

minimum leg circumference sizes without increasing donning difficulty. It is recommended that an ankle zipper be included in the garment design to reduce the amount of garment ease that is required for don/doff. With an added zipper, the three unique minimum leg circumference sizes could be merged into one size with a 28 cm circumference. To achieve the smallest ankle circumference, 18 cm, only 33% actuation contraction is required.

5.7.2 Calf Circumference

The size system presented at the end of Chapter 2 shows that only 13-14 unique garment sizes would be required for men and women if the garment were not required to maintain accurate fit in the calf. Calf variability was found to be larger than the variability at the minimum leg circumference and adds 8 additional sub-sizes to the sizing system, bringing the number of unique sizes up to 104 and 112 for women and men, respectively. This section seeks to reduce this number with active-contracting fabrics. Because significant added dimensional ease in the calf is not required for don/doff [28], actuation contraction only reduces the amount of unique sizes caused by population variability.

Up to 8 unique sizes in 3 cm increments are required to fit the full population at the calf: Men group 1 (25-28 cm), group 2 (28-31 cm), group 3 (31-34 cm), group 4 (34-37 cm), group 5 (37-40 cm), group 6 (40-43 cm), group 7 (43-46), group 8 (46-49); Women group 1 (24-27 cm), group 2 (27-30 cm), group 3 (30-33 cm), group 4 (33-36 cm), group 5 (36-39 cm), group 6 (39-42 cm), group 7 (42-45 cm) group 8 (25-48 cm). A summary of this data is provided in Table 5.3. The total percent change in dimension required for men and women, from the smallest size in group 1 to the largest size in group 8, is 49-50%. Because this range of actuation contraction is higher than active-contracting fabrics can accomplish, the population can be split into two sub-groups. Groups 1-4 (women, 24-36 cm; men 25-37) would require 30-32% actuation contraction to fit all four groups. Additionally, groups 5-8 (women, 36-48 cm; men 37-49 cm) would only require 24-25% actuation contraction to fit all four groups. Consequently, size small would be designed with a calf martensite finish circumference around 37 cm with a active-contracting fabric that can accomplish up 32% actuation contraction. This fabric would ensure that individuals on the lower end of the calf circumference range (i.e. 24, 25 cm) are fit. Likewise, size large would be designed with a calf martensite finish circumference around 49 cm with an active-contracting fabric that can accomplish up to 25% actuation contraction.

Table 5.3: **Actuation Contraction Requirements:** Calf Circumference. [1]

WOMEN	
Calf circumference [cm]	Size Variability
24-27	11%
27-30	10%
30-33	9%
33-36	8%
36-39	8%
39-42	7%
42-45	7%
45-48	6%
MEN	
Calf circumference [cm]	Size Variability
25-28	11%
28-31	10%
31-34	9%
34-37	8%
37-40	8%
40-43	7%
43-46	7%
46-49	6%

5.7.3 Reduced Size System

The results of the supplemental analysis show that a sizing system composed of 104 unique sizes for women and 114 for men can potentially be simplified into 10 sizes for each gender (5 lengths x 1 ankle circumference x 2 calf circumferences), depicted in Table 5.4. While further development and prototyping is required, the analysis presents compelling evidence to continue developing active-contracting fabrics to reduce the challenges associated with achieving population fit for large, highly variable consumer populations.

Table 5.4: **Sizing System for Leg Garment Using Active-Contracting Fabrics:** 104 and 114 sizes for women and men, respectively, previously presented in Chapter 2 can be reduced to 10 sizing using active-contracting fabrics.

WOMEN						
min-leg-to-knee length [cm]		**26-29**	**29-32**	**32-35**	**35-38**	**38-41**
calf girth [cm]	**25-36**	Size 1	Size 2	Size 3	Size 4	Size 5
	36-48	Size 6	Size 7	Size 8	Size 9	Size 10
MEN						
min-leg-to-knee length [cm]		**28-31**	**31-34**	**34-37**	**37-40**	**40-43**
calf girth [cm]	**25-37**	Size 1	Size 2	Size 3	Size 4	Size 5
	37-49	Size 6	Size 7	Size 8	Size 9	Size 10

Chapter 6

Implications & Future Work

The results of the prior anthropometric studies (i.e. Chapter 2 and 3) as well as prior active-contracting fabric characterization work (i.e. Chapters 4 and 5) provide insight into methods for developing active-knit compression garments (CG) that are designed around the dynamic behavior of the body. This final chapter synthesises the work into a discussion of systems design work for applications from consumer clothing to aerospace CGs. The chapter ends with recommendations for future work that will enable the active-knit fabric systems proposed.

6.1 Active-Contracting Fabric Behavior

Before beginning a discussion of garment systems designed with active-contracting fabrics, a summary and synthesis of behavior is presented. The results from Chapters 4 and 5, as well as prior work by [4] revealed that the performance of active-contracting fabrics can be manipulated by design variables: (1) wire diameter, (2) knit index, (3) knit structure, and (4) knit length (i.e. strain). Variables 1-3 can be accomplished in the manufacturing process on the fabric level; however, variable 4 is directly linked to the relationship between garment dimensions and body dimensions. Consequently, consideration of the garment-body interface is crucial to systems performance.

Figure 6.1 depicts the relationship between hypothetical active-contracting fabric performance and fit around the body. On the left is a flow-chart that describes fabric performance when the active-contracting fabric (i.e. martensite free length) is longer in circumference than the circumferential length of the body. In apparel terms, the state when garment dimensions are greater than body dimensions is referred to as positive ease. Alternatively,

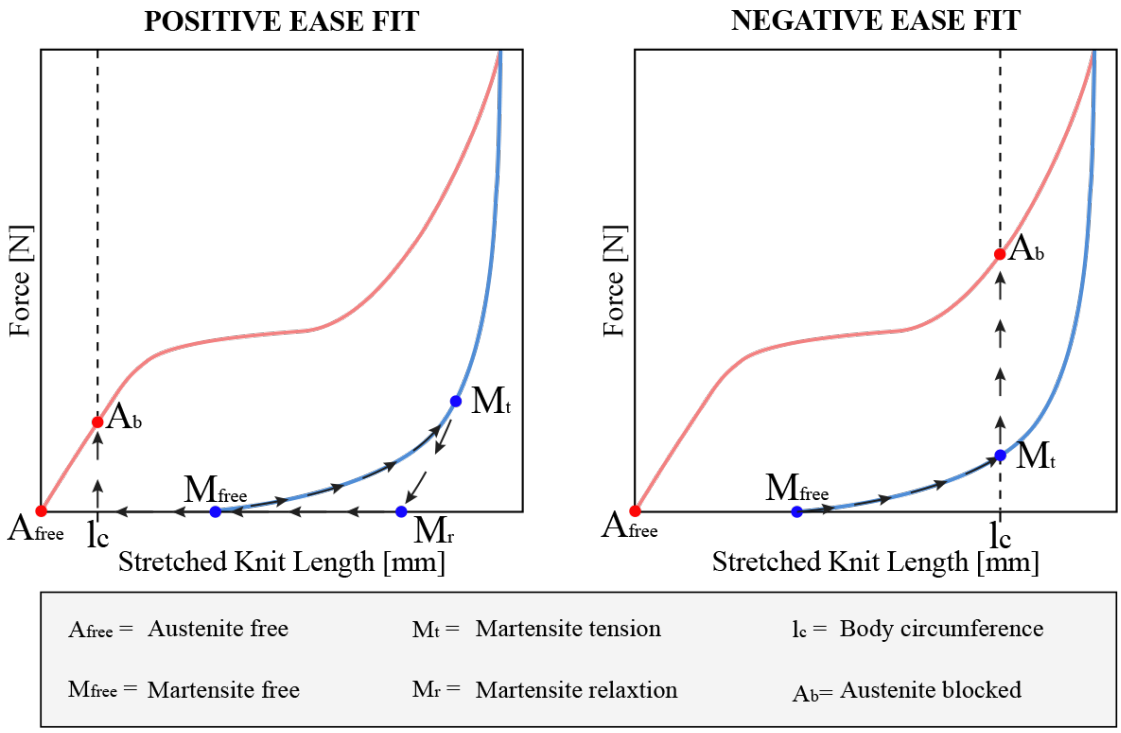

Figure 6.1: **Positive vs Negative Ease Garment Fit Actuation Performance:** Active-contracting fabric curves are fictitious and for illustrative purposes only. Actuation of positive ease active-contracting garments produces body fitting and small forces. Actuation of negative ease active-contracting garments produces a blocked force scenario and high compressive forces.

Figure 6.1 right depicts fabric performance when the active-contracting fabric (i.e. martensite free length) is smaller in circumference than the circumferential length of the body. Negative ease is the state when garment dimensions are smaller than body dimensions. The following sections detail the path and performance of each fit scenario.

6.1.1 Positive Ease: High-Displacement for Fitting

In a positive ease scenarios, active-contractive fabrics function as high-displacement fabrics for garment fitting. In this condition, the initial, oversize garment begins in a martensite free (M_{free}) length, meaning it is inactive and experiencing no-load. The circumferential length of the garment increases from M_{free} to a martensite tension (M_t) length when external forces are placed on the knit to pull the garment over the body. Due to material hysterisis and martensitic detwinning, when that donning load is released, the circumferential length does

not return to M_{free} length, but rather a martensite relaxation (M_r) length. Consequently, the realized contraction upon actuation (i.e. heating) is represented by the distance between lengths M_r and l_c. Furthermore, the actuation contraction potential (without the body present) is the distance between lengths M_r and A_{free}.

While Chapter 5 presents actuation contraction potential as the distance between lengths M_{free} and A_{free}, future work should characterize length M_r to determine true, zero-load actuation contraction potential, as determined by thermomechanical history. Length M_r is difficult to characterize because it is partially dependent on donning forces, forces which are highly variable and dependent on the individual as well as the garment being donned. For example, a pair of leggings might experience high donning forces as someone attempts to pull the small garment over the feet, but a pair of culotte pants might not experience any donning forces because of their characteristic wide pant legs. Additionally, the dimensions of knitted structures after load has been released are highly variable due to fluctuating relationships between knitted loops. Preliminary observations of M_r lengths found length inconsistencies even when the applied load was fixed.

Once the active contracting fabric reduces length from M_r (or M_{free}) to l_c, the knit length hits the circumferential length of the body and is physically blocked from further reducing in length. At this point, small forces are applied to the body, represented by the austenite blocked (A_b) force. Because the circumferential length of the body (l_c) must be less than the circumferential garment length at M_{free}, the force at A_b is always going to be on the lower end of a given knit's overall blocked force potential.

6.1.2 Negative Ease: High-Force for Compression

The same knit architecture (i.e. wire diameter, knit index, stitch type) from Figure 6.1 left, could be used as a high-force fabric for compression applications by modifying the garment-body relationship. As shown in Figure 6.1 right, the number of loops making up the knit is decreased so that the circumferential garment length at M_{free} is less than the circumferential length of the body (l_c). Consequently, the process of donning (i.e. pulling the undersized garment over the body) increases fabric circumferential length and force simultaneously to martensite tension (M_t). Unlike a positive ease garment, in a negative ease scenario, M_t is the point where the fabric length and the circumferential body length converge ($M_t = l_c$). Therefore, M_t length and force are held stable by the body. Once the active-contracting fabric is actuated, the force increases directly from M_t to A_b because

displacement is fixed. As we discovered in Chapter 4, blocking active-contracting fabrics in a state of martensite tension increases actuation force and overall force; therefore, force A_b in Figure 6.1 right is much higher than force A_b in Figure 6.1 left.

While Figure 6.1 and the previous sections discuss fit and the resulting material behavior as a dichotomy, fit is more appropriately considered in a continuum, with positive and negative ease scenarios depicted in Figure 6.1 being two extremes. The following sections discuss how active-contracting fabrics could be used in various application systems and how those systems should be designed, notably pre-fit to the body, to enable desired functional performance.

6.2 Positive Ease for Fitting: Applications & Design

1. Use Cases: Positive ease, active-contracting garments that self-fit and stiffen are ideal for consumer applications, ranging from ready-to-wear (RTW) clothing and accessories to some wearable technologies. Targeted areas of clothing could incorporate active-contracting fabrics at areas such as waistlines, sleeve cuffs, pant cuffs, or shoulder/necklines to anchor clothing to the body. Additionally, active-contracting fabrics incorporated throughout a garment could prevent the need for traditional adjustability notions, such as zippers, buttons, snaps, elastic bands, or drawstrings. Common accessories, like hats, shoe, or wrist watches, could also incorporate active-contracting fabrics to anchor around the head, foot top, or wrist, respectively. Wearable technologies that require anchoring lightweight sensors to the body (e.g. electrocardiograms, inertial measurement units, strain gauges) could reduce the complexity of achieving body proximity and placement necessary for functionality [25]; however, weight of sensors must be considered in relation to active contracting fabric forces at A_b. The force created by the sensors in stationary and mobile conditions must be less than force A_b to prevent unwanted sensor deflection and/or drift. A design approach for garments with incorporated heavy sensors or secondary actuators (e.g. motorized bowden cables, pneumatic actuators) that apply forces higher than fabric actuation forces will be discussed in Section 6.4: Antagonistic System: Applications & Design.

2. Garment Operation & Control: To engage with positive ease, active-contracting garments, the user would pick up the oversized, compliant garment in a martensite state, strain the garment moderately in the donning process, release the detwinned garment on

the body, and allow the garment to contract when actuated. There are pros and cons to designing an system that leverages sensing capabilities of SMA (i.e. strategically heats/cools SMA to control contraction) versus a system that is purely mechanical (i.e. contracts with body heat). Below is a description of each scenario.

Positive ease garments could be designed with SMA material that actuates at body, resulting in a no-power-required system ($A_f \approx 32°C$). At low forces, these austenetic garments could be pulled off the body like elastic bands (i.e. stress-induced martensite) and return to martensite upon submersion in room temperature. The trade-off with this straightforward systems design is the inability to modulate pressure on the body as needed. While dynamic control is not essential in this realm of low-force, positive ease garments, lack of control could have negative repercussion for individuals who have one or more body dimensions that are statistical outliers or lay outside of a designated size category. While the deviation of force is particular to a active-contracting fabric architecture along with the body dimension(s), the result is concentrated force or lack of force in that area. Examples are cysts, localized edema, or structural/anatomical deviations that are unique to individuals and dependent on state of health.

Positive ease garments could also be designed with SMA material that actuates above body temperature, meaning the system requires added heat to apply force to the body. Due to the added system design complexity and low benefit to a low-force system, the control statagy for a dynamically controlled system is outlines in Section 6.3: Negative Ease for Compression.

3. Design Challenges: Anthropometric analysis from Chapters 2-5 reveal that inter-subject variability (population dimensional spread), intra-subject variability (unique body topography), and dynamic variability (posture, orientation) can negatively impact garment fit / functionality and can be competing design priorities. While ideally all three challenges would be addressed in all applications of this technology, the development of positive-ease garments for fitting should focus on the challenges associated with population and individual fit. Positive ease garments (unlike negative ease garments) designed with active-contracting fabrics displace to achieve a stiff and conformal fit around a large spread of body dimensions and unique body shapes. The large, concentrated, and unanticipated pressures associated with dynamic variability, caused by changes in posture or fluid volume, are less critical in the design of positive ease garments because initially over-sized active-contracting garments produce comparatively lower on-body pressure in relation to initially undersized

active-contracting garments, as shown in the hypothetical material curves in Figure 6.1. Additionally, these applications could optimize active-contracting fabrics with low-stiffness behavior. Future work should develop methods to produce uniform target pressures within a range of intra- and inter-subject dimensional variability. Examples of such methods include designing functionally graded garments, a method that was explored in Chapter 5, and developing functional fabrics that plateau in force over a given displacement range, a topic that will be further discussed in 6.5: Future Work.

6.3 Negative Ease for Compression: Applications & Design

1. Use Cases: Successful athletic clothing and accessories (e.g. footwear, compression wraps) are close fitting and generally apply slight compressive forces for therapeutic benefits (e.g. stabilize muscles, increase blood flow, increase proprioception, etc.). Additionally, consumer shapewear (e.g. bodysuits, slimming slips) require higher levels of compression than traditional clothing. Because compression is prioritized over don ease in these applications, a negative ease active-contracting garment is recommended. In these cases the circumferential, martensitic garment length should be less than or equal to circumferential body length. Consequently, donning is enabled by the differential between lengths M_{free} and M_t.

The design of a negative ease, active-contracting garment again necessitates an investigation into donning forces. If donning forces required to stretch the garment from length M_{free} to length M_t is too great, then the garment is not functional to the user (i.e. it cannot be donned). Depending on the garment design, it may be advantageous to combine traditional closures (e.g. hooks and eyes) with active-contracting fabrics to enable don and simultaneously reach higher forces through fabric strain. For example, if a traditional bra were designed with active-contracting fabric in the underband, an area that requires high compression forces, the garment could be stretched around the ribcage and fastened with a traditional hook and eye closure at the back. The inclusion of hook and eye closure enables the underband to begin at a martensite pretension (M_t) length, resulting in higher blocked (A_b) forces once actuated. Similarly, if donning forces are variable throughout the garment, a condition which is common for larger, conformal garments like leggings that require traversing the foot to don (e.g. low donning forces around the thigh, high donning forces around the ankle), closures can be placed selectively to increase martensite tension post-don (e.g. zippers placed around ankles or knees).

2. Garment Operation & Control: While the use of active-contracting fabrics for high-force, consumer applications, such as athelticwear and shapewear, could be simplified by using SMA materials that actuate around skin temperature ($A_f \approx 32°C$), these garments are difficult to doff at high forces. The inclusion of traditional closures, such as zippers, lacing, or hooks and eyes, could enable a purely mechanical (i.e. not dynamic) design for applications that would benefit from minimal complexity. These closures would enable the wearer to stretch the garment over the body, placing it in the required state of pre-tension, as well as serve as release mechanism to enable quick doff while the garment is martensitic. Alternatively, these garments could be designed with SMA that actuates above skin temperature and actuation could be initiated through joule heating with a battery pack. In some scenarios, it may be desirable to apply power to initiate contraction and then turn the power off. In this scenario, an SMA would need to be designed with an extremely low martensite start temperature (e.g. -60°C) so that the garment remains austenetic even after heat is not continuous. In other scenarios, it may be beneficial to strategically increase/decrease heat to precisely increase/decrease pressures on the body. The design of SMA for each scenario will be developed in future work.

3. Design Challenges: Because negative ease active-contracting garments are designed to translate high forces to the body, all fit challenges - inter-subject, intra-subject, and dynamic variability - are magnified. To address the heightened functionality concern and prevent negative medical impacts of over- or under-pressurization, it is recommended that challenges associated with static fit are addressed through traditional RTW techniques previously illustrated in Figure 5.3. Added dimensional ease is not an appropriate design strategy for compression garments because, as shown in data presented in Chapter 4, active-contracting fabrics need to be in a state of pre-tension to reach high actuation forces. Consequently, fit through (1) attached closure adjustability and (2) limited-compliance attachment fabrics are the two traditionally appropriate design solutions for active-contracting compression garments. Figure 6.2A depicts 15 knitted courses of active-contracting fabric (Chapter 4 found that actuation forces do not scale above 15 courses) attached to passive stiff fabric with adjustable closures to accomplish fit. Figure 6.2B depicts the same active-contracting fabric panel composed of 15 knitted courses attached to passive stretch fabric to accomplish fit through strain. Both garment design scenarios A and B require that the active-contracting fabric panel begin unactuated and actuate post-don. Like the adjustable configuration in

Figure 6.2 A, the configuration in Figure 6.2 B transfers the fit challenges from the active-contracting fabric to the passive, extensible fabric. Unlike the configuration in Figure 6.2 A, the configuration in Figure 6.2 B will not translate all active-contracting forces to the body because some forces will be used to displace the extensible fabric until the passive fabric unit tension coequals the active fabric unit tension. Because the passive components to System A are stiff, actuation of active-contracting fabrics results in maximum forces transfered to the body.

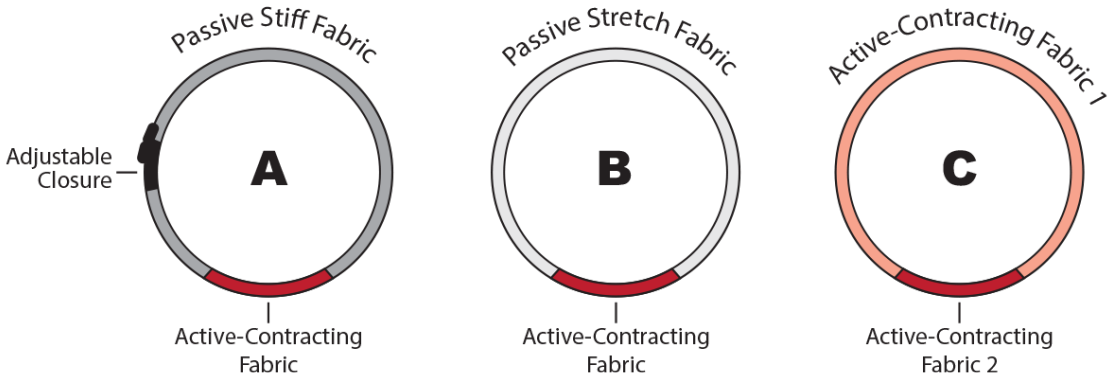

Figure 6.2: **Active-Contracting Fabrics used in Undersized Compression Systems:** Only 15 knitted courses are required in a system to generate maximum force; therefore, the following systems would enable a compression garment that is fitted to the body and place the active-contracting fabric in the required pretension state. (A) Active-contracting fabric (red) is attached to a passive, stiff fabric (gray) that closes and fits around the body with adjustable closures (black). (B) Active contracting fabric (red) is attached to a passive, stretch fabric (light gray) that strains to fit around the body. (C) Active-contracting fabric (red) is joined with a second active-contracting fabric (pink) that actuates at a lower temperature so that the garment first contracts to fit around the body (fabric 1) and then contracts further to apply pressure (fabric 2).

System B in Figure 6.2 is the simplest configuration in terms of design, fabrication, and usability because it does not include attached adjustability mechanisms that can often add mass and complexity to systems. Depending on the application, reduced system forces might be an appropriate trade-off in favor of reduce manufacturing cost and consumer usability. An alternative approach to traditional design approaches A and B is a mechanically antagonistic system presented in Figure 6.2C that uses two active-contracting fabrics that actuate at different temperatures to accomplish fit, garment pre-tension, and compression. The following sections explores the design of the hypothetical system in detail.

6.4 Antagonistic System: Applications & Design

Because active-contracting forces do not scale with added courses, only 15 courses in each circumferential cross-section are required to reach maximum actuation forces on the body. Consequently, the design of high-force CGs could take one of three approaches. (1) The remaining circumference could be a stiff, inextensible fabric that closes around the body with adjustable closures, identical to the approach taken in [5]. The challenge with this approach is conformal fit of inextensible fabrics around the body is difficult to achieve for a population, as discussed in Chapter 2. (2) The remaining circumference could be a compression knit. In this configuration, don/doff would be similar to static CGs (moderately difficult), but the active-contracting fabric panel could increase compression post-don by further reducing garment circumference and increasing pressures. (3) The remaining circumference could be another, active-contracting fabric, producing an antagonistic active-contracting fabric system that equalizes somewhere between the force of Fabric 1 and the force of Fabric 2. The following section explores the design of this novel, fully-functional approach.

6.4.1 Functionality

As shown in Figure 6.3, an ideal method for bypassing the need for traditional adjustable closures required to don/doff a high-force CGs is to create an antogonistic, active-contracting garment that is capable of fitting and compressing. In simplistic terms, the garment could be primarily composed of one active-contracting fabric (Fabric 1) whose function is to provide garment fit. A second panel (Fabric 2) could be added to add compression force to the system. These fabrics would be actuated one after the other.

Figure 6.3 depicts this color-coded garment (blue = martensite; red = austenite) (1) beginning compliant and oversized in relation to body dimensions. (2) Slight M_t forces are applied to the garment as it is pulled over the body, causing slight martensitic garment strain. (3) Once the garment is on the body, force and length are released to M_r, martensite relaxation. (4) As the garment temperature transitions from cool, ambient temperature to warm body temperature, the garment actuates and self-fits to the shape and size of the body. (5) The high-force compression panels would be subsequently actuated and controlled through battery-powered joule heating. Depending on the behavior of the material used, this battery-powered step could be continuous and dialed up and down to precisely increase or decrease pressure. Alternatively, if SMA is designed with a low martensite start temperature (e.g. $M_s = 0°\text{C}$), the garment could be temporarily powered to induce austenite and then

powered off, knowing that the garment will not return to a martensite state until exposed to freezing temperatures. In this instance, the garment would require a zipper release to enable doff and could be stored in the freezer until the following wear.

To further define the antagonistic system, Figure 6.4 describes the interaction of two, hypothetical active-contracting fabrics connected around a hypothetical limb circumference. The major benefit of this system is that the garment can be donned with little-to-no M_t forces and still reach high A_t forces without the addition of sewn closures. The following sections break down the phases from no-forces, to fitting-forces, to compression-forces.

Phase 1: Two different contractile SMA knitted actuator fabrics (Fabric 1 & Fabric 2) are joined so that the combined length ($L1_{Fabric1} + L1_{Fabric2}$) makes up the circumferential length of the M_{free} garment. Fabric 1 serves as the fabric to accomplish fitting and Fabric 2 serves as the fabric to accomplish compression. In phase one, the circumferential length of the martensitic garment is greater than the circumferential length of the body, making it a positive ease garment. This relationship is described mathematically in Equation 6.1.

$$L1_{Fabric1,M_{free}} + L1_{Fabric2,M_{free}} > l_c \tag{6.1}$$

In Figure 6.4, phase 1 is depicted at the intersection between length 1 (L_1) and force 1 (F_1). For Fabric 1, L_1 is longer than L_1 for Fabric 2; however, the forces equalize so that the force of both fabrics is depicted by the same F_1.

Phase 2: In phase 2, only Fabric 1 is actuated, causing length to decrease from L_1 to L_2. This contraction of Fabric 1 strains Fabric 2 and creates a length increase in Fabric 2 from L_1 to L_2. Because both fabrics are extensible in this case, there is not a true blocked, or fixed length scenario. As Fabric 2 strains to a M_t length, it acts as a weak extension spring that counters the actuation contraction of Fabric 1. Consequently, Fabric 1 increases to an austenite tension (A_t) force on a diagonal path that mirrors the stiffness of Fabric 2's martensite curve. Displacement stops at L_2 (now the length of Fabric 1 is smaller than the length of fabric 2) and force between Fabrics 1 and 2 equalize at the intersection of Fabric 1's austenite curve and the mirror of Fabric 2's martensite curve at F2. Phase 2 can be represented by Equation 6.2,

$$L2_{Fabric1,A_t} + L2_{Fabric2,M_t} \approx L_{body} \tag{6.2}$$

where Fabric 1's austenetic length is less than its martensite length,

$$L2_{Fabric1,A_t} < L1_{Fabric1,M_{free}} \tag{6.3}$$

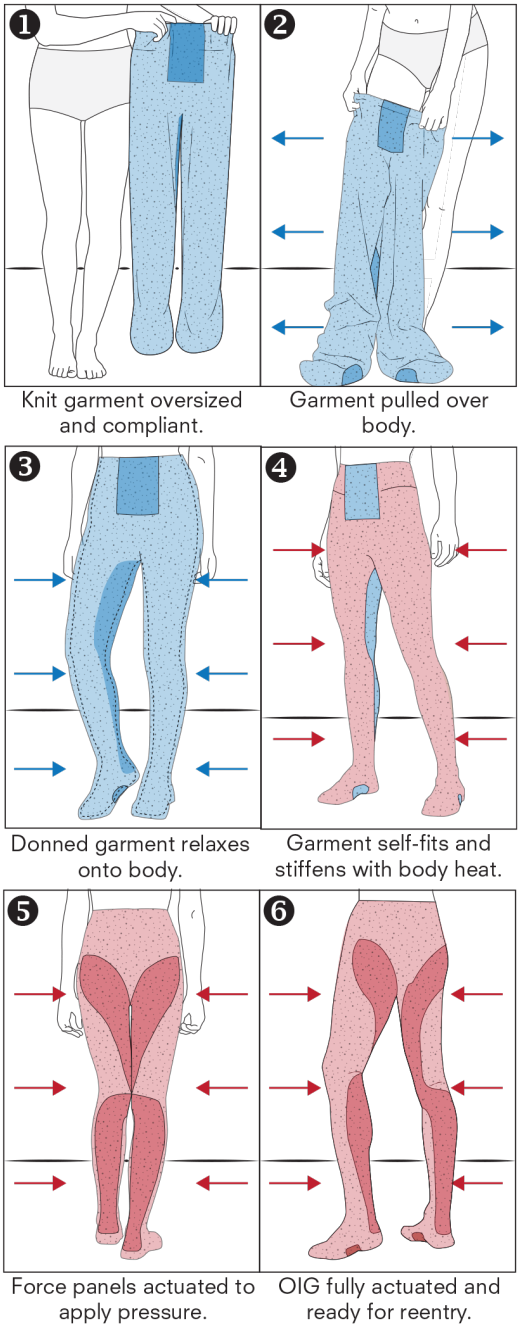

Figure 6.3: **Antogonistic Active-Contracting Garment System:** The majority of the garment would be made out of active-contracting Fabric 1, whose role is to provide garment fitting. Select panels of active-contracting Fabric 2 are included to actuate after Fabric 1 to provide compression post-fitting. Actuated fabrics are depicted in red. Unactuated fabrics ar depicted in blue. Fabric 1 (fitting) is presented in lighter colors. Fabric 2 (compression) is presented in darker colors.

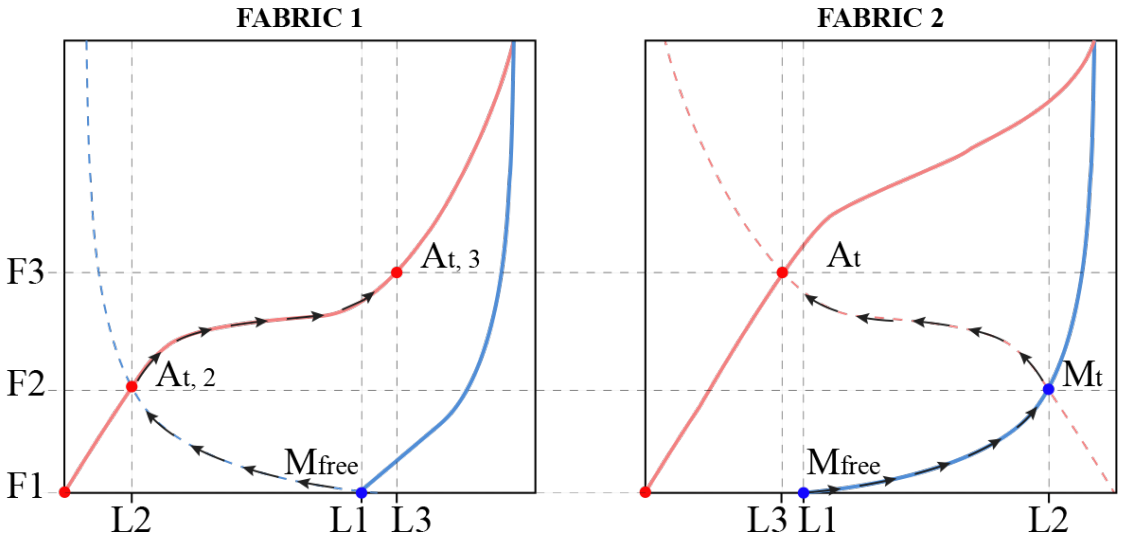

Figure 6.4: **Antagonistic System:** When two active-contracting fabrics are attached together to make up the full circumference of an active-contracting garment, the compressive force after actuating Fabric 1 is represented by Force 2 (F2). When Fabric 2 subsequently actuated, the total system force rises from F2 and F3.

and Fabric 2's tensioned martensite length is greater than its no-load martensite length.

$$L2_{Fabric2,M_t} > L1_{Fabric2,M_{free}} \tag{6.4}$$

Phase 3: Phase 3 is the final garment actuation step. Because Fabric 1 is already in an actuated state, when Fabric 2 actuates, Fabric 1 behaves superelastically. Fabric 1 incrementally increases force along its austenite path until the A_t forces of Fabric 1 equalize with the A_t forces of Fabric 2. Rather than producing a length-controlled, blocked force, Fabric 2 attempts to contract against elastic tension caused by Fabric 1, causing an increase in force and decrease in length along a path that mirrors Fabric 1's austenite path. The overall force that is achieved by the antagonistic system is determined by the intersection of Fabric 2's austenite curve and Fabric 1's mirrored austenite curve.

Figure 6.5 presents an alternative visual for the mechanically antagonistic system using flat knit panels as if a cross-sectional circumference were sliced and laid flat. The three stacked depictions of the garment system correspond with Phases 1, 2, & 3 described above. The design of a fully-functional, antagonistic compression system is in early stages of conceptualization and development, but proposes compelling future systems research. The following section explores forthcoming work that could enable such an antagonistic systems

design as well as further active-contracting fabric research.

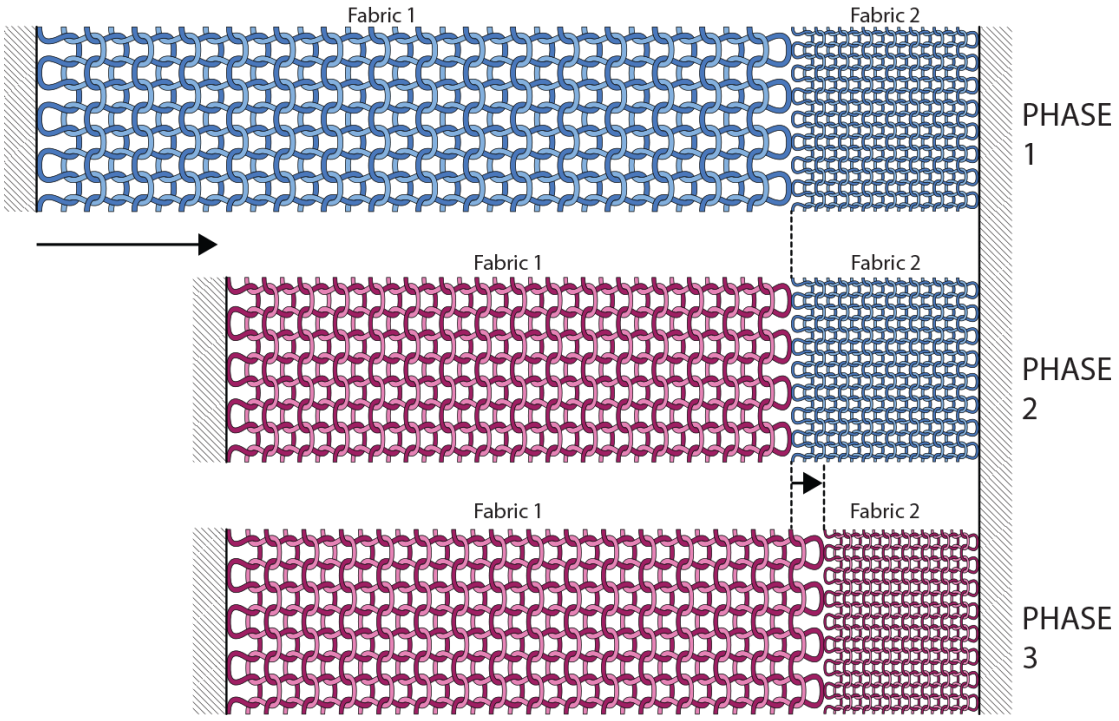

Figure 6.5: **Antagonistic System:** Two active-contracting fabrics are attached together to make up the full circumference of an active-contracting garment. The behavior of Fabrics 1 and 2 correspond with the material curves illustrated in Figure 6.4. Phases 1, 2, and 3 correspond with internal positions described in Section 6.4.1: Functionality. Blue knits indicate a martensite state while red knit indicate an austenite state. The materials curves used to represent this relationship are fictitious and for illustrative purposes only.

6.5 Future Work

Future work will be conducted to verify mathematically approximated pressure ranges through three-dimensional pressure testing, increase actuation forces through SMA yarn development, tailor SMA actuation temperature and develop corresponding control strategies, and further develop novel performance features, such as auxetic and force-plateauing behavior. This work concludes with a discussion of each area of future work.

6.5.1 Pressure Testing

While on-body pressures have been calculated to make comparisons between prototype swatch materials, true normal force pressures tests need to be conducted to validate these calculations. The fabric swatches will be fabricated in 30 x 15 cm swatches to simulate a lower leg compression sleeve. As shown in Figure 6.6, the testing will be conducted on a plexiglass cylinder with a circumference of 30 cm and radius of 0.05 meters to approximate an average limb circumference and relate to pressure calculations from prior force testing. The plexiglass surface will be covered with a layer of 1/8 polyurethane foam, as specified in [7] to simulate the bodys soft tissue. Three force sensitive resisters (FSR) (111N 0-25 lbs, FlexiForce B201, Tekscan, Boston, MA, USA) will be used to gather point pressure in the center of each knit sample, as depicted in Figure 6.6. The raw sensor data will be calibrated using an Instron tensile testing machine that can apply known forces to the sensor. A 10 point calibration (0-25 lbs) will be used for maximum accuracy. Small teflon pucks will be placed underneath each FSR to reduce flex which has been found to generate unpredictable results. Before conducting tests with active knits, the setup will be validated by applying known pressures (i.e. 20, 40, 60, 80 mmHg) with a calibrated blood pressure cuff, 5 times each. This initial test will allow us to better approximate pressure capabilities of active-contracting fabrics.

6.5.2 Tailor Actuation Temperature & Develop Control Strategies

All characterization in this work was conducted with high-temperature actuator wire (A_f = 90°C). Future work should develop SMA actuator wire with an A_f temperature close to or slightly above skin temperature. Figure 6.7 presents a chart of possible control strategies for active-contracting garments. If actuation is controlled through joule heating, an active-contracting knit with low hysteresis could be used to enable pressure to be dialed up and down with electrical power (system 2). Alternatively, an active-contracting fabric with high hysteresis that increases force upon cool-down could be used. In this case (system 1), the garment would be electrically powered to reach A_f temperature and would be subsequently turned off. If the body temperature were above the M_s temperature, the system would stay active without power. Systems 3-10 describe various methods to actuate the system through contact heating. The SMA materials could be designed with an actuation temperature at skin temperature so that the system actuates upon donning (systems 3-4). Active-contracting fabrics could be designed into the garment (system 3) or attached to the garment

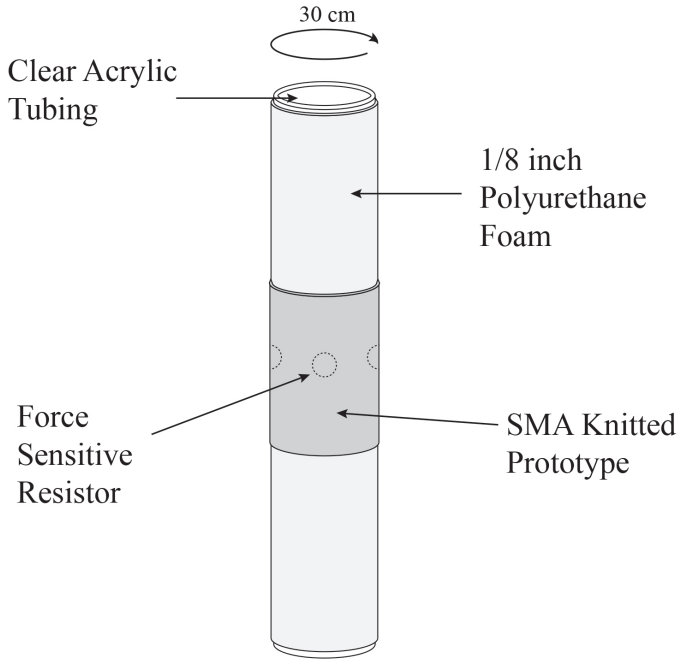

Figure 6.6: **Pressure Testing Setup.**

with modular panels that could be zipped on and off as needed (system 4). More complex methods of contact heating include systems 5-10 that use fluid, like NASA's liquid cooling garment, and phase change materials to modify active-contracting garment temperature.

Figure 6.8 evaluates systems 1-10 described in Figure 6.7 in terms of system trade-offs. In terms of garment wearability, pressure control (the ability to increase or decrease pressure as needed) and thermal comfort are important to users. Figure 6.8 shows that a neutral system that does not require added cold or heat to function is only possible if body heat is the actuation stimulus. In these scenarios (systems 1, 3, 4), the garment is either always tight until it is doffed or the garment is designed with modular active regions that are snapped or zipped on and off to add or relieve pressure.

Cooling and heating are two methods to create controllable CGs. Added heat is easily accomplished through joule heating (system 2). Added cooling would be more difficult to accomplish through liquid cooling channels or phase change materials (PCM). In this case, the active materials would be designed to actuate at body temperature and the hysteresis cool-down curve would need to increase in force upon slight cooling, as shown in Figure 6.7. While the strategy chosen is dependent on the application, it is likely a combination of contact body heating (system 3) and joule heating (system 1) are pursued.

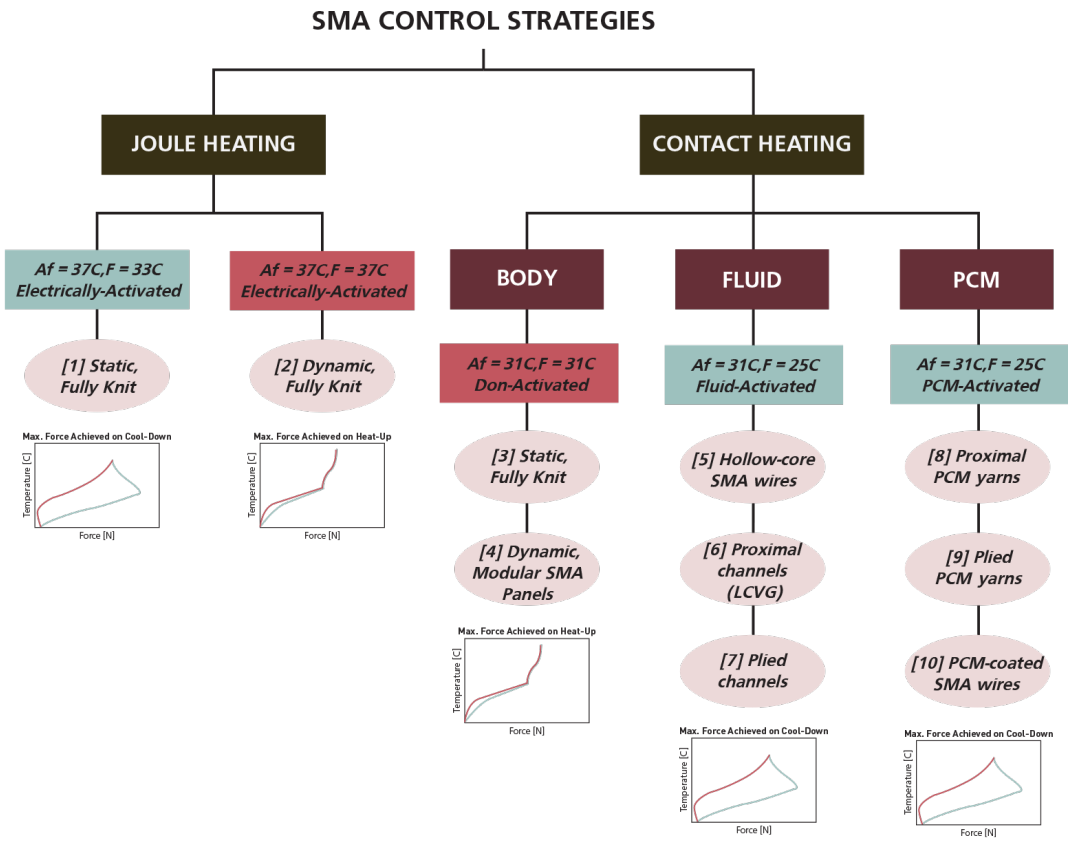

Figure 6.7: **Control Strategies for Active-Contracting Garments:** Various methods of joule heating and contact heating can be used to power active-contracting fabrics.

6.5.3 Increased Force Behavior

The active-contracting fabrics evaluated in this work are all composed of SMA wires. Future work will look at methods to increase active-contracting forces through SMA yarn development. These yarns would incorporate many SMA wires spun with traditional fibers (e.g. kevlar, wool, polyester). Passive textiles are commonly constructed with yarns made of bundles of staple fibers or filaments (i.e. multifilaments), rather than monofilaments (e.g. wire), to increase flexibility and improve fabric hand. Multifilament yarns, or yarns made with many filament fibers, are stronger than either monofilament or staple fiber yarns. Additionally, yarn are typically twisted together to increases frictional forces. Motivated by passive yarn engineering techniques, we hypothesize that active textiles constructed with multifilament SMA yarns, rather than a monofilament SMA, will increase active textile

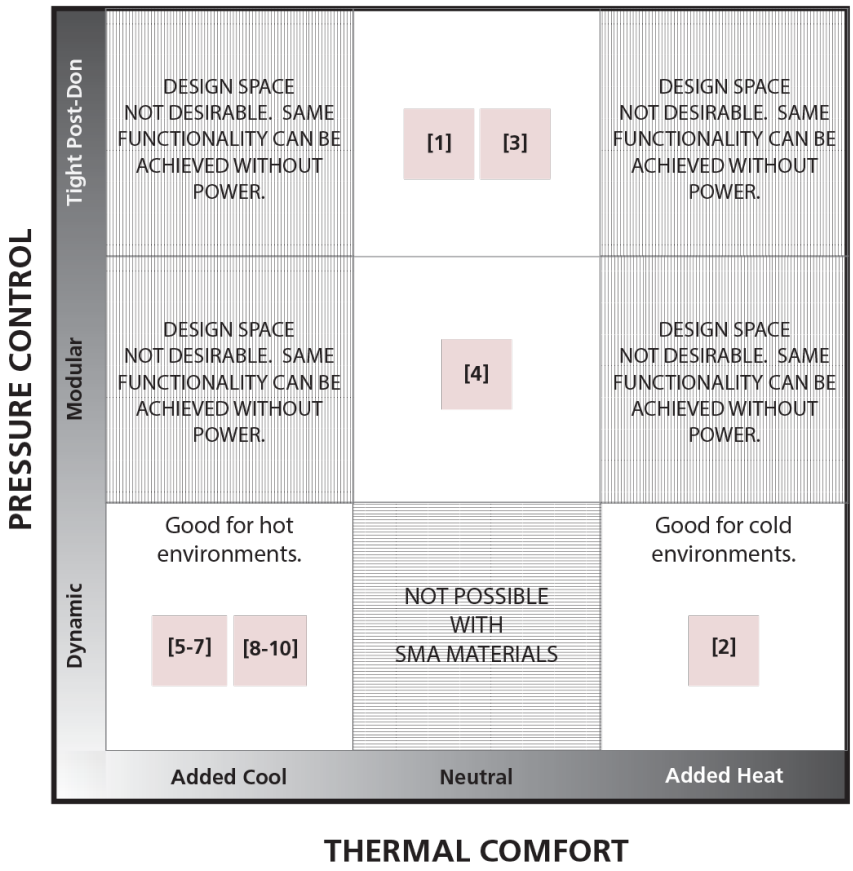

Figure 6.8: **Trade-off Between Dynamic Control and Thermal Balance:** Each strategy to power active-contracting fabrics presented in Figure 6.7 has design trade-offs presented here.

strength and flexibility. Additionally, we hypothesize that the addition of yarn twist will increase active textile contractive force through added shear stress. Figure 6.9 depicts yarn variables that could be modified to increase actuation contraction: (1) number of SMA filaments, (2) twists per inch, and (3) number of yarn plys.

6.5.4 Edge Effects & Garment Shaping

While the prior analysis of active-contracting fabrics presented in Chapter 4 only evaluates rectangular fabric samples, to construct active-contracting garment for the body the knitted fabric must be shaped to match the dimensions of the body. Shaping, or gradually changing the dimensions of a knitted fabrics, is generally accomplished by selectively

adding or subtracting loops to make the fabric wider or narrower (e.g. ankle circumference, thigh circumference) as well as longer or shorter (e.g. back leg length, front leg length). Through the construction of the prototype garment in Chapter 5, we determined that actuation of shaped edges perform differently than the center of the fabric. When edge loops were stacked over each other to subtract a column of knitted wales, actuation in that area produced fabric curling. Alternatively, when edge loops were spread out to add a column of knitted wales, actuation in that area produced amplified fabric contraction, a behavior that is consistent with prior knit index research [4].

While future research should explore the mechanical behavior of edge conditions created through garment shaping, further development of active-contracting fabric behavior may change the observed behavior. Preliminary analysis of SMA yarns used in the construction of active-contracting fabrics have shown that the new structures behave more cohesively than monofilament SMA knits. Specifically, the force-extension curves are smoother and exhibit little-to-no loop slippage that creates jagged force-extension curves that characterize monofilament SMA knit performance. Additionally, the structures are more compact because added fiber fills out the loop enclosed areas. This preliminary analysis suggests that the complex behavior of shaped edges may be mitigated, or at least lessened through yarn design; however, future research should be dedicated to characterizing edge effects once active-contracting fabrics are tailored to the application.

Figure 6.9: **Experimental Yarn Design:** Multifilament yarns can be designed with systematically varied SMA filaments (4 wires vs 8 wires), twists per inch (3 TPI vs 9 TPI), and yarn plies (1 twisted yarns vs 2 twisted yarns twisted together).

6.5.5 Auxetic Behavior

Preliminary experiments with fabricating and knitting SMA yarns show that active- contracting fabrics can exhibit auxetic behavior, specifically, contracting in x- and y-directions. See Figure 6.10. This behavior could be particularly useful for areas of the body that expand and contract between postures. For instance, during knee flexion, the skin on the back on the knee contracts and the skin on the front of the knee expands to facilitate motion. Similarly, the front on the pelvis contracts and the back of the thighs expand when transitioning from a standing to a sitting posture. Consequently, more work should be conducted to determine the suitability of auxetic active contracting fabrics for select areas of the body to preserve full range of motion.

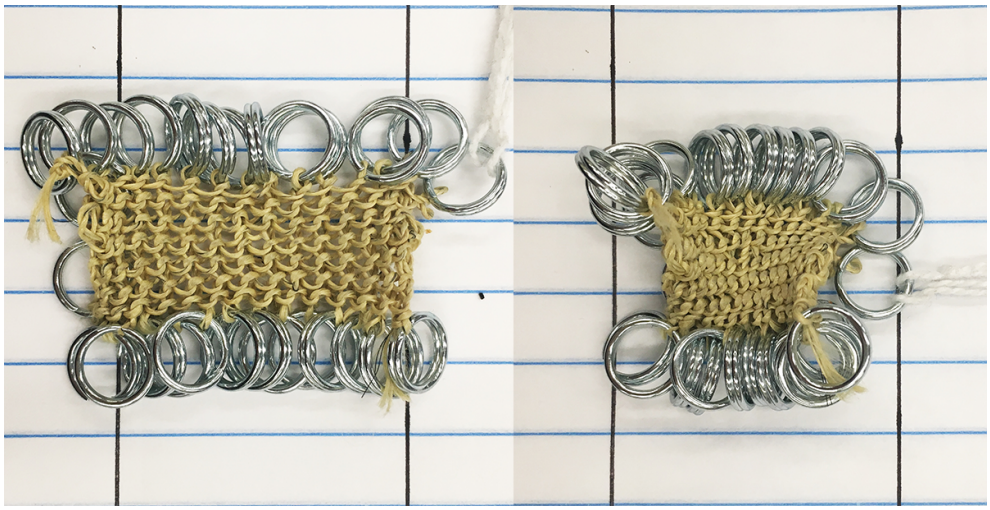

Figure 6.10: **Auxetic Active-Contracting Fabric:** Preliminary samples of knitted SMA yarn show an auxetic behavior that may be useful for future garment development to preserve mobility.

6.5.6 Force-Plateauing Behavior

Certain passive elastic fabrics are capable of plateauing force across a range of displacements to enable pressure stabilization with small changes in body circumference [84]. For instance, in 2011 Lee et al. reference a spandex fabric that experiences a small change in pressure (e.g. ± 3 mmHg) with a relatively large change in body circumference (e.g. ± 3 cm). This plateauing behavior is highly-desirable for on-body compression applications to prevent

large swings in pressure, as detailed in Chapter 3. Consequently, force-plateauing active-contracting fabrics would enable the design of a purely highly-simplified, purely mechanical system that exerts a consistent force of the body within a given range of dimensional change. The enormous benefit of such a fabrics deserves further investigation, development, and refinement for compression garment applications.

It is possible that active-contracting knits could be designed to have a similar force-plateau behavior within a range of length displacements. As shown in Figure 6.11, some active-contracting knits exhibit superelastic behavior that suggests force plateauing is possible. Upon increase from Length 1 to Length 2, forces are approximately stable. This means that a garment that uses this fabric around the knee would not exert increased forces around the knee upon knee flexion; however, hysteretic behavior would cause a decrease in force upon knee extension that could not be restored until subsequent knee flextion. In other words, the plateauing behavior of active-contracting fabrics only occurs upon length increase and is not reversible. Additional analysis should be conducted to identify the magnitude of these force plateaus and determine what variables cause them to appear or disappear.

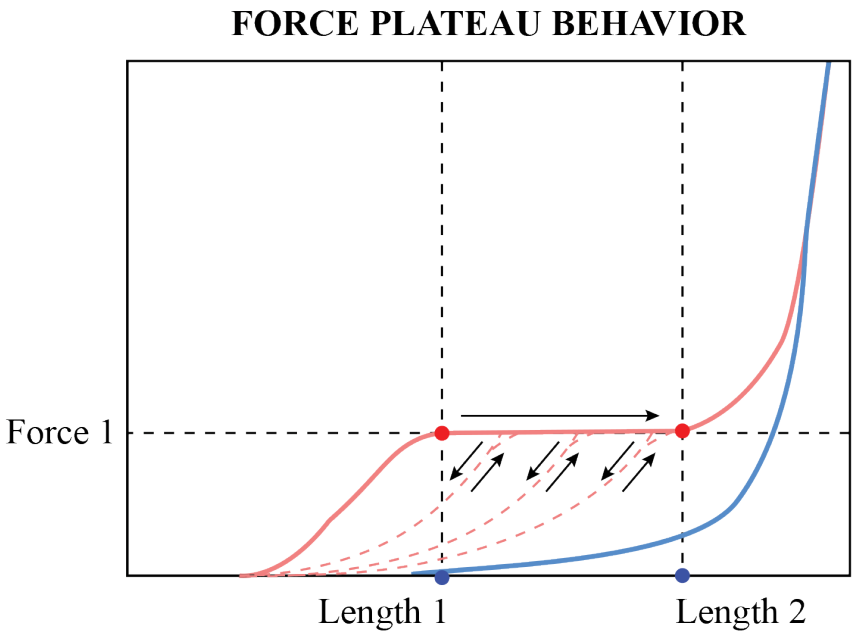

Figure 6.11: **Force Plateauing Behavior of Active-Contracting Fabrics:** Some active-contracting fabrics appear to plateau in force between certain knit lengths. As long as the length increases, force is stable. If length decreases, however, hysteresis causes a drop in force that is not recovered until the knit returns to the maximum length. This behavior could prevent large increases in forces around joints that negatively effect therapeutic benefits.

References

[1] SizeUSA. Technical report.

[2] R. Granberry, J. Duvall, L.E. Dunne, and B. Holschuh. An analysis of anthropometric geometric variability of the lower leg for the fit and function of advanced functional garments. In *Proceedings - International Symposium on Wearable Computers, ISWC*, volume Part F1305, 2017.

[3] A. C.K. Chan. *The development of apparel sizing systems from anthropometric data*. Woodhead Publishing Limited, 2014.

[4] Kevin Eschen and Julianna Abel. Effect of Geometric Design Parameters on Contractile SMA Knitted Actuator Performance. In *Proceedings of the ASME Conference on Smart Materials, Adaptive Structures and Intelligent Systems*, Snowbird, UT, 2017.

[5] J. Duvall, R. Granberry, C. Johnson, K. Kelley, B. Johnson, M. Joyner, L. E. Dunne, and B. Holschuh. The Design and Development of Active Compression Garments for Orthostatic Intolerance. *ASME Journal of Medical Devices*, 2017.

[6] C. J. Wildin, A. C W Hui, C. N A Esler, and P. J. Gregg. In vivo pressure profiles of thigh-length graduated compression stockings. *British Journal of Surgery*, 85(9):1228–1231, 1998.

[7] Lisa Macintyre. Designing pressure garments capable of exerting specific pressures on limbs. *Burns*, 33(5):579–586, 2007.

[8] Ashwin Rao, A R Srinivasa, and J N Reddy. *Design of Shape Memory Alloy (SMA) Actuators*. 2015.

[9] P. J. Myers-McDevitt. *Complete guide to size specification and technical design*. Fairchild Books, New York, 2nd editio edition, 2009.

[10] Steven H. Platts, Jennifer A. Tuxhorn, L. Christine Ribeiro, Michael B. Stenger, Stuart M C Lee, and Janice V. Meck. Compression garments as countermeasures to orthostatic intolerance. *Aviation Space and Environmental Medicine*, 80(5 PART 1):437–442, 2009.

[11] T Jennings, L Tripp, L Howell, D Loukoumidis, and C Goodyear. The Effects of Anti-Ballooing G-Suit and a Buttstrap G-Suit on G-Tolerance. In *Aerospace and Electronics Conference*, pages 799–802, 1989.

[12] Stuart M C Lee, Jamie R. Guined, Angela K. Brown, Michael B. Stenger, and Steven H. Platts. Metabolic consequences of garments worn to protect against post-spaceflight orthostatic intolerance. *Aviation Space and Environmental Medicine*, 82(6):648–653, 2011.

[13] Kunihiko Tanaka, Patrick Danaher, Paul Webb, and Alan R. Hargens. Mobility of the elastic counterpressure space suit glove. *Aviation Space and Environmental Medicine*, 80(10):890–893, 2009.

[14] Rong Liu, Yi Lin Kwok, Yi Li, Terence Loa, Xin Zhang, and Xiao Qun Dai. Objective Evaluation of Skin Pressure Distribution of Graduated Elastic Compression Stockings. *Dermatologic Surgery*, 31(6):615–624, 2005.

[15] Rong Liu, Yi Lin Kwok, Yi Li, Terence T. Lao, and Xin Zhang. Skin pressure profiles and variations with body postural changes beneath medical elastic compression stockings. *International Journal of Dermatology*, 46(5):514–523, 2007.

[16] Colin Quinn, Brian Deegan, John Cooke, Sheila Carew, Ailish Hannigan, Colum Dunne, and Declan Lyons. Therapeutic use of compression stockings for orthostatic hypotension: An assessment of patient and physician perspectives and practices. *Age and Ageing*, 44(2):339–342, 2015.

[17] L Christine Ribeiro, Stuart M. C. Lee, Angela K. Brown, Michael B. Stenger, and Steven H. Platts. Countermeasures to Space-flight-induced Orthostatic Hypotension. Technical report, NASA, Houston, 2009.

[18] Julianna Abel, Jonathan Luntz, and Diann Brei. Hierarchical architecture of active knits. *Smart Materials and Structures*, 22(12):16, 2013.

[19] Bradley T Holschuh and Dava J Newman. Morphing Compression Garments for Space Medicine and Extravehicular Activity Using Active Materials. *Aerospace medicine and human performance*, 87(2):84–92, 2016.

[20] D.C. Lagoudas, editor. *Shape Memory Alloys: Modeling and Engineering Applications*. Springer Science+Business Media, LLC, New York, 2008.

[21] Rachael Granberry, Lucy E Dunne, and Bradley Holschuh. Effects of Anthropometric Variability and Dimensional Change Due to Posture on Orthostatic Intolerance Garments. In *International Conference on Environmental Systems*, Charleston, 2017.

[22] R. Granberry, K. Eschen, B. Holschuh, and J. Abel. Active-Contracting, Variable-Stiffness Fabrics for Self-Fitting Wearables. In *ASME Conference on Smart Materials, Adaptive Structures & Intelligent Systems*, San Antonio, TX, 2018.

[23] Susan M. Watkins and Lucy E. Dunne. *Functional Clothing Design: From Sportswear to Spacesuits*. New York, 2015.

[24] Deepti Guptaa. Functional clothing- definition and classification. *Indian Journal of Fibre and Textile Research*, 36(4):312–326, 2011.

[25] Linsey Griffin, Crystal Compton, and Lucy E. Dunne. An analysis of the variability of anatomical body references within ready-to-wear garment sizes. *Proceedings of the 2016 ACM International Symposium on Wearable Computers - ISWC '16*, pages 84–91, 2016.

[26] Alan T. Asbeck, Kai Schmidt, and Conor J. Walsh. Soft exosuit for hip assistance. *Robotics and Autonomous Systems*, 73:102–110, 2015.

[27] Matthew B Yandell, Dmitry Popov, Brendan T Quinlivan, Conor Walsh, Kathleen O 'donnell, and Karl E Zelik. Systematic evaluation of human-exosuit physical interfaces. 2011.

[28] Mary L. Davis-Meyers. The Development of American Menswear Pattern Drafting Technology, 1822 to 1860. *Clothing and Textiles Research Journal*, 10(3):12–20, 1992.

[29] H. Jaffe and N Relis. *Draping for Fashion Design*. Regents/Prentice Hall, Englewood Cliffs, 2nd editio edition, 1993.

[30] Gilbert S. Daniels and H. C. Jr. Meyers. Anthropometry of Male Basic Trainees. Technical report, Wright Air Development Center, 1953.

[31] Lucy Dunne. Beyond the second skin: an experimental approach to addressing garment style and fit variables in the design of sensing garments. *International Journal of Fashion Design, Technology and Education*, 3(3):109–117, 2010.

[32] Crystal Compton. *Fit for Sace: Leveraging a Novel Skin Contact Measurement Technique Towards a More Efficient Liquid Cooled Garment.* PhD thesis, University of Minnesota, 2016.

[33] Compression Store, 2018.

[34] R L Summers, S Platts, J G Myers, and T G Coleman. Theoretical analysis of the mechanisms of a gender differentiation in the propensity for orthostatic intolerance after spaceflight. *Theor Biol Med Model*, 7:8, 2010.

[35] J V Meck, C J Reyes, S a Perez, a L Goldberger, and M G Ziegler. Marked exacerbation of orthostatic intolerance after long- vs. short-duration spaceflight in veteran astronauts. *Psychosomatic Medicine*, 63(6):865–873, 2001.

[36] H. Edgell, A. Grinberg, N. Gagné, K. R. Beavers, and R. L. Hughson. Cardiovascular responses to lower body negative pressure before and after 4 h of head-down bed rest and seated control in men and women. *Journal of Applied Physiology*, 113(10):1604–1612, 2012.

[37] Wendy W Waters, Michael G Ziegler, Janice V Meck, W Wendy, Michael G Ziegler, and V Janice. Postspaceflight orthostatic hypotension occurs mostly in women and is predicted by low vascular resistance. pages 586–594, 2002.

[38] Deborah L. Harm, Richard T. Jennings, Janice V. Meck, Michael R. Powell, Lakshmi Putcha, Clarence P. Sams, Suzanne M. Schneider, Linda C. Shackelford, Scott M. Smith, and Peggy A. Whitson. Invited Review: Gender Issues Related to Spaceflight: a NASA Perspective. *Journal of Applied Physiology*, 91:2374–2383, 2001.

[39] Janice M Fritsch-Yelle, Peggy A Whitson, Roberta L Bondar, and Troy E Brown. Subnormal norepinephrine release relates to presyncope in astronauts after spaceflight. *Journal of Applied Physiology*, 81(5):2134–2141, 1996.

[40] Marlene S. Grenon, Xinshu Xiao, Shelley Hurwitz, Natalie Sheynberg, Christine Kim, Ellen W. Seely, Richard J. Cohen, and Gordon H. Williams. Why Is Orthostatic Tolerance Lower in Women than in Men? Renal and Cardiovascular Responses to Simulated Microgravity and the Role of Midodrine. *Journal of Investigative Medicine*, 54(4):180–190, 2006.

[41] S Choi and S P Ashdown. 3D body scan analysis of dimensional change in lower body measurements for active body positions. *Textile Research Journal*, 81(1):81–93, 2011.

[42] Elaine Nicpon EN Marieb and Katja Hoehn. *Human Anatomy & Physiology*, volume Chapter 18. 2013.

[43] A. E. Nicogossian. The Apollo-Soyuz Test Project Medical Report. Technical report, NASA, Washington D.C., 1977.

[44] A LeBlanc, C Lin, L Shackelford, V Sinitsyn, H Evans, O Belichenko, B Schenkman, I Kozlovskaya, V Oganov, A Bakulin, and T Hedrick. Muscle volume, MRI relaxation times (T2), and body composition after spaceflight. *Journal of applied physiology (Bethesda, Md. : 1985)*, 89(6):2158–2164, 2000.

[45] Satish R. Raj. The postural tachycardia syndrome (POTS): Pathophysiology, diagnosis & management. *Indian Pacing and Electrophysiology Journal*, 6(2):84–99, 2006.

[46] Herbert O. Sieker, John F. Burnum, John B. Hickman, and Kenneth E. Penrod. Treatment of Postural Hypotension with a Counter-Pressure Garment. *JAMA: The Journal of the American Medical Association*, 161(2):132–135, 1956.

[47] J C Denq, T L Opfer-Gehrking, M Giuliani, J Felten, V A Convertino, and P A Low. Efficacy of compression of different capacitance beds in the amelioration of orthostatic hypotension. *Clin Auton Res*, 7(6):321–326, 1997.

[48] Kathryn L. Leuders. ISS Crew Transportation and Services Requirements Document CCT-REQ-1130. Technical report, NASA, 2015.

[49] Erica Arverud, Jorge Azevedo, Fausto Labruto, and Paul W. Ackermann. Adjuvant compression therapy in orthopaedic surgery-an evidence-based review. *European Orthopaedics and Traumatology*, 4(1):49–57, 2013.

[50] Katarzyna Ochalek, Tomasz Gradalski, and Hugo Partsch. Preventing early postoperative arm swelling and lymphedema manifestation by compression sleeves after axillary lymph node interventions in breast cancer patients: A randomized controlled trial. *Journal of pain and symptom management*, 2017.

[51] Waldemar L Olszewski, Pradeep Jain, Govinda Ambujam, Marzanna Zaleska, Marta Cakala, and Tomasz Gradalski. Tissue fluid pressure and flow during pneumatic compression in lymphedema of lower limbs. *Lymphatic research and biology*, 9(2):77–83, 2011.

[52] Hsin Yung Chen, Hsiang Yang, Huang Ju Chi, and Hsin Ming Chen. Physiological effects of deep touch pressure on anxiety alleviation: The weighted blanket approach. *Journal of Medical and Biological Engineering*, 33(5):463–470, 2013.

[53] Kirsten Krauss. The Effects of Deep Touch Pressure on Anxiety. *The American journal of occupational therapy. : official publication of the American Occupational Therapy Association*, 41(6):366–373, 1987.

[54] Mickey Losinski, Katie Cook, Shanna Hirsch, and Sara Sanders. The Effects of Deep Pressure Therapies and Antecedent Exercise on Stereotypical Behaviors of Students With Autism Spectrum Disorders. *Behavioral Disorders*, 42(4):196–208, 2017.

[55] Nancy L. VandenBerg. The use of a weighted vest to increase on-task behavior in children with attention difficulties. *American Journal of Occupational Therapy*, 55(6):621–628, 2001.

[56] A. Ben-Sasson, A. S. Carter, and M. J. Briggs-Gowan. Sensory over-responsivity in elementary school: Prevalence and social-emotional correlates. *Journal of Abnormal Child Psychology*, 37(5):705–716, 2009.

[57] L. J. Olson and H. J. Moulton. Use of Weighted Vests in Pediatric Occupational Therapy Practice. *Physical & Occupational Therapy in Pediatrics*, 24(3):23–43, 2004.

[58] Get Pumped for Athleisure Beauty (Insights & Breakthroughs). *Global Cosmetic Industry*, 184(2):9(1), 2016.

[59] RAL-GZ 387-1:2008, RAL Deutsches Institut fur Gutesicherung und Kennzeichnung e.V.

[60] EU ENV 12718: 2001, Comite Europeen de Normalisation.

[61] Jai Prakash Sharma and Rashmi Salhotra. Tourniquets in orthopedic surgery. *Indian journal of orthopaedics*, 46(4):377–83, 2012.

[62] James P Henry, Owen L Slaughter, and Theodore Greiner. A Medical Massage Suit for Continuous Wear. *Angiology*, 6(5):482–494, 1955.

[63] Leslie Klenerman. Historical Background. In *The Tourniquet Manual Principles and Practice*, chapter 1, pages 1–16. Springer London, 2003.

[64] J W Frazier, T Gordon, and L J Meeker. Anti-G Suit Pressure-How Much is Just Right? In *Proceedings of the IEEE 1988 National Aerospace and Electronics Conference*, pages 897–902, 1988.

[65] Michael B. Stenger, Stuart M C Lee, Christian M. Westby, L. Christine Ribeiro, Tiffany R. Phillips, David S. Martin, and Steven H. Platts. Abdomen-high elastic gradient compression garments during post-spaceflight stand tests. *Aviation Space and Environmental Medicine*, 84(5):459–466, 2013.

[66] Joan M Hayes, Cheryl A Lehman, and Paula Castonguay. Graduated Compression-Stockings: Updating Practice, Improving Compliance. *MedSurg Nursing*, 11(4):163, 2002.

[67] N. B. Morgan and M. Broadley. Taking the art out of smart! - Forming processes and durability issues for the application of NiTi shape memory alloys in medical devices. *Medical Device Materials: Proceedings of the Materials & Processes for Medical Devices Conference*, pages 247–252, 2003.

[68] W. J. Buehler, J. V. Gilfrich, and R. C. Wiley. Effect of Low-Temperature Phase Changes on the Mechanical Properties of Alloys near Composition TiNi. *Journal of Applied Physics*, 34(5):1475–1477, 1963.

[69] D. Spencer. Knitting technology. *Knitting International*, 103(1229):22, 1996.

[70] C. Reichman. *Knitting Dictionary*. American Society of Knitting Technologists, New York, 1966.

[71] A. Cohen, I. Johnson, and J. Pizzuto. *J. J. Pizzuto's Fabric Science*. Fairchild Books, New York, 10th edition, 2012.

[72] Julianna Abel, Jonathan Luntz, and Diann Brei. Hierarchical architecture of active knits. *Smart Materials and Structures*, 22(12):16, 12 2013.

[73] Jessica A. Hill, Glyn Howatson, Ken A. van Someren, Stuart Davidson, and Charles R. Pedlar. The variation in pressures exerted by commercially available compression garments. *Sports Engineering*, 18(2):115–121, 2015.

[74] A J Best, S Williams, A Crozier, R Bhatt, P J Gregg, and A C W Hui. Graded Compression Stocking in Elective Orthopaedic Surgery: An Assessment of the In Vivo Performance of Commercially Available Stockings in Patients Having Hip and Knee Arthroplasty. *The Journal of Bone and Joint Surgery*, 82(1):116–118, 2000.

[75] German Institute for Quality Assurance. Medical Compression Hosiery. (January), 2000.

[76] W. Y. Leung, D. W. Yuen, Sun Pui Ng, and S. Q. Shi. Pressure Prediction Model for Compression Garment Design. *Journal of Burn Care & Research*, 31(5):716–727, 2010.

[77] Lisa Macintyre and Margot Baird. Pressure garments for use in the treatment of hypertrophic scars - A review of the problems associated with their use. *Burns*, 32(1):10–15, 2006.

[78] J M Abel, P Mane, B Pascoe, J Luntz, and D Brei. Experimental investigation of active rib stitch knitted architecture for flow control applications. *Active and Passive Smart Structures and Integrated Systems 2010*, 7643(PART 1):1–12, 2010.

[79] Deepti Gupta. *Anthropometry and the design and production of apparel: An overview.* Number 2005. Woodhead Publishing Limited, 2014.

[80] Lutz Walter, George Alexander Kartsounis, and Stefano Carosio. *Transforming clothing production into a demand-driven, knowledge-based, high-tech industry: The leapfrog paradigm.* 2009.

[81] Norsaadah Zakaria. *Body shape analysis and identification of key dimensions for apparel sizing systems.* Woodhead Publishing Limited, 2014.

[82] W. M. Huang, Z. Ding, C. C. Wang, J. Wei, Y. Zhao, and H. Purnawali. Shape memory materials. *Materials Today*, 13(7-8):54–61, 2010.

[83] E. H. Weber. *The Sense of Touch.* Academic Press for Experimental Psychology Society, London, 1978.

[84] Steven H Platts, Stuart M C Lee, Christian M Westby, L Christine Ribeiro, and B Michael. Compression stockings may ameliorate orthostatic intolerance in astronauts after short-duration space flight. Technical report, National Aeronautics and Space Administration.

Appendix A

Performance Plots

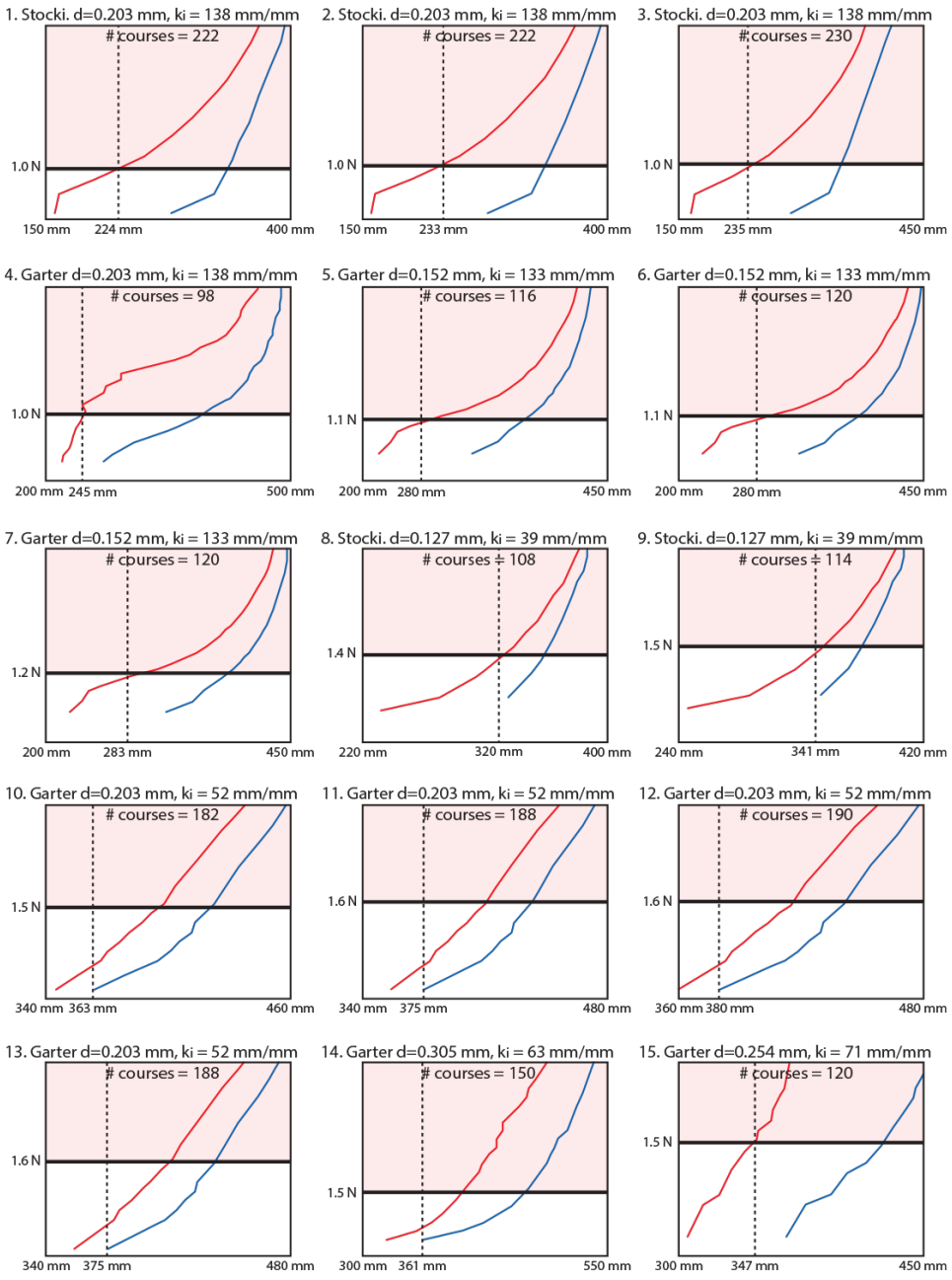
1. Stocki. d=0.203 mm, ki = 138 mm/mm
courses = 222
1.0 N
150 mm
224 mm
400 mm
2. Stocki. d=0.203 mm, ki = 138 mm/mm
courses = 222
1.0 N
150 mm
233 mm
400 mm
3. Stocki. d=0.203 mm, ki = 138 mm/mm
courses = 230
1.0 N
150 mm
235 mm
450 mm
4. Garter d=0.203 mm, ki = 138 mm/mm
courses = 98
1.0 N
200 mm
245 mm
500 mm
5. Garter d=0.152 mm, ki = 133 mm/mm
courses = 116
1.1 N
200 mm
280 mm
450 mm
6. Garter d=0.152 mm, ki = 133 mm/mm
courses = 120
1.1 N
200 mm
280 mm
450 mm
7. Garter d=0.152 mm, ki = 133 mm/mm
courses = 120
1.2 N
200 mm
283 mm
450 mm
8. Stocki. d=0.127 mm, ki = 39 mm/mm
courses = 108
1.4 N
220 mm
320 mm
400 mm
9. Stocki. d=0.127 mm, ki = 39 mm/mm
courses = 114
1.5 N
240 mm
341 mm
420 mm
10. Garter d=0.203 mm, ki = 52 mm/mm
courses = 182
1.5 N
340 mm
363 mm
460 mm
11. Garter d=0.203 mm, ki = 52 mm/mm
courses = 188
1.6 N
340 mm
375 mm
480 mm
12. Garter d=0.203 mm, ki = 52 mm/mm
courses = 190
1.6 N
360 mm
380 mm
480 mm
13. Garter d=0.203 mm, ki = 52 mm/mm
courses = 188
1.6 N
340 mm
375 mm
480 mm
14. Garter d=0.305 mm, ki = 63 mm/mm
courses = 150
1.5 N
300 mm
361 mm
550 mm
15. Garter d=0.254 mm, ki = 71 mm/mm
courses = 120
1.5 N
300 mm
347 mm
450 mm

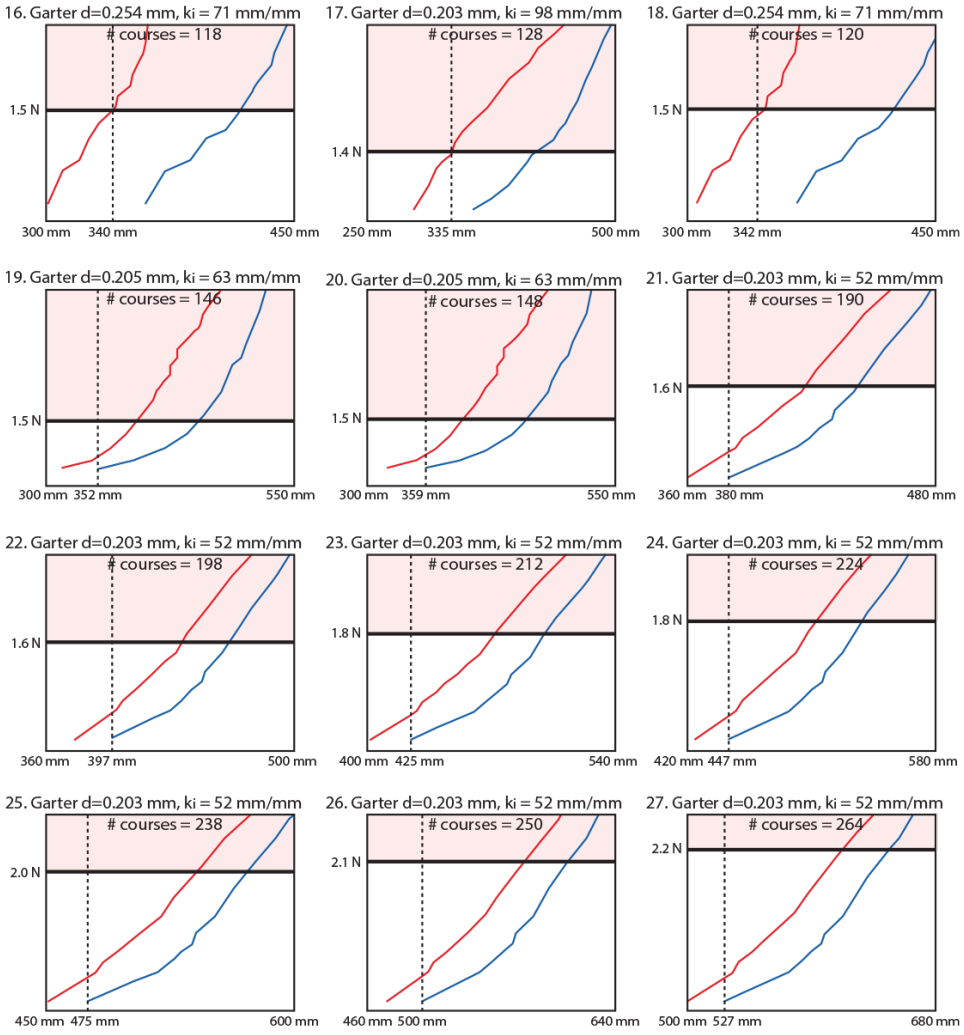
16. Garter d=0.254 mm, ki = 71 mm/mm
courses = 118
1.5 N
300 mm
340 mm
450 mm
17. Garter d=0.203 mm, ki = 98 mm/mm
courses = 128
1.4 N
250 mm
335 mm
500 mm
18. Garter d=0.254 mm, ki = 71 mm/mm
courses = 120
1.5 N
300 mm
342 mm
450 mm
19. Garter d=0.205 mm, ki = 63 mm/mm
courses = 146
1.5 N
300 mm
352 mm
550 mm
20. Garter d=0.205 mm, ki = 63 mm/mm
courses = 148
1.5 N
300 mm
359 mm
550 mm
21. Garter d=0.203 mm, ki = 52 mm/mm
courses = 190
1.6 N
360 mm
380 mm
480 mm
22. Garter d=0.203 mm, ki = 52 mm/mm
courses = 198
1.6 N
360 mm
397 mm
500 mm
23. Garter d=0.203 mm, ki = 52 mm/mm
courses = 212
1.8 N
400 mm
425 mm
540 mm
24. Garter d=0.203 mm, ki = 52 mm/mm
courses = 224
1.8 N
420 mm
447 mm
580 mm
25. Garter d=0.203 mm, ki = 52 mm/mm
courses = 238
2.0 N
450 mm
475 mm
600 mm
26. Garter d=0.203 mm, ki = 52 mm/mm
courses = 250
2.1 N
460 mm
500 mm
640 mm
27. Garter d=0.203 mm, ki = 52 mm/mm
courses = 264
2.2 N
500 mm
527 mm
680 mm

Appendix B

Garment Patterns

① knit 2 pieces Garter | d = 0.203 mm | ki = 52 mm/mm

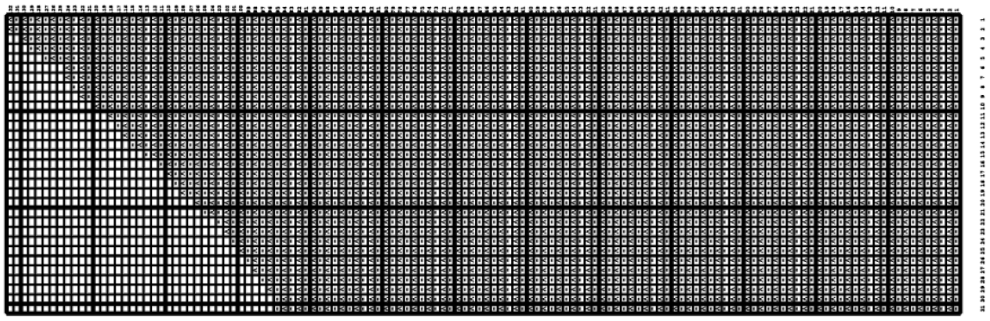

② double pattern Garter | d = 0.205 mm | ki = 63 mm/mm

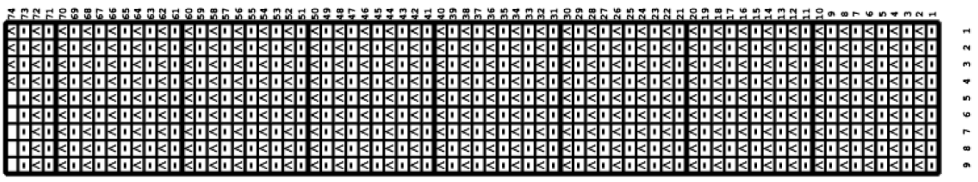

③ double pattern Garter | d = 0.254 mm | ki = 71 mm/mm

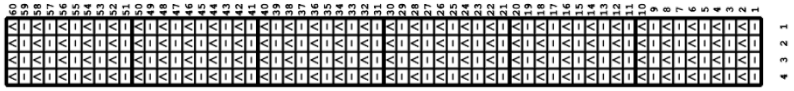

④ double pattern Garter | d = 0.203 mm | ki = 98 mm/mm

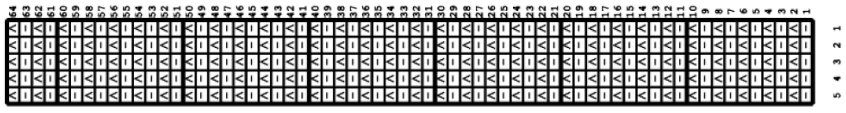

Knit Stitch Purl Stitch Garter: Knit and Purl Stitches Stockinette: Knit Stitches

⑤ double pattern Garter | d = 0.254 mm | ki = 71 mm/mm

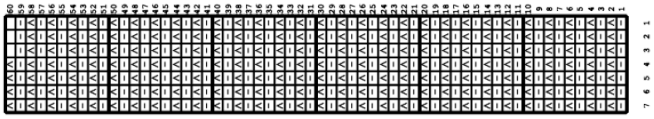

⑥ double pattern Garter | d = 0.305 mm | ki = 63 mm/mm

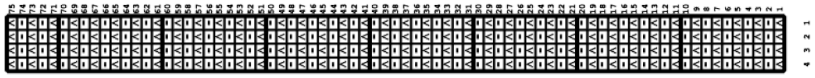

⑦ knit 1 piece Garter | d = 0.203 mm | ki = 52 mm/mm

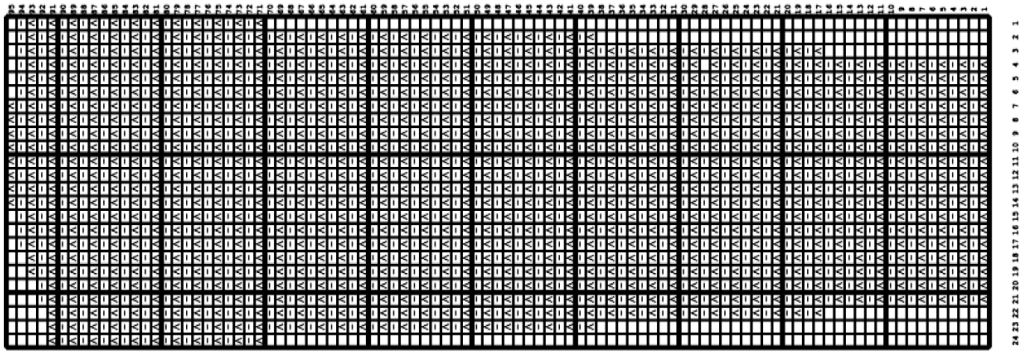

⑦ knit 1 piece Garter | d = 0.203 mm | ki = 52 mm/mm

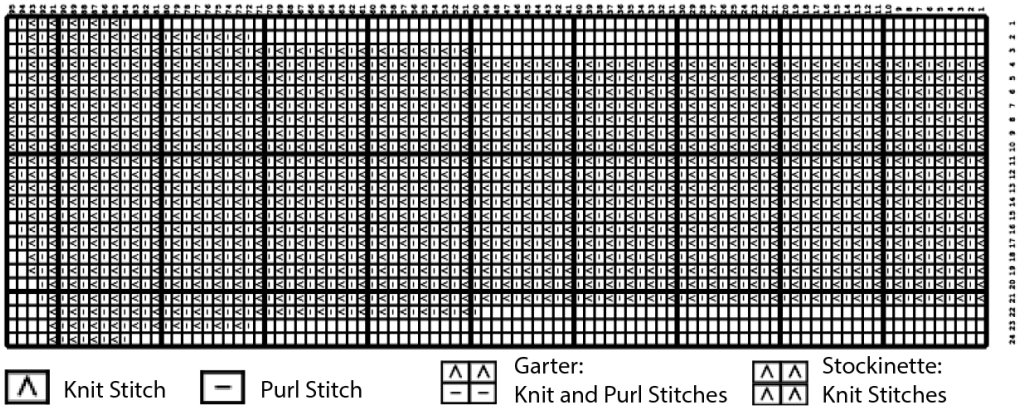

⑧ knit 2 pieces Stockiette | d = 0.127 mm | ki = 39 mm/mm

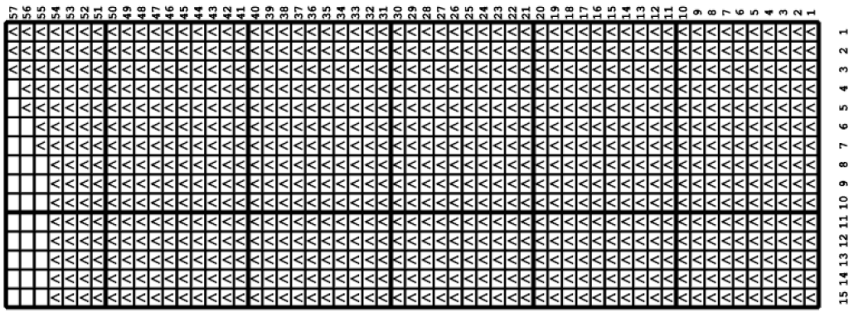

⑨ knit 2 pieces Garter | d = 0.152 mm | ki = 133 mm/mm

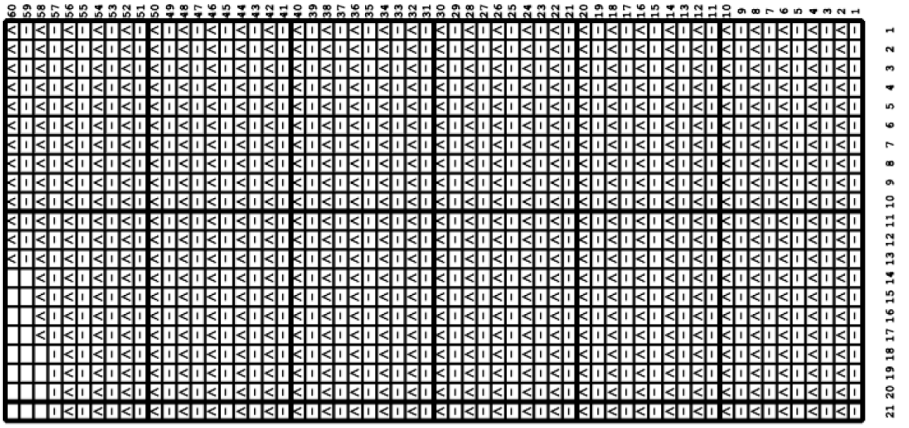

⑩ double pattern Garter | d = 0.203 mm | ki = 138 mm/mm

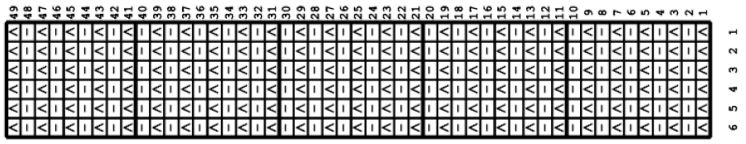

⑩ knit 2 pieces Stockinette | d = 0.203 mm | ki = 138 mm/mm

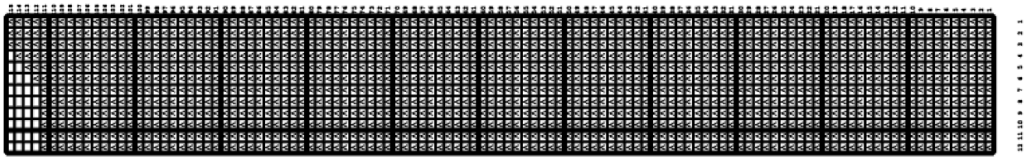

Knit Stitch | Purl Stitch | Garter: Knit and Purl Stitches | Stockinette: Knit Stitches

Table B.1: Acronyms

Acronym	Meaning
A – – – – – – –	– – – – – – –
$A_{L1,L2,L3,...,Ln}$	Austenite lengths
A_b	Austenite blocked
A_f	Austenite finish
A_{free}	Austenite free
$A_{l,m}$	Loop enclosed area, martensite free
A_s	Austenite start
A_t	Austenite tension
ADHD	Attention deficit hyperactivity disorder
AGS	Antigravity suit
ANOVA	Analysis of variance
ANSUR	Anthropometric Survey of US Army Personnel
ASD	Autism spectrum disorder
ASTM	American Society for Testing & Materials
B – – – – – – –	– – – – – – –
$\beta_{0,1,2,3,...,n}$	Regression coefficients
BMI	Body mass index
C – – – – – – –	– – – – – – –
C	Spring index
$c_{n,body}$	Circumference of the body at a given cross section
$c_{n,garment}$	Circumference of the garment at a given cross section
CAESAR	Civilian American & European Surface Anthropometry Resource
CG	Compression garment
CPI	Cycles per inch
D – – – – – – –	– – – – – – –
δ	Displacement
d	Wire diameter
DVT	Deep vein thrombosis
E – – – – – – –	– – – – – – –

Continued on next page

Table B.1 – continued from previous page

Acronym	Meaning
ECG	Electrocardiogram
F – – – – – – –	– – – – – – –
F	Force [N]
F_{app}	Force applied
F_{crit}	Critical force at which pressure reached 1333 Pa
$F\hat{W}$	Force applied at maximum work
G – – – – – – –	– – – – – – –
GAD	Generalized anxiety disorder
I – – – – – – –	– – – – – – –
IQR	Interquartile range
K – – – – – – –	– – – – – – –
K_i	Knit index
kPa	Kilopascal
L – – – – – – –	– – – – – – –
l	Length along knitted courses
$L_{1,2,3,...n}$	Lengths along knitted courses
l_c	Circumferential body length
l_{ss}	Length along courses of strained sample knit
M – – – – – – –	– – – – – – –
$M_{L1,L2,L3,...,Ln}$	Martensite lengths
M_f	Martensite finish
M_{free}	Martensite free
M_r	Martensite relaxation
M_s	Martensite start
M_t	Martensite tension
mmHg	Millimeters of mercury
N – – – – – – –	– – – – – – –
NiTi	Nickel titanium, Nitinol
O – – – – – – –	– – – – – – –
OH	Orthostatic hypotension

Continued on next page

Table B.1 – continued from previous page

Acronym	Meaning
OI	Orthostatic intolerance
OIG	Orthostatic intolerance garment
P – – – – – – –	– – – – – – –
p	Pressure [Pa]
P_{crit}	Critical press = 1333 Pa
Pa	Pascal
POTS	Postural orthostatic tachycardia syndrome
R – – – – – – –	– – – – – – –
r	Radius [m]
RTW	Ready-to-wear
S – – – – – – –	– – – – – – –
σ_θ	Hoop stress
SE	Superelastic effect
SIM	Stress induced martensite
SMA	Shape memory alloy
SMA-CG	Shape memory alloy compression garments
SME	Shape memory effect
SMM	Shape memory material
T – – – – – – –	– – – – – – –
T	Unit tension [N/m]
t	Fabric thickness
T_{skin}	Skin temperature
W – – – – – – –	– – – – – – –
w	Width along knitted wales
X – – – – – – –	– – – – – – –
$\bar{x}$	Statistical mean
$x_{1,2,3,...,n}$	Dependent variables
Y – – – – – – –	– – – – – – –
Y	Independent variable
Z – – – – – – –	– – – – – – –

Continued on next page

Table B.1 – continued from previous page

Acronym	Meaning
ζ	Actuation contraction
$\#_g$	Number of knitted courses making up a garment
$\#_s$	Number of knitted courses making up a sample, 15